

Westinghouse Non-Proprietary Class 3

WCAP-17116-NP
Revision 0

September 2009

**Westinghouse BWR ECCS
Evaluation Model:
Supplement 5 – Application
to the ABWR**



WCAP-17116-NP
Revision 0

**Westinghouse BWR ECCS Evaluation Model:
Supplement 5 – Application
to the ABWR**

J. Blaisdell*
LOCA Analysis and Methodology

D. Shum*
LOCA Analysis and Methodology

September 2009

Reviewer: P. Kottas*
LOCA Analysis and Methodology

Approved: J. Ghergurovich*
LOCA Analysis and Methodology

*Electronically approved records are authenticated in the electronic document management system.

Westinghouse Electric Company LLC
P.O. Box 355
Pittsburgh, PA 15230-0355

© 2009 Westinghouse Electric Company LLC
All Rights Reserved

TABLE OF CONTENTS

LIST OF TABLES.....v

LIST OF FIGURES.....vii

ACRONYMS AND ABBREVIATIONSix

1 OBJECTIVE1-1

 1.1 BACKGROUND.....1-1

2 SUMMARY AND CONCLUSIONS2-1

3 OVERVIEW OF THE BWR/ABWR LOCA METHODOLOGY3-1

 3.1 GOBLIN.....3-1

 3.2 CHACHA-3D.....3-1

4 ABWR EVALUATION MODEL.....4-1

 4.1 DESCRIPTION OF THE ABWR4-1

 4.2 DESCRIPTION OF ABWR ECCS4-3

 4.2.1 Reactor Core Isolation Cooling (RCIC)4-3

 4.2.2 High Pressure Core Flooder (HPCF)4-3

 4.2.3 Residual Heat Removal (RHR).....4-3

 4.2.4 Automatic Depressurization System (ADS)4-3

 4.2.5 Emergency Power4-4

 4.3 DESCRIPTION OF ABWR EVALUATION MODEL.....4-4

 4.3.1 GOBLIN Model.....4-4

 4.3.2 CHACHA-3D Model.....4-6

 4.3.3 ABWR ECCS Performance Methodology.....4-6

 4.4 RESPONSE OF THE ABWR SYSTEMS TO A LOCA WITH LOSS OF OFF SITE
POWER.....4-10

 4.4.1 Reactor Scram.....4-10

 4.4.2 Steam Line Isolation4-10

 4.4.3 Feedwater Isolation.....4-10

 4.5 BREAKS INSIDE CONTAINMENT4-11

 4.5.1 HPCF Line Break.....4-11

 4.5.2 Main Steam Line Break (MSLB).....4-25

 4.5.3 Feedwater Line Break (FWLB)4-35

 4.5.4 RHR Suction Line Break4-47

 4.5.5 RHR Injection Line Break4-49

 4.5.6 Drain Line Break.....4-56

 4.6 BREAKS OUTSIDE CONTAINMENT4-60

 4.6.1 Steam Line Break Outside Containment Results4-60

 4.7 SUMMARY OF LIMITING CASES4-64

 4.7.1 Case with Minimum Inventory4-66

 4.7.2 Case with Maximum Peak Cladding Temperature.....4-66

5 QUALIFICATION OF ABWR EVALUATION MODEL5-1

 5.1 RECIRCULATION PUMP MODEL5-1

 5.2 INTERNAL PUMP COASTDOWN.....5-3

 5.2.1 Okiluoto 1 Pump Trip5-3

| | | |
|-------|---|------|
| 5.3 | PREDICTION OF BOILING TRANSITION..... | 5-4 |
| 5.3.1 | FRIGG Loop Comparison..... | 5-5 |
| 6 | COMPLIANCE WITH 10 CFR 50 APPENDIX K..... | 6-1 |
| 6.1 | SOURCES OF HEAT DURING THE LOCA..... | 6-1 |
| 6.1.1 | Initial Stored Energy in the Fuel..... | 6-1 |
| 6.1.2 | Fission Heat | 6-2 |
| 6.1.3 | Decay of Actinides..... | 6-2 |
| 6.1.4 | Fission Product Decay | 6-3 |
| 6.1.5 | Metal-Water Reaction Rate..... | 6-4 |
| 6.1.6 | Reactor Internals Heat Transfer | 6-4 |
| 6.2 | SWELLING AND RUPTURE OF THE CLADDING AND FUEL ROD THERMAL PARAMETERS..... | 6-4 |
| 6.3 | BLOWDOWN PHENOMENA..... | 6-5 |
| 6.3.1 | Break Characteristics and Flow | 6-5 |
| 6.3.2 | Frictional Pressure Drops..... | 6-7 |
| 6.3.3 | Momentum Equation | 6-8 |
| 6.3.4 | Critical Heat Flux..... | 6-8 |
| 6.3.5 | Post-CHF Heat Transfer Correlations..... | 6-9 |
| 6.3.6 | Pump Modeling..... | 6-11 |
| 6.3.7 | Core Flow Distribution During Blowdown | 6-11 |
| 6.4 | POST-BLOWDOWN PHENOMENA; HEAT REMOVAL BY THE ECCS..... | 6-12 |
| 6.4.1 | Single Failure Criterion..... | 6-12 |
| 6.4.2 | Containment Pressure | 6-12 |
| 6.4.3 | Calculation of Reflood Rate..... | 6-12 |
| 6.4.4 | Steam Interaction with Emergency Core Cooling Water | 6-12 |
| 6.4.5 | Refill and Reflood Heat Transfer..... | 6-12 |
| 6.4.6 | Convective Heat Transfer Coefficients for Boiling Water Reactor Fuel Rods Under Spray Cooling..... | 6-13 |
| 6.4.7 | The Boiling Water Reactor Channel Box Under Spray Cooling..... | 6-13 |
| 7 | REFERENCES..... | 7-1 |
| | APPENDIX A ROADMAP TO THE METHODOLOGY CHANGES | A-1 |
| | APPENDIX B ABWR LOCA ANALYSIS MODEL INPUT PARAMETERS | B-1 |

LIST OF TABLES

| | | |
|-----------|--|------|
| Table 4-1 | Line Breaks Inside Containment | 4-11 |
| Table 4-2 | HPCF Line Break Results | 4-12 |
| Table 4-3 | Steam Line Break Results | 4-26 |
| Table 4-4 | Feedwater Line Break Results..... | 4-36 |
| Table 4-5 | RHR Suction Line Break Results..... | 4-47 |
| Table 4-6 | RHR Injection Line Break Results..... | 4-49 |
| Table 4-7 | Drain Line Break Results | 4-56 |
| Table 4-8 | Main Steam Line Break Outside Containment Results..... | 4-61 |
| Table 4-9 | Summary of Break Spectrum Study Results | 4-64 |

LIST OF FIGURES

| | |
|---|------|
| Figure 3-1 Flow of Information Between Computer Codes (parallel channel mode)..... | 3-2 |
| Figure 4-1 Schematic of ABWR Reactor Vessel Internals | 4-2 |
| Figure 4-2 Schematic of ECCS Divisions | 4-4 |
| Figure 4-3 Typical GOBLIN Nodalization for ABWR | 4-9 |
| Figure 4-4 Core Flow Rate Sensitivity – Dome Pressure and GOBLIN PCT | 4-15 |
| Figure 4-5 Core Flow Rate Sensitivity – System Mass and ECCS Flow Rate | 4-16 |
| Figure 4-6 Core Flow Rate Sensitivity – Upper Plenum Void and Hot Assembly Exit Quality | 4-17 |
| Figure 4-7 Steam Line Isolation Sensitivity –Dome Pressure and GOBLIN PCT..... | 4-18 |
| Figure 4-8 Steam Line Isolation Sensitivity – Break Flow Rate and System Mass | 4-19 |
| Figure 4-9 Break Size Sensitivity – Dome Pressure and PCT | 4-20 |
| Figure 4-10 Break Size Sensitivity – System Mass and ECCS Flow Rate | 4-21 |
| Figure 4-11 Break Size Sensitivity – Upper Plenum Void and Hot Assembly Exit Quality | 4-22 |
| Figure 4-12 Assembly Power Sensitivity – Exit Cladding Temperature vs. Channel Peaking Factor ... | 4-23 |
| Figure 4-13 Assembly Power Sensitivity – GOBLIN PCT vs. Channel Peaking Factor | 4-24 |
| Figure 4-14 Schematic of Steam Line Break inside Containment | 4-25 |
| Figure 4-15 Core Flow Rate Sensitivity – Dome Pressure and Break Flow Rate..... | 4-28 |
| Figure 4-16 Core Flow Rate Sensitivity – System Mass and ECCS Flow Rate | 4-29 |
| Figure 4-17 Core Flow Rate Sensitivity – GOBLIN PCTs | 4-30 |
| Figure 4-18 Core Flow Rate Sensitivity – Upper Plenum Void and Hot Assembly Exit Quality | 4-31 |
| Figure 4-19 Break Size Sensitivity – Break Flow Rates | 4-32 |
| Figure 4-20 Break Size Sensitivity – Dome Pressure and System Mass..... | 4-33 |
| Figure 4-21 Break Size Sensitivity – GOBLIN PCTs | 4-34 |
| Figure 4-22 Schematic of Feedwater Line Break..... | 4-35 |
| Figure 4-23 Core Flow Rate Sensitivity – Dome Pressure and GOBLIN PCTs | 4-38 |
| Figure 4-24 Core Flow Rate Sensitivity – System Mass and ECCS Flow Rates | 4-39 |
| Figure 4-25 Core Flow Rate Sensitivity – Upper Plenum Void and Hot Assembly Exit Quality | 4-40 |
| Figure 4-26 Steam Line Isolation Sensitivity – Dome Pressure and GOBLIN PCTs | 4-41 |
| Figure 4-27 Steam Line Isolation Sensitivity – Break Flow Rate and System Mass | 4-42 |
| Figure 4-28 Break Location Sensitivity – System Mass and ECCS Flow Rates | 4-43 |

| | |
|--|------|
| Figure 4-29 Break Size Sensitivity – Dome Pressure (Short-term and Long-term)..... | 4-44 |
| Figure 4-30 Break Size Sensitivity – GOBLIN PCTs..... | 4-45 |
| Figure 4-31 Break Size Sensitivity – System Mass and ECCS Flow Rates..... | 4-46 |
| Figure 4-32 Schematic of RHR Suction Line Break..... | 4-48 |
| Figure 4-33 Core Flow Rate Sensitivity – GOBLIN PCTs..... | 4-50 |
| Figure 4-34 Core Flow Rate Sensitivity – Upper Plenum Void and Hot Assembly Exit Quality | 4-51 |
| Figure 4-35 Steam Line Isolation Sensitivity – Dome Pressure and GOBLIN PCT..... | 4-52 |
| Figure 4-36 Break Size Sensitivity – GOBLIN PCT and System Mass..... | 4-53 |
| Figure 4-37 Core Flow Rate Sensitivity – GOBLIN PCT | 4-54 |
| Figure 4-38 Core Flow Rate Sensitivity – Dome Pressure and System Mass..... | 4-55 |
| Figure 4-39 Schematic of Drain Line Break | 4-57 |
| Figure 4-40 Comparison of DLB to RHRSLB – GOBLIN PCTs | 4-58 |
| Figure 4-41 Comparison DLB to RHRSLB – Dome Pressure and System Mass..... | 4-59 |
| Figure 4-42 Schematic of Steam Line Break Outside Containment | 4-60 |
| Figure 4-43 Steam Line Break Outside Containment – GOBLIN PCT | 4-62 |
| Figure 4-44 Steam Line Break Outside Containment – Dome Pressure and System Mass | 4-63 |
| Figure 4-45 Summary of Peak Cladding Temperature Results vs. Break Size | 4-65 |
| Figure 4-46 Summary of Minimum Inventory Results vs. Break Size | 4-66 |
| Figure 4-47 Peak Cladding Temperature For Limiting Case..... | 4-68 |
| Figure 5-1 Calculated ABWR Pump Trip Transient..... | 5-3 |
| Figure 5-2 Comparison of Core Channel Inlet Flow Rate for OL1 Pump Trip Transient..... | 5-4 |
| Figure 5-3 FRIGG Loop Test Section | 5-6 |
| Figure 5-4 Comparison of Measured and Predicted Dryout Times..... | 5-7 |

ACRONYMS AND ABBREVIATIONS

| | |
|---------|--|
| ADS | automatic depressurization system |
| ASD | adjustable speed drive |
| BAF | bottom of active fuel |
| CPR | critical power ratio |
| CTG | combustion turbine generator |
| EDG | emergency diesel generator |
| HPCF | high pressure core flooder |
| LHGR | linear heat generation rate |
| LPFL | low pressure flooder |
| LTR | licensing topical report |
| LWL | low water level |
| MAPLHGR | maximum average planar linear heat generation rate |
| MOV | motor operated valve |
| OLI | Okiluoto 1 |
| PCT | peak cladding temperature |
| PLR | part-length rod |
| RIP | reactor internal pump |
| RWCU | reactor water clean-up |
| TCV | turbine control valve |
| TMOL | thermal mechanical operating limit |
| TSV | turbine stop valve |
| TVO | Teollisuuden Voima Oy |

1 OBJECTIVE

The Safety Evaluation Report (SER) for the Westinghouse boiling water reactor (BWR) emergency core cooling system (ECCS) Evaluation Model which is contained in RPB 90-93-P-A (Reference 1), concludes that the Evaluation Model is acceptable for large and small break applications involving BWR/2 through BWR/6 plants. The objective of this Licensing Topical Report (LTR) is to provide a basis for extending the applicability of the Evaluation Model to the Advanced Boiling Water Reactor (ABWR).

Since the response of the ABWR to a LOCA event is quite different than for a BWR with external recirculation pumps, different features of the Evaluation Model take on more importance and require additional qualification.

For example, the speed of internal recirculation pumps responds to a loss of power more quickly than external recirculation pumps. This results in boiling transition in the coolant channel in the first few seconds of the LOCA transient. Also, the absence of external recirculation piping connecting to the reactor vessel significantly reduces the loss of inventory due to postulated breaks in the attached piping. As a result, the phenomena of extended clad heat-up associated with core uncover is absent in the ABWR design. The only significant cladding heatup predicted is due to early boiling transition in the hot channels as a result of the rapid decrease in core flow, which is independent of the ECCS equipment.

[

] ^{a,c}

The LTR provides additional qualification of the internal pump model and benchmarks the system performance code GOBLIN to a series of dryout tests.

1.1 BACKGROUND

The licensing of the Westinghouse BWR reload safety analysis methodology for U.S. applications was begun by Westinghouse Electric Corporation in 1982 with the submittal of various LTRs. These reports describe codes and methodology developed by Westinghouse Atom AB, formerly known as ABB Atom (and ASEA Atom) of Sweden. Appendix A of this report provides a roadmap showing where various features of the Evaluation Model are described or revised.

In 1988 ABB Atom continued the licensing of the BWR reload methodology that was started by Westinghouse in 1982. The transfer of the licensing effort was formally facilitated by ABB's re-submittal of NRC-approved LTRs under ABB ownership.

After the acquisition of Combustion Engineering by the parent company of ABB Atom, the U.S. operations of ABB Atom were consolidated within ABB Combustion Engineering, which became the cognizant organization for BWR reload fuel application in the U.S. CENPD-300-P-A (Reference 2) describes the ABB BWR reload methodology that is currently used for U.S. reload applications.

ABB nuclear businesses were acquired by Westinghouse Electric Company LLC (the successor company of the Westinghouse Electric Corporation nuclear business) in April 2000.

The Westinghouse BWR ECCS Evaluation Model was originally approved by the NRC in 1989 and is described in RPB 90-93-P-A (Reference 2) and RPB 90-94-P-A (Reference 3). This methodology was first revised in 1996 to extend its application to SVEA-96 fuel. These revisions are described in CENPD-283-P-A (Reference 4) and CENPD-293-P-A (Reference 5). Two other revisions were made to the methodology in 2003 and 2004, primarily to improve the fuel rod cladding rupture model and to extend the application to SVEA-96 Optima2 fuel. These changes are described in WCAP-15682-P-A (Reference 6) and WCAP-16078-P-A (Reference 7) respectively.

2 SUMMARY AND CONCLUSIONS

The ABWR LOCA transient assumed to occur coincident with a loss of off site power is different than a typical BWR LOCA transient in two important ways:

- The core flow rate decreases quickly due to the rapid coastdown of the reactor internal pumps (RIPs) following the loss of power¹.
- The elevations of potential large pipe break sites are above the top of the active core.

The first difference results in early boiling transition before the reactor scram occurs. The reduction in heat transfer results in an increase in cladding temperature. The decrease in core power caused by increased voiding and reactor scram results in a rapid reduction in cladding temperature. As a result, the cladding temperature excursion is short-lived. The second difference, in conjunction with the actuation of the robust ECCS, results in nearly continuous two-phase cooling of the core. The typical extended core uncover phase of the BWR loss of coolant accident (LOCA) transient does not occur in the ABWR. As a result, the peak cladding temperature (PCT) occurs before ECCS actuation and is independent of ECCS performance.

This LTR provides the basis for extending the Westinghouse BWR ECCS Evaluation Model to the ABWR. This version of the Evaluation Model is identified as USA7.

As discussed in Section 3, the methodology makes use of two computer codes, GOBLIN and CHACHA. These are the same codes used in the Westinghouse BWR ECCS performance analysis and no coding changes are necessary to apply these codes to the ABWR.

Section 4 describes the differences in the methodology with respect to typical BWR applications. In summary, the differences are:

- The nodalization for the system/hot assembly thermal-hydraulic response analysis is modified to account for the differences in design between BWRs and ABWRs. Most notably is the replacement of BWR external recirculation loops with ABWR internal recirculation pumps.

- []^{a,c}

- []^{a,c}

Section 4 presents a sample break spectrum analysis for a typical ABWR. The results of this sample break spectrum analysis show that the PCT occurs in the first few seconds and that the hot assembly is

1. A rapid coastdown of all RIPs is assumed, which ignores the effect that the 6 RIPs connected to the MG sets would coast down more slowly.

cooled by a two-phase mixture throughout the event. The case with the highest PCT, as predicted by the system/hot channel analysis, was further analyzed in a lattice heatup calculation using the CHACHA code to determine the MAPLHGR. As shown, the MAPLHGR [

] ^{a,c}.

Section 5 of the topical report presents additional qualification for the GOBLIN code. A detailed description of the recirculation pump model is provided with emphasis on how the pump model is biased to ensure that a conservatively fast pump coastdown is predicted. A comparison of a predicted ABWR pump coastdown to a pump coastdown time constant specification (minimum safety analysis limit) is presented.

Section 5 also presents a comparison of GOBLIN test predictions of FRIGG loop transient dryout experiments. The predictions included comparisons to experiments with three different axial power shapes, decreasing flow rates, and increasing test section powers. The comparisons showed that GOBLIN predicted the time of boiling transition conservatively for all relevant test data.

Section 6 describes how the ABWR ECCS Evaluation Model complies with the requirements of 10 CFR 50 Appendix K and Section 7.

Appendix A provides an overview of the Westinghouse BWR/ABWR ECCS Evaluation Model methodology. A roadmap is provided to indicate what changes have been made to the methodology over the years and where the changes are described.

Appendix B provides a table of input parameters that were used to develop the GOBLIN system/hot channel analysis model. The data in the table is representative of an ABWR, but should not be assumed to be applicable to any particular plant.

3 OVERVIEW OF THE BWR/ABWR LOCA METHODOLOGY

The methodology and computer codes used for the ABWR are essentially the same as for the BWRs and are being applied in a manner that is generally consistent with the NRC approval for the BWR. The specific differences are described in Section 4.

The GOBLIN series of computer codes uses one-dimensional assumptions and solution techniques to calculate the ABWR transient response to both large- and small-break LOCAs. The series is comprised of two major computer codes, GOBLIN and CHACHA-3D. The flow of information between these codes is shown in Figure 3-1.

3.1 GOBLIN

GOBLIN performs the analysis of the LOCA blowdown and reflood thermal-hydraulic transient for the entire reactor, including the interaction with various control and safety systems. The GOBLIN code has what is referred to as the 'DRAGON' option that can be driven by boundary conditions supplied by the GOBLIN system analysis calculation. This option may be used to analyze the hot assembly in a series fashion rather than in parallel with the system response analysis. The parallel-channel calculation is accomplished by running GOBLIN with two or more parallel channels where one of the channels represents the hot assembly and the other(s) represents the remainder of the core. The latter approach is used in the examples presented in this report.

3.2 CHACHA-3D

The CHACHA-3D code performs detailed fuel rod mechanical and thermal response calculations at a specified axial level within the hot assembly previously analyzed by DRAGON or the multi-channel GOBLIN model. All necessary fluid boundary conditions are obtained from the hot channel calculation. CHACHA-3D determines the temperature distribution of each rod at a specified axial plane throughout the transient. These results are used to determine the PCT and cladding oxidation at the axial plane under investigation. CHACHA-3D also provides input for the calculation of total hydrogen generation.

The flow of information between these codes is shown in Figure 3-1. Reference 2 provides a detailed description of these codes. References 4, 5 and 7 describe updates to the various components of the computer codes.

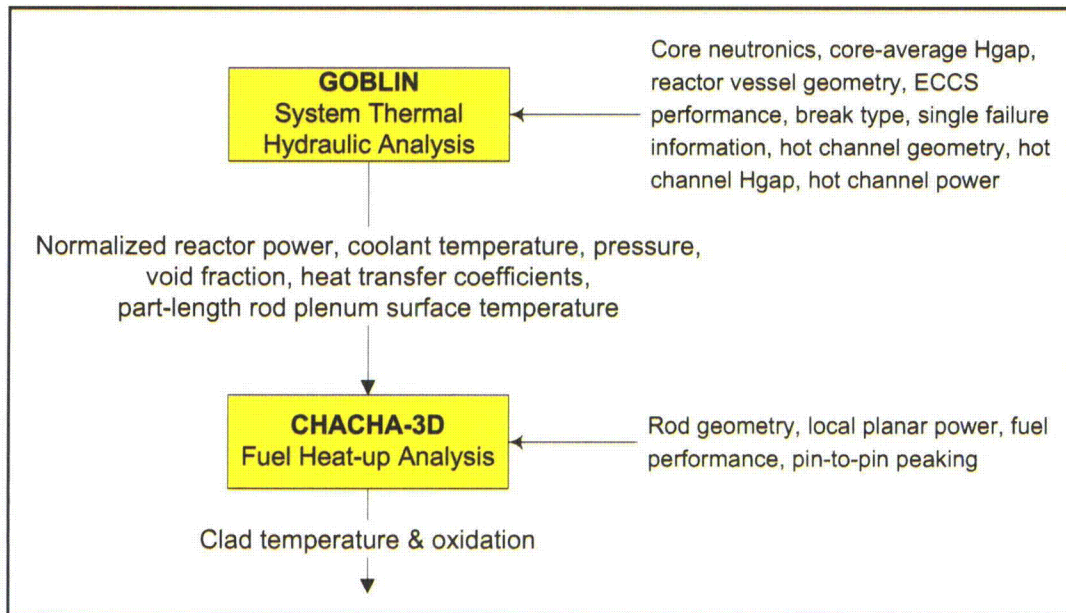


Figure 3-1 Flow of Information Between Computer Codes (parallel channel mode)

4 ABWR EVALUATION MODEL

4.1 DESCRIPTION OF THE ABWR

Figure 4-1 shows a cross section of the ABWR reactor vessel. The internals are similar to the BWR/3 to BWR/6 except that there are no jet pumps and no recirculation line nozzles connected to the lower part of the downcomer. The lack of large piping connecting to the lower part of the annulus, plus the capacity of the ECCS, significantly reduce the potential loss of inventory due to a postulated break in connecting piping. However, the low inertia of the impellers in the 10 variable speed reactor internal pumps (RIPs) cause them to coast down much faster than the larger external recirculation loops. The rapid reduction in core flow rate results in an early departure from nucleate boiling following the loss of offsite power that is assumed coincident with the LOCA.

During normal operation the 10 RIPs provide forced circulation of reactor coolant through the lower plenum of the reactor and up through the lower grid, the reactor core, steam separators, and back down the downcomer annulus. By regulating the flow rate, the reactor power output can be regulated over an approximate range from 70% to 100% without moving control rods. The RIPs are mounted vertically with their drive shafts penetrating the RPV through nozzles arranged in an equally-spaced ring pattern on the bottom head. Adjustable speed drives (ASDs) provide power to the induction motors driving the RIPs. The RIPs are powered from two separate non-safety electrical load groups, each load group supplying 5 RIPs. Within each group, the RIPs are further divided between two 13.8 kV buses. Three RIPs connect via a motor/generator (M/G) set from one bus, and two, not connected to an M/G set, from another bus. On a single failure of a single power distribution component, two RIPs will trip simultaneously and three RIPs will continue to receive power as the M/G set coasts down. A maximum of three RIPs will trip simultaneously on a single failure of a 13.8 kV power system component (i.e., the M/G set). On a complete loss of alternating current (AC) power, the six RIPs connected to the M/G sets will continue to receive power as the M/G sets coast down. While this system would significantly delay the early departure from nucleate boiling following a LOCA, the system is not credited for the analysis of LOCA coincident with loss of offsite power.

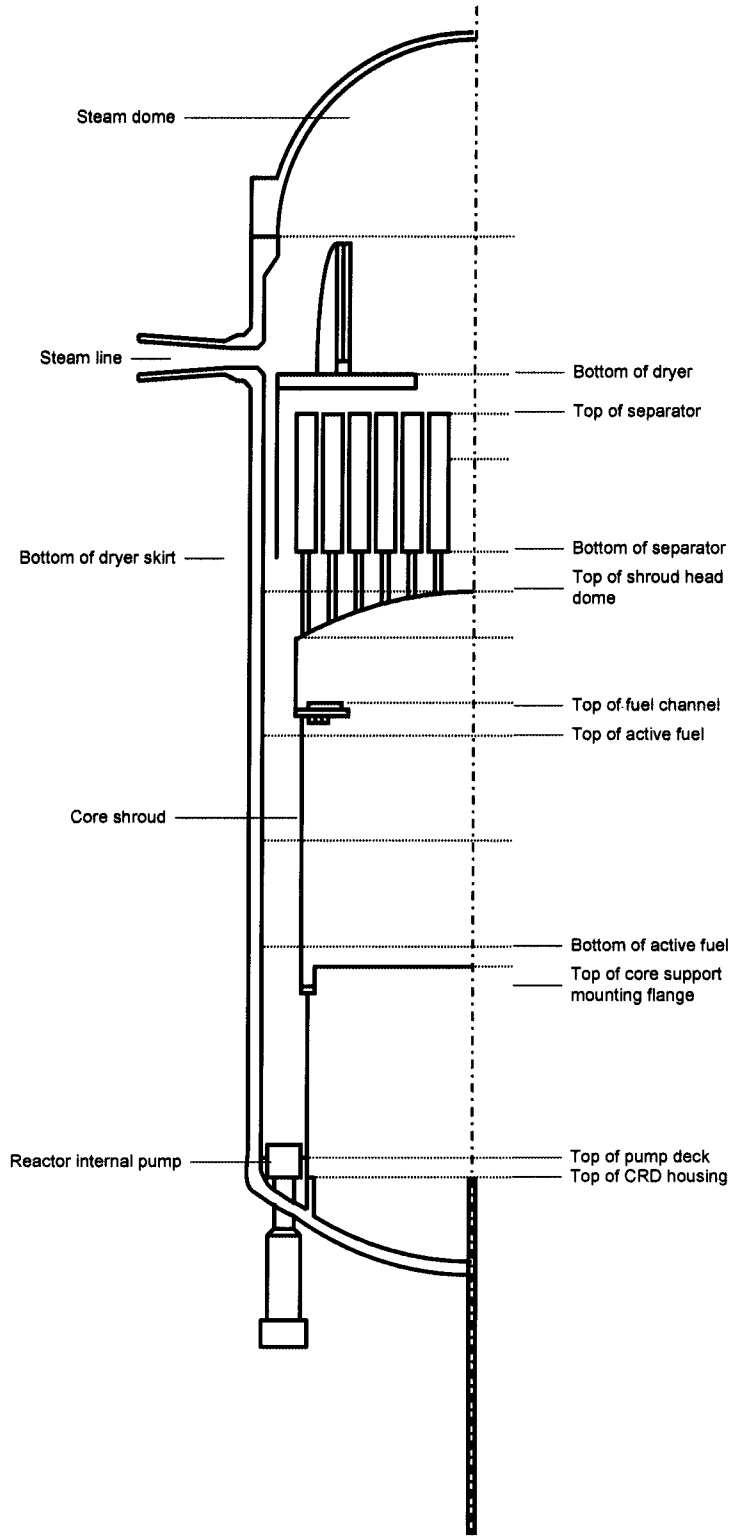


Figure 4-1 Schematic of ABWR Reactor Vessel Internals

4.2 DESCRIPTION OF ABWR ECCS

The ECCS is comprised of a reactor core isolation cooling (RCIC) system, a high pressure core flooder (HPCF) system, a residual heat removal (RHR) system and an automatic depressurization system (ADS).

4.2.1 Reactor Core Isolation Cooling (RCIC)

The RCIC system consists of a single steam-driven turbine that drives a pump. The RCIC turbine steam supply is taken from one of the main steam lines upstream of the first MSIV. The turbine exhausts to the suppression pool. The RCIC pump discharges makeup water to one of the two main feedwater lines. The RCIC pump takes suction from the condensate storage tank (CST) or the suppression pool with the preferred source being the CST.

The RCIC system is initiated automatically when either a high drywell pressure signal or a low water level signal (LWL-2) signal is generated. The RCIC system is designed to deliver water to the RPV while the system is fully pressurized.

4.2.2 High Pressure Core Flooder (HPCF)

The HPCF is made up of two loops that deliver water to the RPV via two independent spargers above the core. The system is capable of injecting water into the reactor vessel over the entire operating pressure range. Both divisions take primary suction from the CST and secondary suction from the suppression pool. In the event the CST water level falls below a predetermined setpoint, the pump suction transfers automatically to the suppression pool.

The HPCF system is initiated automatically when either a high drywell pressure signal or a LWL-1.5 signal is generated.

4.2.3 Residual Heat Removal (RHR)

The RHR system consists of three independent loops that inject water into the RPV and/or remove heat from the reactor core or containment. In the low pressure flooder (LPFL) mode, each loop draws water from the suppression pool and injects water into the RPV outside of the core shroud via one of the feedwater lines on one loop and via the core cooling subsystem discharge return line on two loops.

The LPFL mode of RHR is initiated automatically when either a high drywell pressure signal or a LWL-1 signal is generated. Since the piping system is not designed for high system pressure, the injection valves require that the system pressure be below a pressure permissive setpoint before they will open.

4.2.4 Automatic Depressurization System (ADS)

If the RCIC and HPCF systems cannot maintain the RPV water level, the ADS, which is independent of any other ECCS, reduces RPV pressure so that flow from the RHR system operating in the LPFL mode enters the RPV in time to cool the core and limit fuel cladding temperature. The ADS is comprised of eight safety relief valves (SRVs). Each of the selected SRVs is equipped with an air accumulator and

check valve that ensures that the valves can be held open following failure of the air supply to the accumulators.

The system is designed so that a single active or passive component failure including power buses, electrical and mechanical parts, cabinets, and wiring will not disable ADS. A timer in the ADS is initiated when a high drywell pressure signal and a LWL-1 are present. If these conditions persist when the time delay expires, the ADS valves will open and steam will be discharged to the suppression pool.

4.2.5 Emergency Power

The ABWR has three emergency diesel generators (EDGs) to power the ECCS equipment in the event of a loss of normal power. Failure of one EDG will disable one of the LPFL pumps. RCIC is independent of the EDG and is available in the case of a station blackout. Failure of either of the other two EDGs will disable one HPCF pump and one LPFL pump. Figure 4-2 shows the breakdown of ECCS equipment by electrical division. The ECCS can also be manually powered by the combustion turbine generator (CTG). However, power supply from the CGT is not credited in the LOCA analysis.

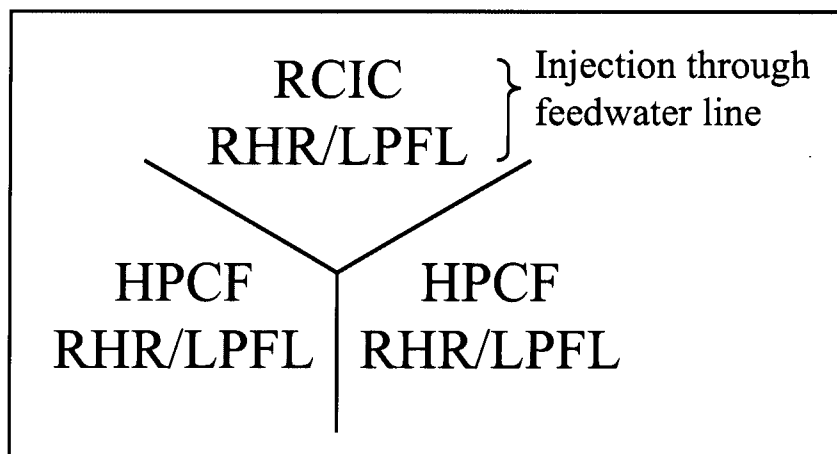


Figure 4-2 Schematic of ECCS Divisions

4.3 DESCRIPTION OF ABWR EVALUATION MODEL

4.3.1 GOBLIN Model

4.3.1.1 Nodalization

The typical ABWR GOBLIN nodalization for the Westinghouse ABWR Evaluation Model is shown in Figure 4-3. This nodalization scheme has been developed based on previous nodalization studies (References 3, 4 and 7). The major difference in the ABWR ECCS performance Evaluation Model is the increased number of nodes to model the active core. The benchmarking of the FRIGG loop experiments, as described in Section 5.3, showed improved results when []^{a,c} were used to model the heated test section. GOBLIN nodalization of the ABWR may be changed, depending on the application of the model, to ensure that the appropriate thermal/hydraulic phenomena are captured in sufficient detail.

The steam dome is represented by a single control volume. During a LOCA transient with total loss of offsite power, the steam line is isolated rapidly by closure of the turbine stop valves (TSVs), fast closure of the turbine control valves (TCVs) or closure of the main steam isolation valves (MSIVs) and the steam dome is generally a stagnant vapor space.

The upper and lower downcomer regions are made up of nine sub-volumes. Feedwater as well as RCIC and LPCF injection are directed into the upper portion of the lower downcomer. Two-phase mixture level tracking is calculated throughout the entire downcomer. This means that the actual volume boundary nearest the mixture level is placed at the location of the mixture level. More detail about the level tracking feature is provided in Section 3.3.2 of Reference 2.

The lower plenum is divided into four control volumes. The lowermost sub-volume receives flow from the RIPs. This noding is similar in detail to the noding used in the BWR Evaluation Model.

The core is represented by five parallel channels, two channels representing the average core and its associated water-cross channel, two channels representing the hot assembly and its associated water-cross channel, and the fifth channel representing the core bypass region. The four channels representing average core and hot assembly channels, including their respective water cross, are comprised of []^{a,c} each. The active region of the core and hot assembly are represented by []^{a,c}. There are unheated sub-volumes at the top and bottom.

The core bypass and guide tube region are connected. These regions are partitioned into a total of seven control volumes, two of which represent the guide tubes. This noding is also similar to the noding detail used in the BWR Evaluation Model.

The upper plenum is divided into four sub-volumes. Three of the sub-volumes represent the region above the active core and one sub-volume represents the standpipes and steam separators. This is a region where the HPCF flow is injected. This noding is also similar in detail to the BWR Evaluation Model.

4.3.1.2 Hot Assembly Power

The ABWR design does not result in the hot assembly uncovering for any break in piping connected to the reactor pressure vessel (RPV), even when the limiting single active failure of ECCS equipment is assumed. As a result, the hot assembly power in the ABWR LOCA analysis may be established in a conservative manner [

] ^{a,c}. The process used is as follows:

The methodology assumes a symmetrical axial power shape (chopped cosine) with a 1.5 axial peaking factor. It is recognized that the axial power shape at the beginning of cycle is bottom peaked and that the peak power location generally moves upward during the cycle to become slightly top-peaked at the end of cycle. However, the axial shape used in the analysis is reasonably conservative and representative. The power at the hottest axial node is set to correspond to [

] ^{a,c}. The resulting initial assembly power is considerably higher than any that would occur during operation. This is confirmed for each reload.

The break spectrum analysis is performed using the predicted PCT in the GOBLIN hot assembly to identify the limiting break size/location case that will be subsequently evaluated in the CHACHA heatup calculation. The single failures of ECCS equipment have no impact on this analysis since the PCT occurs before any of the ECCS equipment has actuated. The break spectrum/single failure analysis results are also used to confirm that the performance of the ECCS equipment is sufficient to ensure that any uncover is minimal and there is no appreciable cladding heat-up.

When the limiting break size/location has been determined, the boundary conditions from the hot assembly node applicable to the lattice being evaluated are applied to a CHACHA heatup calculation. The nodal power in the CHACHA heatup calculation is set so that []^{a,c}. The resulting conditions from the analysis are shown to be less than the 10 CFR 50.46 criteria, with regard to PCT and maximum local oxidation. []^{a,c}

4.3.2 CHACHA-3D Model

The CHACHA calculations performed in this report were for the SVEA-96 Optima2 fuel design. However, any fuel design approved by the NRC can be considered. The CHACHA-3D model is identical to the model described in Section 5.3 of Reference 7. Previous sensitivity studies described in Section 4.3.1 of Reference 3 and Section 6.3.1 of Reference 4 have shown little sensitivity to fuel rod nodding. The standard fuel rod nodding, which consists of seven radial nodes having equal volume to represent the fuel pellet and three nodes having equal radial increments to represent the cladding, is used. Similarly, the channel/water cross is represented by a single node with a constant thickness. Since previous studies have shown little sensitivity to channel thickness, the average thickness of the channel and water cross structures is used.

4.3.3 ABWR ECCS Performance Methodology

The reactor coolant pressure boundary contains numerous connecting pipes of varying lengths, diameters, and elevations. A postulated LOCA may be initiated by a break in connecting piping of a wide range of sizes and locations. A 10 CFR 50 Appendix K LOCA analysis requires that the worst possible single failure of the ECCS be assumed when demonstrating ECCS performance. A spectrum of pipe breaks sizes, locations, and single failures is necessary in the evaluation of an ECCS performance.

4.3.3.1 Break Spectrum

For typical LOCA Evaluation Models, the limiting break is the combination of break size, location, and single failure that yields the highest calculated PCT. However in the case of the ABWR, the PCT is not a sufficient measure of ECCS performance.

There is a short duration cladding temperature excursion in the first few seconds of a LOCA due to the rapid loss of core flow after the RIPs lose power. This temperature excursion occurs whether or not a LOCA has occurred and the magnitude of the PCT is independent of ECCS performance. Even though the return to nucleate boiling is prevented in the Evaluation Model, the cladding temperature reduces quickly as the reactor power reduces and the hot assembly remains cooled by a two-phase mixture throughout the rest of the ABWR LOCA transient.

The purpose of the ECCS in the ABWR design is to provide sufficient makeup to the core to prevent heat-up of the cladding subsequent to initial brief heat-up caused by boiling transition associated with the rapid decrease in core flow. Therefore, in the case of the ABWR, the relative performance of the ECCS is best determined by comparing the minimum system inventories for the various cases analyzed and showing that adequate core cooling is not interrupted at any core location. A demonstration of this analysis is presented in Section 4.4 and the case that resulted in the least inventory during the transient is described in Section 4.7.1.

4.3.3.2 Compliance with Acceptance Criteria

The Code of Federal Regulations, 10 Part 50.46 prescribes the following five acceptance criteria for an ECCS performance evaluation for light water nuclear power reactors:

1. Peak cladding temperature – The calculated maximum fuel element cladding temperature shall not exceed 2200°F
2. Maximum cladding oxidation – The calculated total oxidation of the cladding shall nowhere exceed 0.17 times the total cladding thickness before oxidation.
3. Maximum hydrogen generation – The calculated total amount of hydrogen generated from the chemical reaction of the cladding with water or steam shall not exceed 0.01 times the hypothetical amount that would be generated if all the metal in the cladding cylinders surrounding the fuel, excluding the cladding surrounding the plenum volume, were to react.
4. Coolable geometry – Calculated changes in core geometry shall be such that the core remains amenable to cooling.
5. Long-term cooling – After any calculated successful initial operation of the ECCS, the calculated core temperature shall be maintained at an acceptably low value and decay heat shall be removed for the extended period of time required by the long-lived radioactivity remaining in the core.

As discussed in Section 4.3.3.1, the PCT that occurs during a LOCA for an ABWR is not associated with the performance of the ECCS because it occurs before the ECCS is actuated. However, there is a requirement to demonstrate that the 10 CFR 50.46 criteria are met for all postulated LOCAs. The following process is used to demonstrate that these criteria are met:

1. The GOBLIN system response analysis includes an analysis of the hot assembly that has been initialized at a conservative initial power per Section 4.3.1.2. The maximum cladding temperature and the node where it occurs are recorded for each of the break spectrum analyses and single failure studies.
2. The GOBLIN case resulting in the maximum peak cladding temperature is determined.
3. Boundary conditions from the limiting case (e.g., convective heat transfer coefficient, normalized power, rod plenum surface temperatures), which are appropriate for the lattice being evaluated,

are extracted from the GOBLIN system response analysis for the limiting break scenarios(s) as established by the maximum cladding temperature calculated by GOBLIN.

4. These boundary conditions are provided to the hot plane analysis using CHACHA and the nodal power is increased in the CHACHA analysis so that the hottest fuel rod in the lattice is at a linear heat generation rate corresponding to the TMOL.
5. The PCT, maximum oxidation and transient oxidation are recorded and used to demonstrate that the acceptance criteria are met.

The three remaining criteria, maximum hydrogen generation, coolable geometry and long term cooling, are clearly met by the ABWR. The short duration of the cladding heatup and the low maximum cladding temperature ensure that the transient cladding oxidation will be below the established acceptance criterion. For similar reasons, the fuel cladding will retain sufficient ductility to maintain the fuel structure intact and amenable to long-term cooling which is ensured by the long-term operation of the ECCS.

a,c

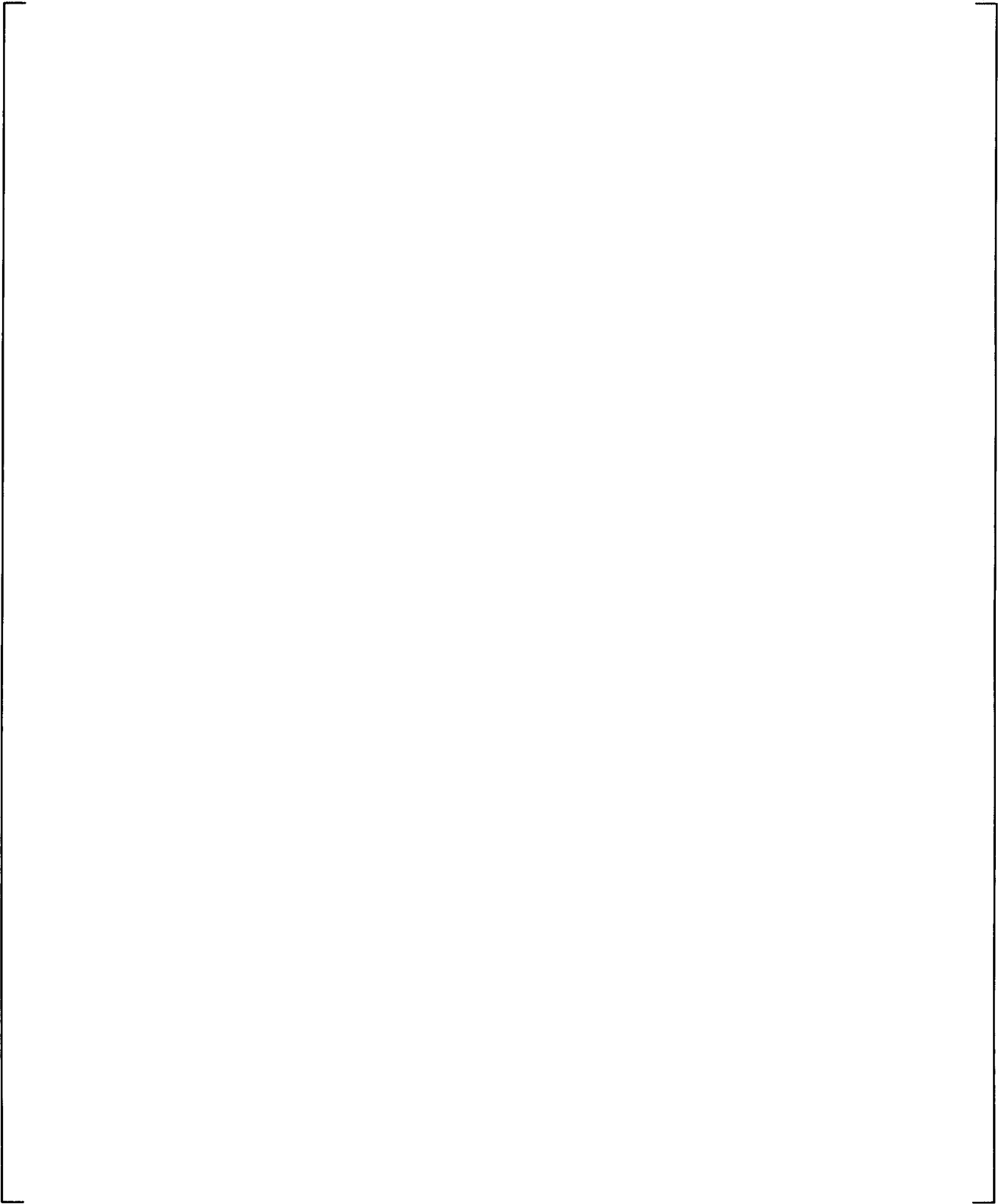


Figure 4-3 Typical GOBLIN Nodalization for ABWR

4.4 RESPONSE OF THE ABWR SYSTEMS TO A LOCA WITH LOSS OF OFF SITE POWER

In the ABWR there are one high pressure reactor core isolation (RCIC) system, two high pressure core flooders (HPCF) systems, three low pressure flooders (LPFL) systems available for any postulated pipe break, and the automatic depressurization system (ADS) available to mitigate a postulated LOCA. Given a break and the limiting single failure, there remains at least one high pressure and one low pressure injection system available to mitigate the event. Although loss of offsite power is assumed to occur at the start of the event, the analysis bounds the various time delays by assuming that the Emergency Diesel Generators (EDGs) start on the low water level ECCS initiation signal plus a fixed time delay. Since the EDGs start also on a high drywell pressure signal that occurs prior to the low water level signal in general, this assumption results in a conservative start time for ECC systems.

4.4.1 Reactor Scram

There are three automatic reactor scram signals that might occur following a LOCA with coincident loss of off site power:

- Water level < LWL 3
- Drywell pressure > High drywell pressure signal
- MSIV stem position < 0.9 (steam line break)

With the exception of high drywell pressure, the other two reactor scram signals will be modeled.

4.4.2 Steam Line Isolation

The steam line will isolate following a LOCA. The two MSIVs on each steam line, which receive a close signal on LWL 1.5 or on high steam flow are the safety grade system for isolating the steam lines. However, sensitivity studies, which are described in this report, show that an earlier and faster steam line isolation is conservative because it reduces the amount of voiding in the core as the pumps coast down due to its impact on system pressure. Therefore, it is assumed that the control grade fast closure of the turbine control valves (TCVs) isolates the steam lines on the generator trip signal coincident with the loss of offsite power.

4.4.3 Feedwater Isolation

The feedwater pumps lose motive power on the loss of off site power. Although the feedwater pumps would coastdown due to inertia, the feedwater flow is assumed to ramp to zero flow in 1 second.

4.5 BREAKS INSIDE CONTAINMENT

Since the ABWR has no external recirculation lines, the largest line breaks are those postulated in a steam line, a feedwater line, or the RHR shutdown suction line. In comparison to external recirculation loop BWRs, the maximum ABWR line break size is only ~15% of the maximum double-ended recirculation line break. In addition, all of the large ABWR lines are located above the core. Breaks in smaller lines such as the RHR injection line, the HPCF injection line, and the bottom head drain line are also considered along with smaller breaks in the larger connecting lines. Table 4-1 lists the breaks considered inside the containment and the corresponding limiting single failure. Note that the limiting single failure is based on minimum inventory predicted during the event because failures in ECCS equipment do not impact the predicted PCT which occurs before any ECCS equipment is activated. The limiting single failure is the one that provides the least makeup when considering the impact of the break location on the ECCS. The breaks listed in Table 4-1 are piping systems with RPV penetrations. There are other branch lines that connect to these lines such as reactor water clean-up (RWCU), RCIC injection line, and the RCIC turbine steam supply line. Breaks in these lines are bounded by the break spectrum of lines that connect directly to the RPV.

A conservative assumption made in the ABWR LOCA analysis is that all offsite AC power is lost simultaneously with the initiation of the LOCA. In this case, four of the RIPs will automatically trip off. If reactor water level continues to drop and reaches LWL-2, the remaining six RIPs will be tripped, three immediately and the final three after a preset time delay. However, in the analysis, all of the RIPs are assumed to coast down rapidly as a result of the loss of power. The resulting rapid core flow coastdown produces a calculated departure from nucleate boiling in the hot assemblies within a fraction of a second after the accident. If offsite power were available, the RIPs would continue to run until a LWL-2 signal is generated and the pump coastdown would not begin until after the reactor scram.

| Break Location | Available ECCS | | | | Remarks |
|---------------------------------|----------------|------|------|-----|--|
| | RCIC | HPCF | LPFL | ADS | |
| HPCF Line Break | 1 | 0 | 2 | 8 | HPCF break + single failure of 1 EDG |
| Main Steam Line Break | 1 | 1 | 2 | 8 | Single failure of 1 EDG RCIC side MSLB |
| | - | 1 | 2 | 8 | |
| Feedwater Line Break | - | 1 | 2 | 8 | RCIC side FWLB + single failure of 1 EDG LPFL side FWLB + single failure of 1 EDG |
| | 1 | 1 | 1 | 8 | |
| RHR Shutdown Suction Line Break | 1 | 1 | 2 | 8 | Single failure of 1 EDG |
| RHR Injection Line Break | 1 | 1 | 1 | 8 | LPFL break + single failure of 1 EDG |
| Drain Line Break | 1 | 1 | 2 | 8 | Single failure of 1 EDG |

4.5.1 HPCF Line Break

There are two HPCF injection nozzles that attach to the RPV near the elevation of the shroud dome. Each nozzle is connected to one of the two HPCF loops. Each injection line is isolated from the RPV by

two valves, one a testable check valve and the other a normally closed motor operated valve (MOV), which opens on the HPCF actuation signal. Internal piping connects each nozzle to a sparger within the upper plenum of the reactor. Each sparger contains a number of nozzles which distribute the injected water above the core.

In the event of a break in the HPCF injection line between the check valve and the RPV, coolant from the RPV will discharge directly into the drywell. The flow of coolant exiting the RPV is limited by the combined flow area of the sparger nozzles. A break in the injection line will prevent any makeup from the water injected from the affected HPCF system. The limiting single active failure is the failure of the EDG that powers the unaffected HPCF loop. This results in the following available equipment:

1 RCIC + 2 LPFL + 8 ADS

Because the combined flow area of the sparger nozzles is small, the system pressure is maintained by the SRVs until actuation of ADS. The RCIC system receives an actuation signal when the measured water level decreases below LWL-2. The LPFL system and ADS delay timer receive an actuation signal when the measured water level decreases below LWL-1. Although the LPFL pumps will start, the LPFL injection valve will not open until the system pressure decreases below a permissive setpoint.

4.5.1.1 HPCF Line Break Results

Six cases were run with the power in the hot assembly set to simulate the hot rod at the TMOL. Table 4-2 summarizes the results of those cases. As shown, the variations in PCT are small when the steam line is isolated by TCV fast closure. The variations in minimum mass for a given break size were minimal. The minimum system mass increases with decreasing break size as expected.

| Case | Core Flow | Break Location | Break Size | Steam Line Isolation | PCT (GOBLIN) | Minimum Mass |
|-------|-----------|----------------|------------|----------------------|--------------|--------------|
| hpcf3 | 90% | HPCF Line | 100% | TCV fast closure | 708°C | 133.3 E3 kg |
| hpcf4 | 111% | HPCF Line | 100% | TCV fast closure | 692°C | 132.2 E3 kg |
| hpcf5 | 90% | HPCF Line | 100% | Pressure regulator | 661°C | 133.7 E3 kg |
| hpcf7 | 90% | HPCF Line | 75% | TCV fast closure | 708°C | 138.1 E3 kg |
| hpcf8 | 90% | HPCF Line | 50% | TCV fast closure | 708°C | 143.6 E3 kg |
| hpcf9 | 90% | HPCF Line | 25% | TCV fast closure | 708°C | 151.3 E3 kg |

4.5.1.2 Sensitivity Studies

Core Flow Rate

Cases hpcf3 and hpcf4 show the effects of different initial core flow rates. The higher initial core flow rate will result in a higher initial mass in the core due to lower void content and additional margin to dryout.

Figure 4-4 compares the system pressure response and the maximum cladding temperature in the hottest GOBLIN node. As shown, the initial pressure responses are identical. However, ADS actuation occurs sooner for the base case, 90% core flow rate, because the water level decreases to the ADS actuation setpoint, LWL-1, sooner. The figure also shows that the PCT is slightly higher in the base case which is a result of an earlier transition to dryout.

Figure 4-5 compares the system mass and ECCS flow rates. Although the initial mass is slightly higher in the high core flow case (hpcf4), there is a delay in the start of RCIC and LPFL injection which delays recovery. As a result, the minimum inventory is slightly less in the high core flow rate case.

Figure 4-6 compares the upper plenum average void and hot assembly exit quality. As shown, there is a period of time when the upper plenum does not contain any liquid (i.e., the void fraction becomes 1.0). This is because the break is located in the upper plenum and it eventually loses all liquid inventory. However, the figure also shows that the hot assembly exit quality indicates two-phase flow throughout the transient.

Steam Line Isolation

Cases hpcf3 and hpcf5 compare different ways of isolating the steam lines. The first, or base, case isolates the steam line by fast closure of the TCVs. The second case assumes that the pressure regulator controls the TCVs to maintain system pressure. As shown in Table 4-2, the PCT was lower in the second case. The minimum inventories were nearly identical.

As shown in Figure 4-7, the dome pressure responses are quite different. The base case maintains a higher pressure until ADS actuation. In this case, the initial system pressure is controlled by the opening and closing of the SRVs. The second case (hpcf5) shows the effect of the pressure regulator closing the TCVs where system pressure is held approximately constant until the MSIV closure setpoint, LWL-1.5, is reached. After MSIV closure, the system pressure increases until ADS is actuated. The figure also shows that the base case has a higher PCT which is due to reactivity feedback effect caused by the impact of the pressure response on the void distribution.

As shown in Figure 4-8, the initial break flow rate is higher when the steam line is isolated by the pressure regulator as in case hpcf5. This is because the combined break area (HPCF line and steam line) is larger as the steam is discharging through the TCVs for a longer time. The additional loss of inventory results in earlier ADS actuation, earlier actuation of the LPFL pumps, and earlier recovery. However, the minimum system masses are nearly identical.

Break Size

Cases hpcf3, hpcf7, hpcf8 and hpcf9 show the effects of different break sizes. As shown in Table 4-2, the PCTs are the same for all cases and the minimum inventory decreases as break size increases.

Figure 4-9 compares the dome pressure and PCT responses. As shown, the initial pressure responses are the same because the pressure is controlled by the opening and closing of the SRVs until ADS actuation. Since the loss of inventory occurs at a slower rate as the break size decreases, the water level reaches the

ADS actuation setpoint later as break size decreases. The figure also shows that the PCT, which occurs early due to the reduction in core flow, is independent of break size.

Figure 4-10 shows the effect of break size on system inventory and ECCS flow rate. As shown, the system mass decreases at a faster rate for the larger breaks, but recovery starts sooner due to earlier actuation of the LPFL pumps. As a result, the largest break has the smallest minimum inventory.

Figure 4-11 shows the upper plenum average void fraction and hot assembly exit quality for each of the break sizes. As shown, all cases have a period of time where the upper plenum void fraction becomes one. This is due to the break location being in the upper plenum. However, Figure 4-11 also shows that the hot assembly exit quality is substantially less than one, indicating that the hot assembly is cooled by a two-phase mixture throughout the transient.

Assembly Power

Although the hot assembly does not uncover during the event, assemblies with lower power do experience a short-term uncover at the upper elevations for the HPCF injection line break. The difference in behavior between high and low power assemblies is due to the amount of steam generated in the two-phase region of the assembly. For high power assemblies, there is sufficient steam generation to swell the two-phase mixture to the top of the channel. However, for low power assemblies, the top of the two-phase mixture may not reach the exit of the channel. Sensitivity studies were performed where the power in the single channel was reduced. Figure 4-12 compares the cladding temperatures at the exit of the heated channel for several channel peaking factors. As shown, for peaking factors of 1.2 and lower, there is a temperature excursion after 280 seconds which recovers following LPFL injection.

Figure 4-13 compares the PCTs for several channel peaking factors. As shown, the highest power channel has the highest peak cladding temperature, occurring during the RIP coastdown phase of the event. Although the lower power bundles do not experience the early boiling transition during the RIP coastdown phase, there is a short duration heatup that occurs prior to LPFL injection when the system inventory is low. As shown, there is a channel peaking factor between 0.9 and 0.3 where this heatup will reach a maximum. However, the PCT during this heatup phase is of the same order as the initial cladding temperature.

The HPCF line break was the only break to exhibit this behavior because this is the only break located inside the core shroud region.

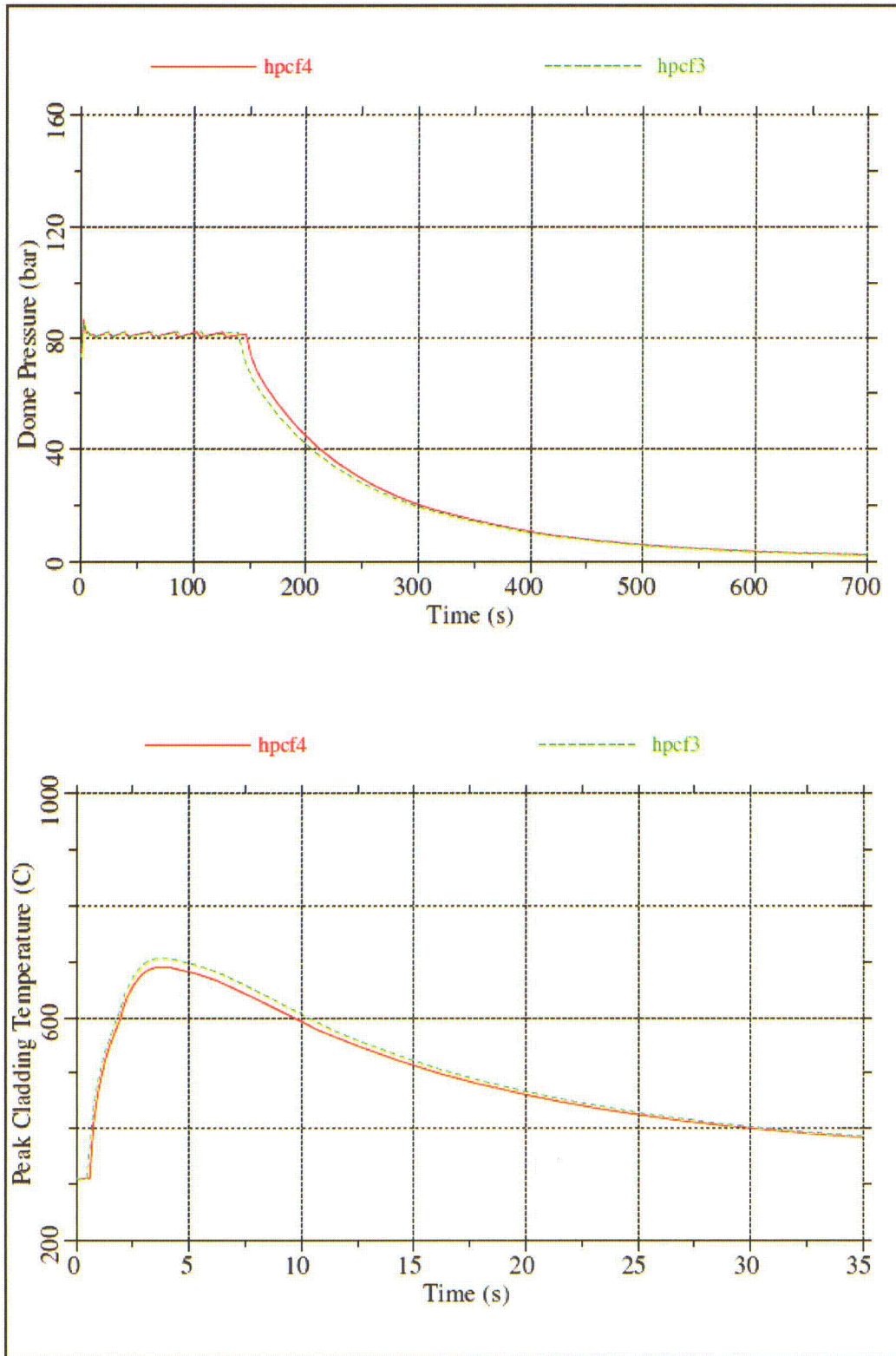


Figure 4-4 Core Flow Rate Sensitivity – Dome Pressure and GOBLIN PCT

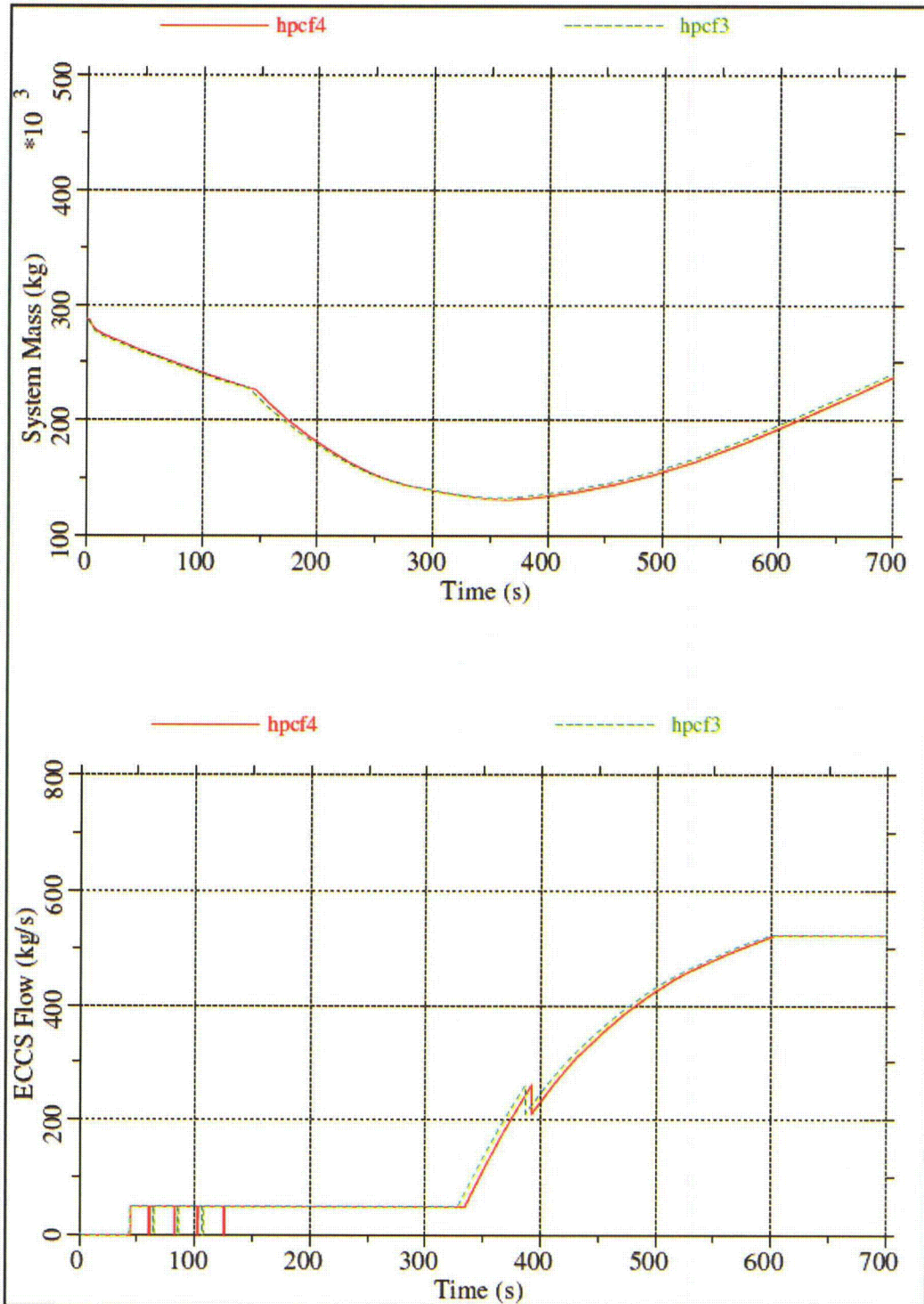


Figure 4-5 Core Flow Rate Sensitivity – System Mass and ECCS Flow Rate

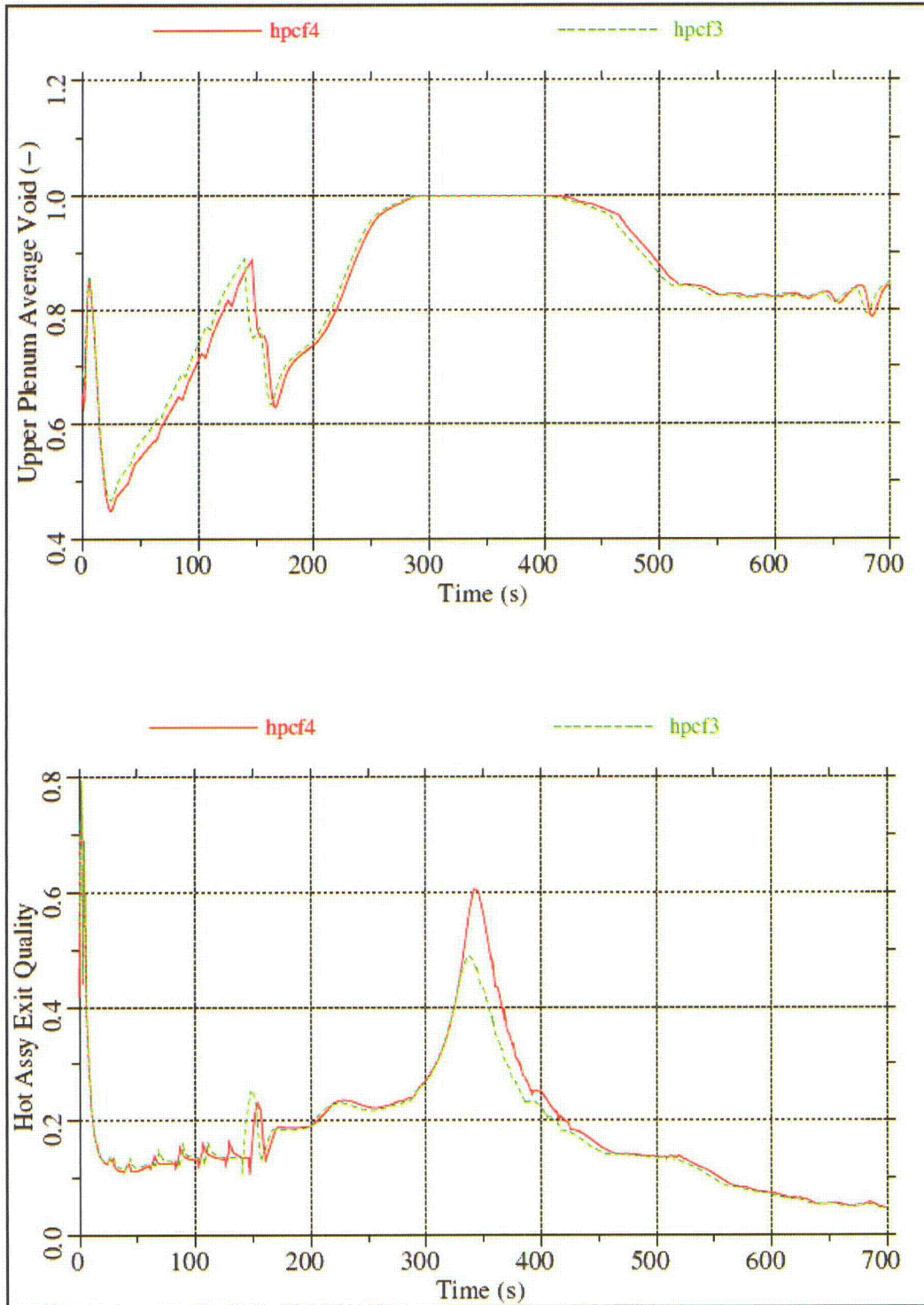


Figure 4-6 Core Flow Rate Sensitivity – Upper Plenum Void and Hot Assembly Exit Quality

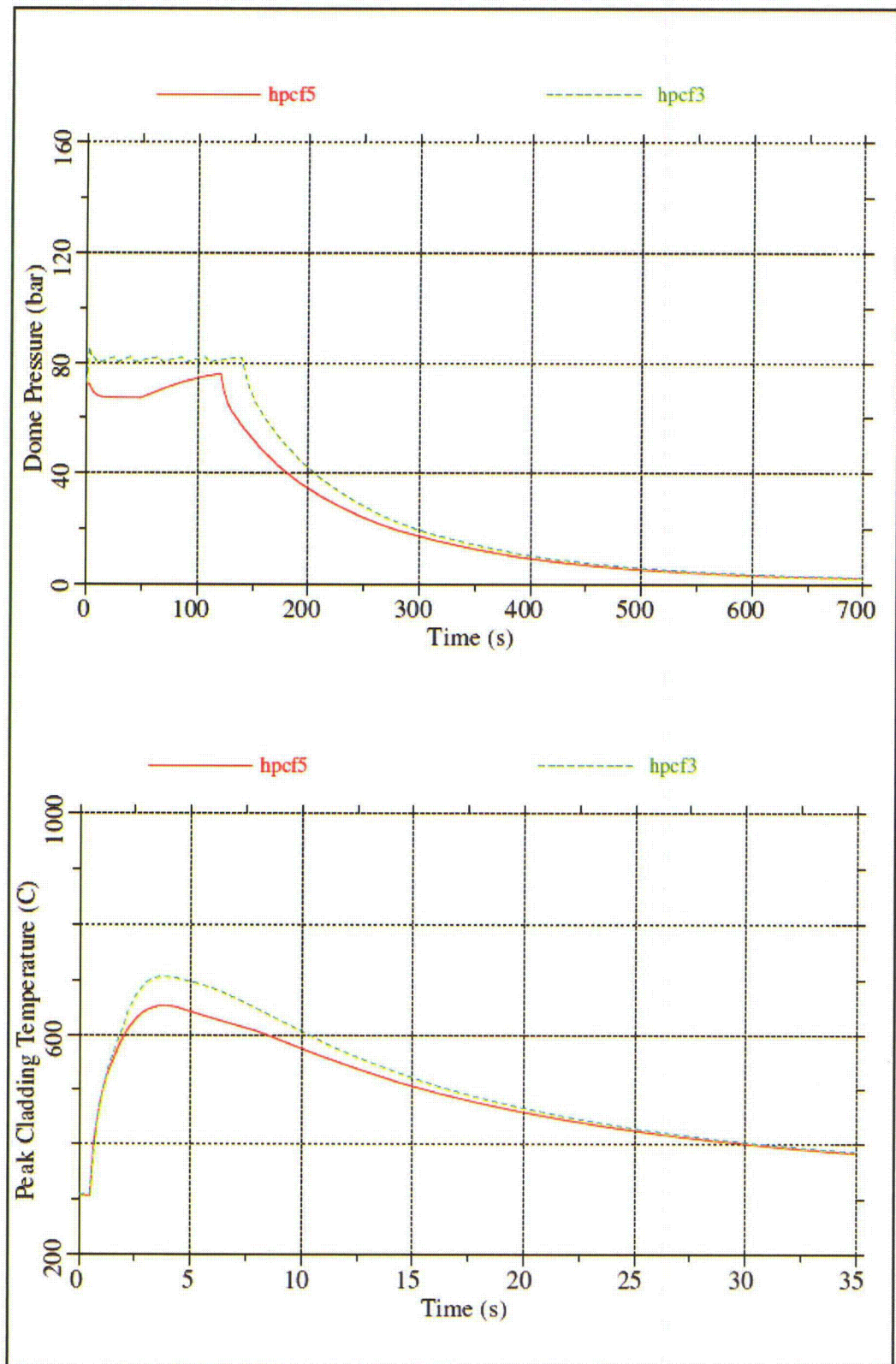


Figure 4-7 Steam Line Isolation Sensitivity –Dome Pressure and GOBLIN PCT

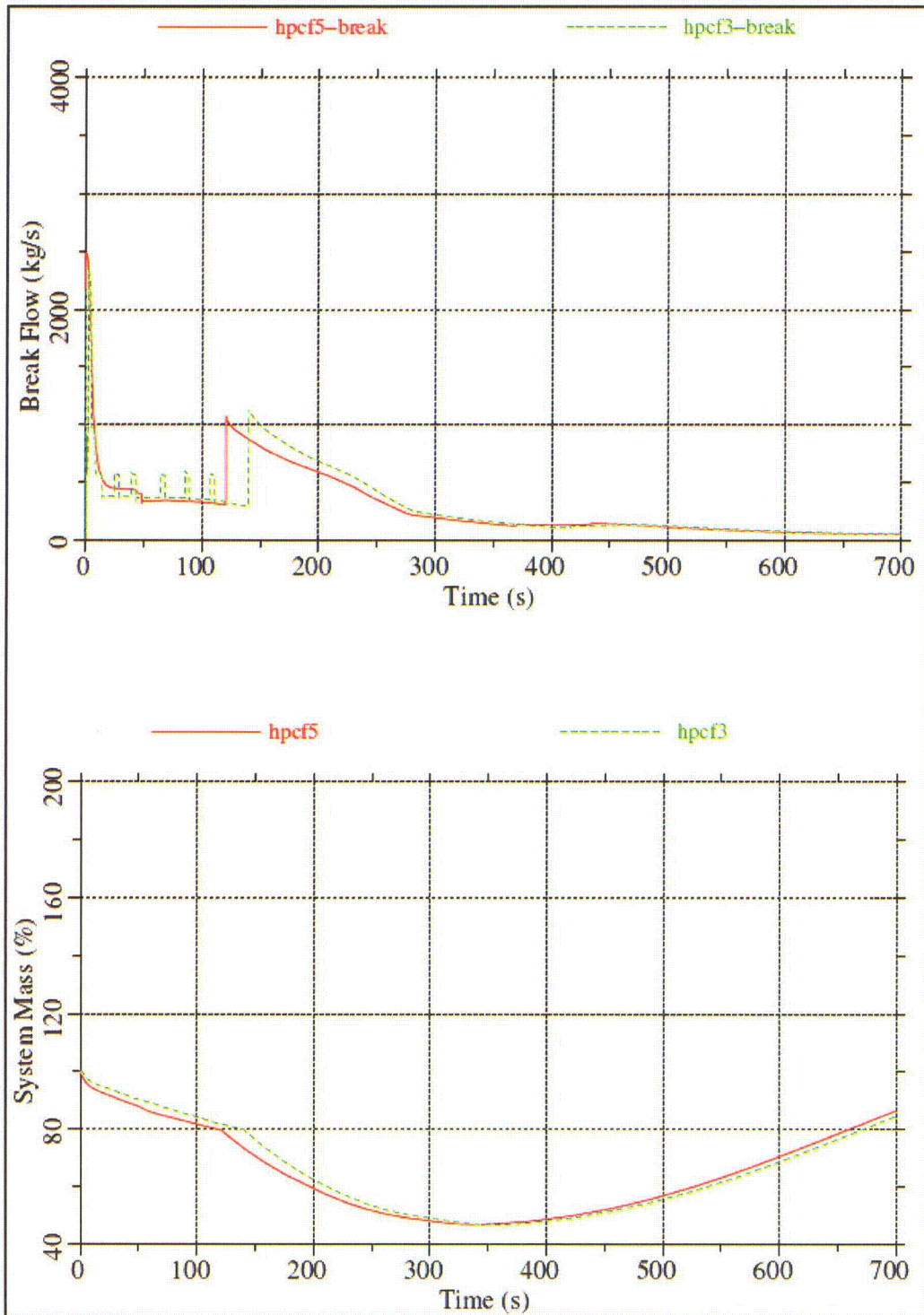


Figure 4-8 Steam Line Isolation Sensitivity – Break Flow Rate and System Mass

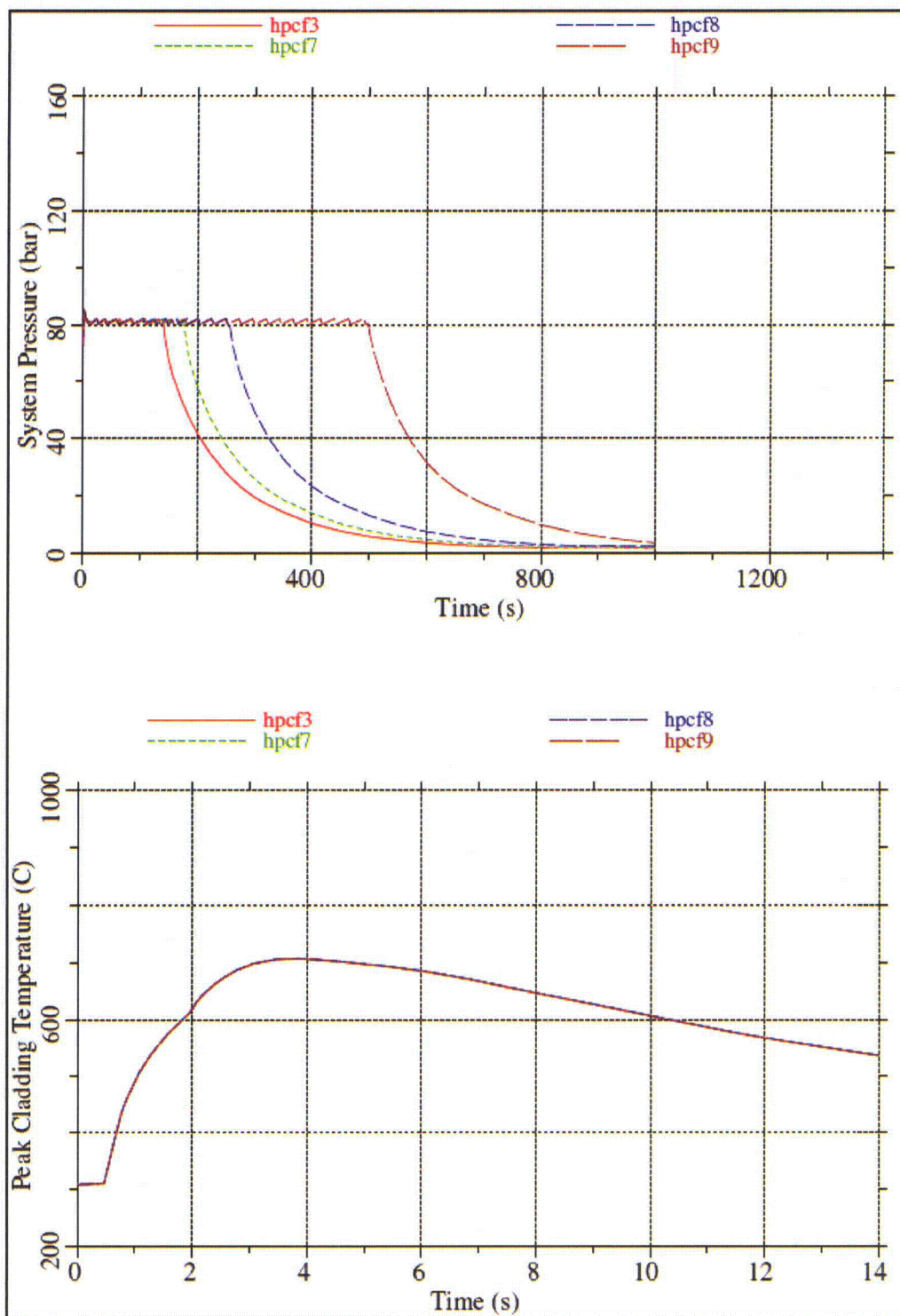


Figure 4-9 Break Size Sensitivity – Dome Pressure and PCT

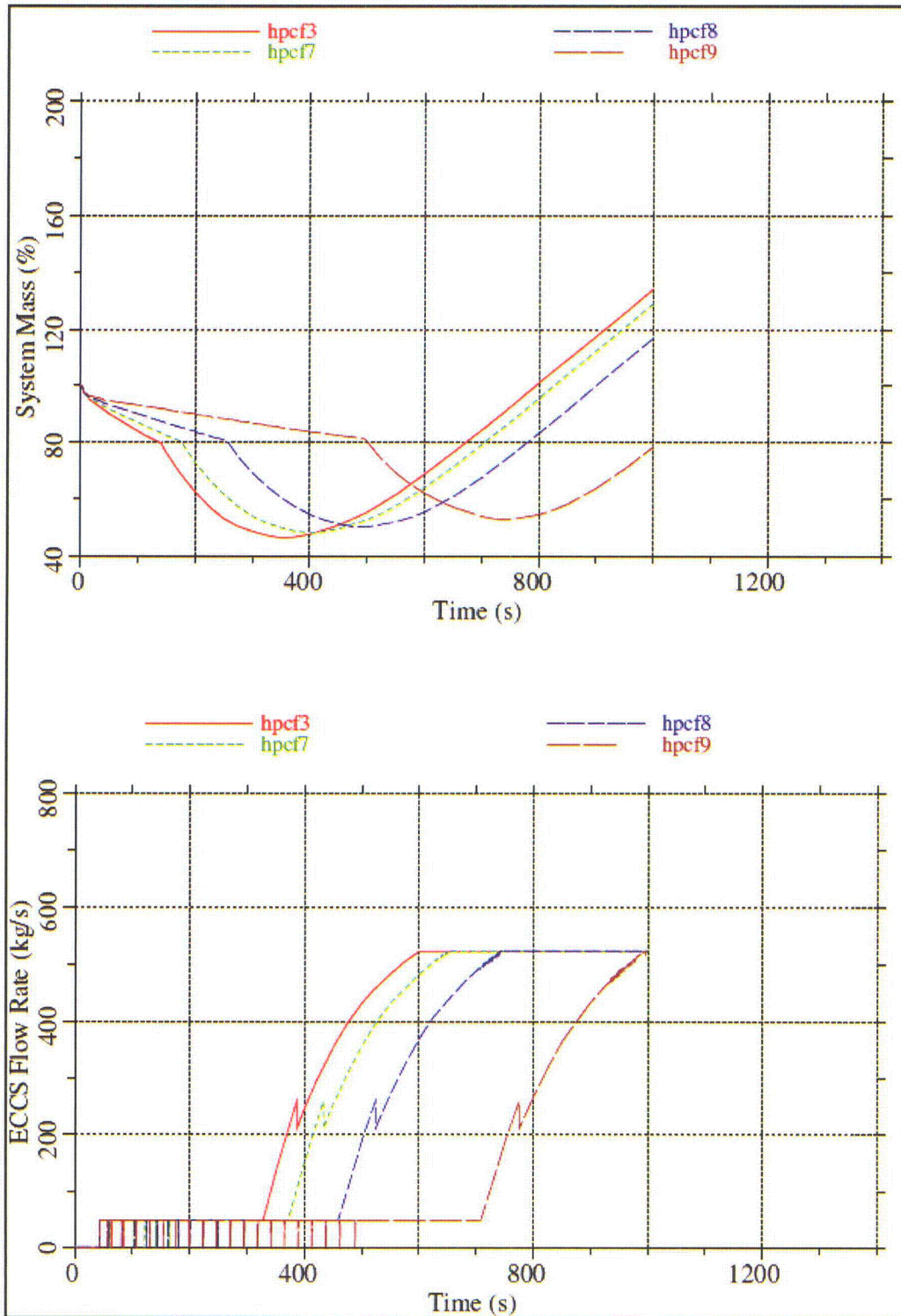


Figure 4-10 Break Size Sensitivity – System Mass and ECCS Flow Rate

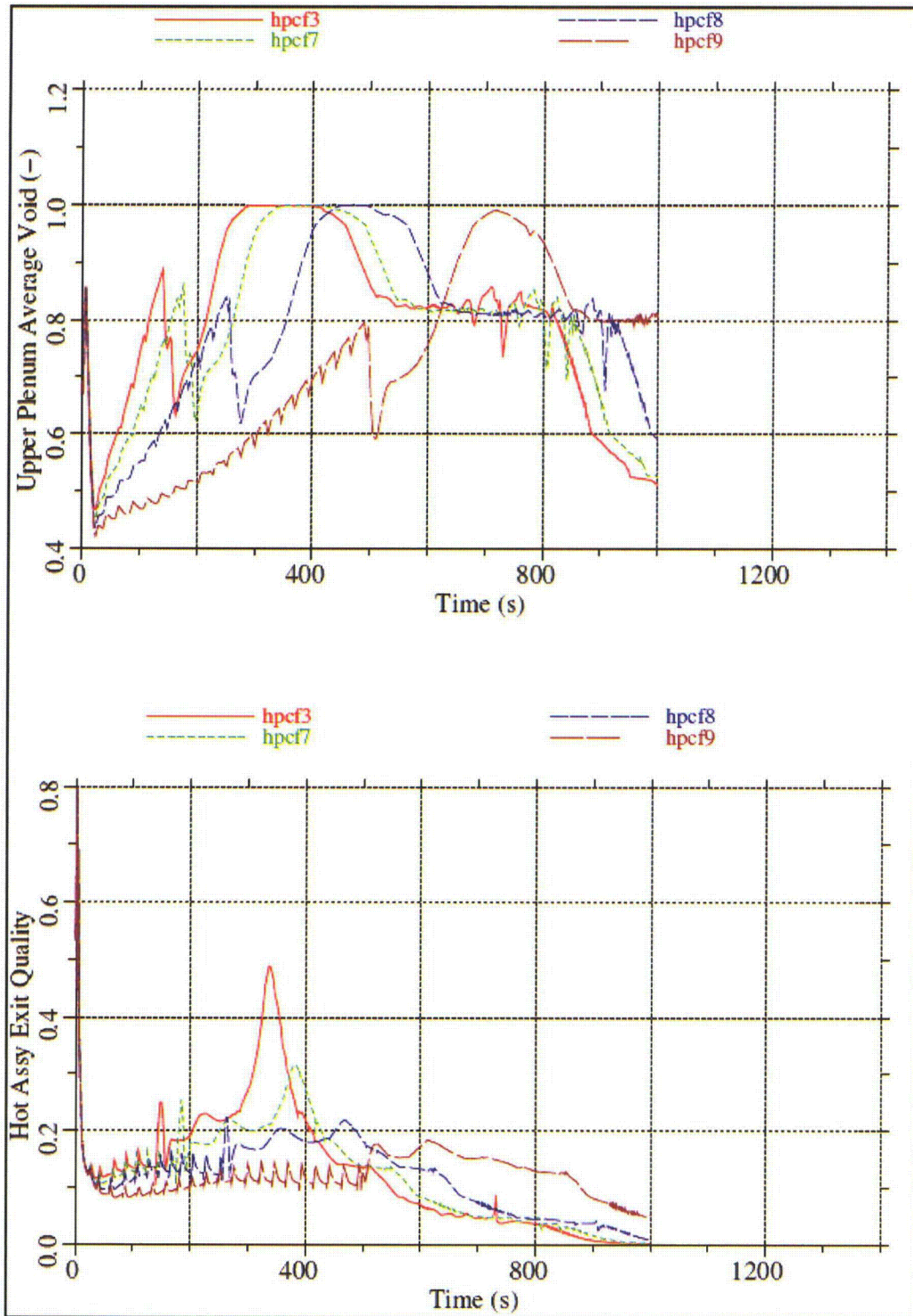


Figure 4-11 Break Size Sensitivity – Upper Plenum Void and Hot Assembly Exit Quality

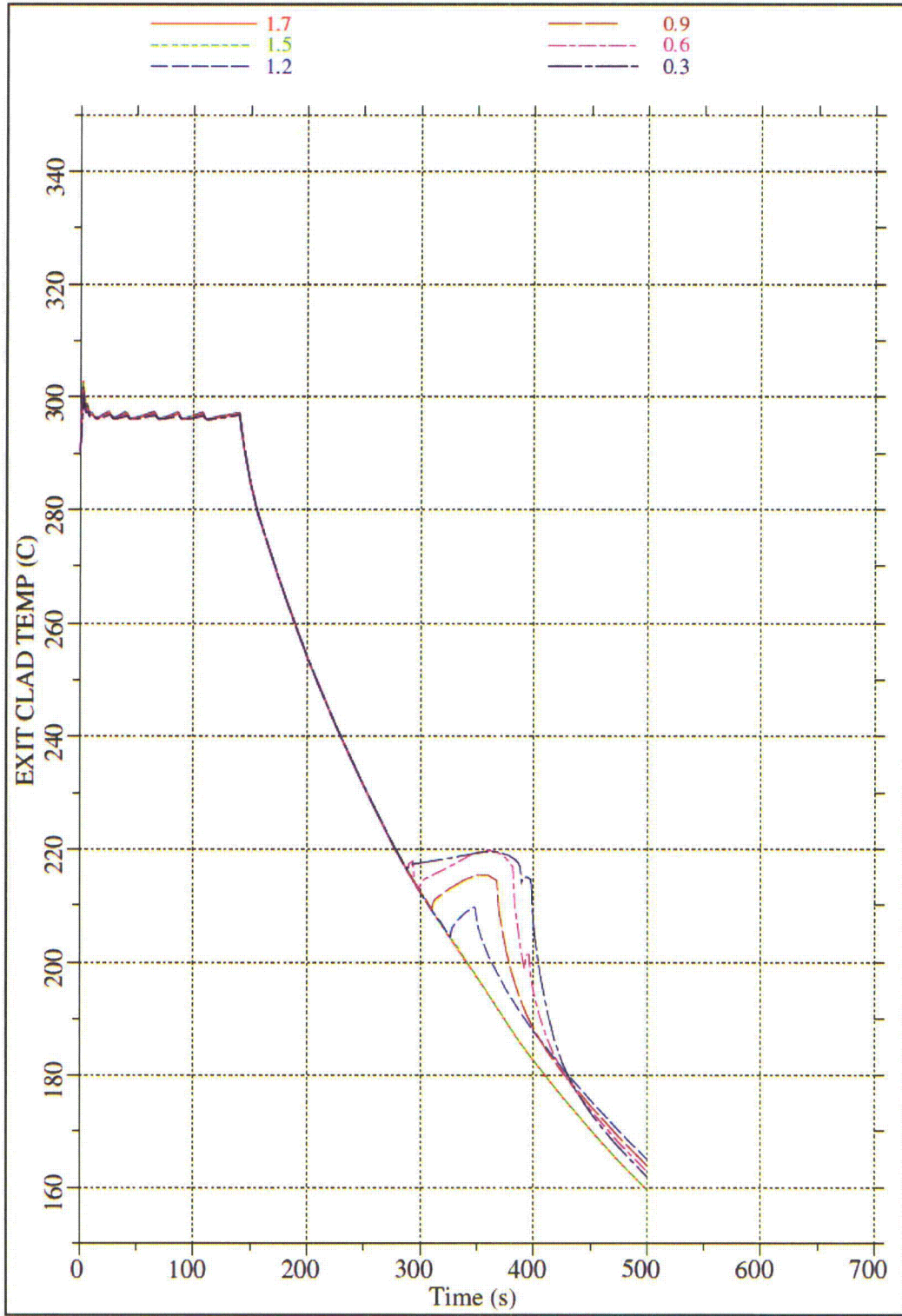


Figure 4-12 Assembly Power Sensitivity – Exit Cladding Temperature vs. Channel Peaking Factor

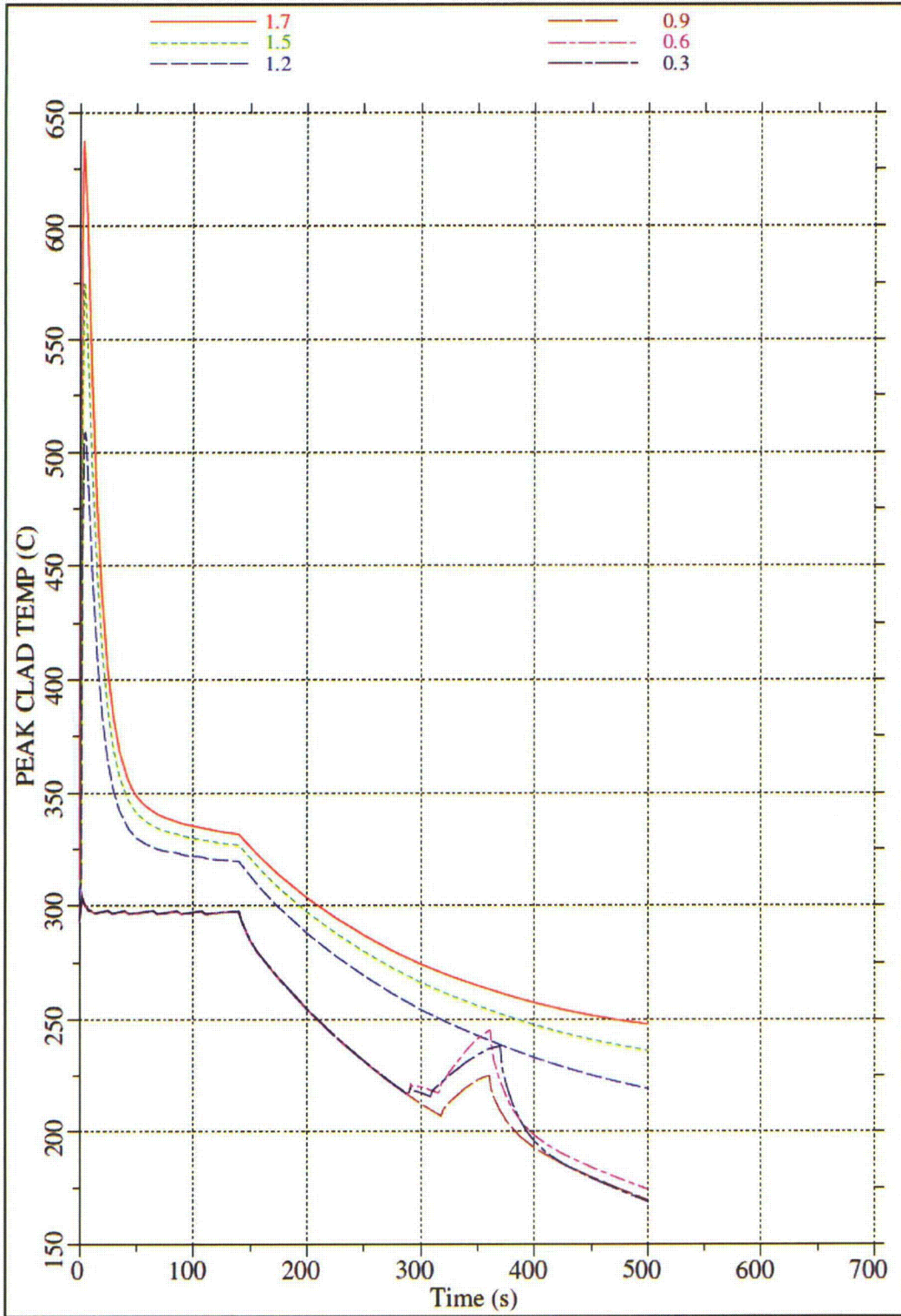


Figure 4-13 Assembly Power Sensitivity – GOBLIN PCT vs. Channel Peaking Factor

4.5.2 Main Steam Line Break (MSLB)

There are four main steam lines that attach to the reactor pressure vessel (RPV) at an elevation just above the bottom of the steam dryer. Each steam line nozzle has an integral flow restrictor, which limits the steam flow in the event of a steam line rupture. Each steam line can be isolated from the turbine by closure of the two MSIVs in each line. One MSIV is located inside the drywell; the other MSIV is located outside the drywell. In addition to the MSIVs, there are TCVs and TSVs between the steam header and the turbine. These valves can also isolate the steam lines from the turbine following a loss of electrical load. A main steam line break inside containment is a result of a break in one of the steam lines between the RPV and the first MSIV.

For a large steam line break coincident with loss of off-site power, the steam lines would be isolated from the turbine by fast-closure of the TCVs. Steam from the RPV would flow through the broken steam line directly to the break and from the intact steam lines through the steam header and back into the drywell via the broken steam line. The flow from the intact steam lines would continue until the MSIVs in the broken steam line close. As shown in Figure 4-14, once the MSIVs are closed, the break flow is only from the RPV through the broken line.

The MSIV closure is actuated by either the LWL-1.5 signal or the high steam flow signal. For large steam line breaks, the high steam flow signal would occur almost instantly. For small steam line breaks, the MSIVs would isolate on a LWL-1.5 signal.

The limiting single active failure that results in the least injection capability is the failure of the EDG that powers a HPCF pump and a LPFL pump with the steam line break located in the line that feeds the RCIC turbine. This results in the following available equipment:

1 HPCF + 2 LPFL + 8 ADS

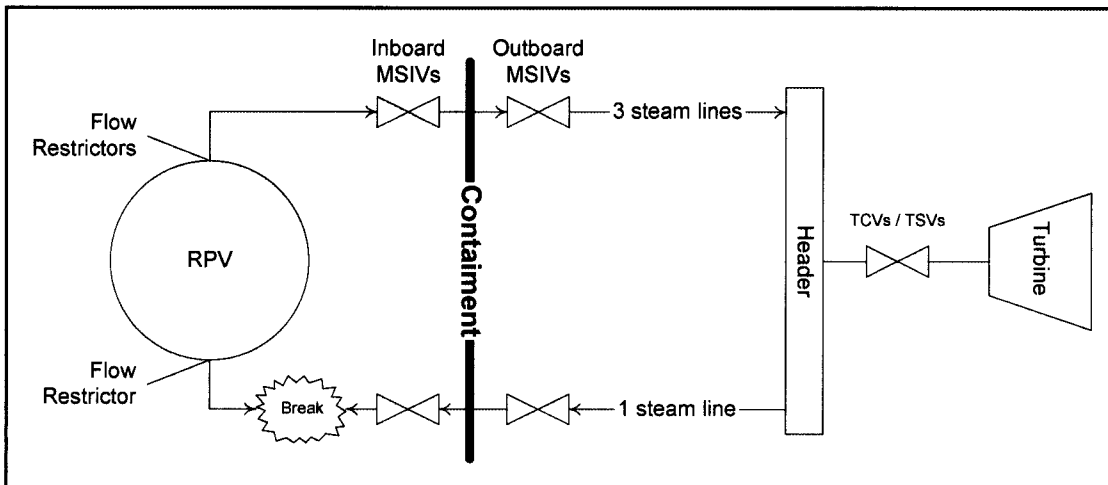


Figure 4-14 Schematic of Steam Line Break inside Containment

4.5.2.1 Main Steam Line Break Results

Four cases were run with the power in the hot assembly set to simulate a nodal power where the hot rod would be at the TMOL. As shown in Table 4-3, the variation in PCT and minimum mass were small.

| Case | Core Flow | Break Location | Break Size⁽¹⁾ | Steam Line Isolation | PCT (GOBLIN) | Minimum Mass |
|-------------|------------------|-----------------------|---------------------------------|-----------------------------|---------------------|---------------------|
| mslb6 | 90% | RCIC side | 200% | TCV fast closure | 657°C | 164.1 E3 kg |
| mslb6a | 111% | RCIC side | 200% | TCV fast closure | 648°C | 162.6 E3 kg |
| mslb7 | 90% | RCIC side | 150% | TCV fast closure | 654°C | 164.1 E3 kg |
| mslb8 | 90% | RCIC side | 100% | TCV fast closure | 656°C | 164.1 E3 kg |

Note:
1. Steam line breaks are simulated as double-ended breaks. However, MSIVs isolate steam line side of the break.

4.5.2.2 Sensitivity Studies

Core Flow Rate

Cases mslb6 and mslb6a compare the impact of initial core flow rate on steam line break results. As shown in Table 4-3, the case with the lowest initial core flow rate had the highest PCT.

Figure 4-15 compares the dome pressure and break flow rate responses for cases mslb6 and mslb6a. As shown, the first case depressurizes more rapidly in the first 20 seconds. This is a result of differing break flow during this period of time. In the base case the break flow quality is one until ~ 18 seconds. In the second, higher core flow, case the break flow quality transitions to a two-phase mixture at ~ 4 s. This causes the different depressurization rates mentioned above. As a result of the additional mass in the core, the break flow transitions from steam to a two-phase mixture sooner in the second case.

Figure 4-16 compares the system mass and ECCS flow rate for the two cases. As shown, the ECCS actuation for the second case, mslb6a, is slightly sooner. In this case the higher break flow compensated for the higher initial system mass resulting in an earlier actuation of the ECCS pumps. However, the minimum inventories were nearly identical.

Figure 4-17 compares the GOBLIN PCTs. As shown, the base case had the highest PCT. The higher initial core flow rate in the second case provides additional margin to dryout. As a result, dryout occurs later in the second case and the PCT is lower.

Figure 4-18 compares the upper plenum average void fraction and hot assembly exit quality. As shown, a two phase mixture exists in the upper plenum and there is a two-phase mixture exiting the hot assembly throughout the transient.

Break Size

Cases mslb6, mslb7 and mslb8 simulate double-ended breaks of the steam line between the reactor pressure vessel and the first MSIV. The first case, mslb6, represents a full double-ended rupture of the steam line. However, the vessel side of the break is limited in flow area because of the integral flow restrictor which has a flow area that is approximately 30% of the main steam line flow area. The second case represents a 75% steam line break. In this case, the vessel side of the break continues to be limited by the flow restrictor, but the turbine side of the break is reduced in flow area below that of the combined flow area of the three intact steam line flow restrictors. The third case represents a 50% steam line break. In this case, the vessel side of the break continues to be limited by the flow restrictor, but the steam line side of the break would be further reduced. In all cases, the MSIV closure signal was generated by the high steam flow signal due to the flow out of the break.

As shown in Figure 4-19, the break flow from the steam line side decreases with decreasing break size, but the effect is small due to closure of the MSIVs. As shown in Figure 4-20 and Figure 4-21, the effect of changing break size on system pressure, system mass, and PCT is also minimal.

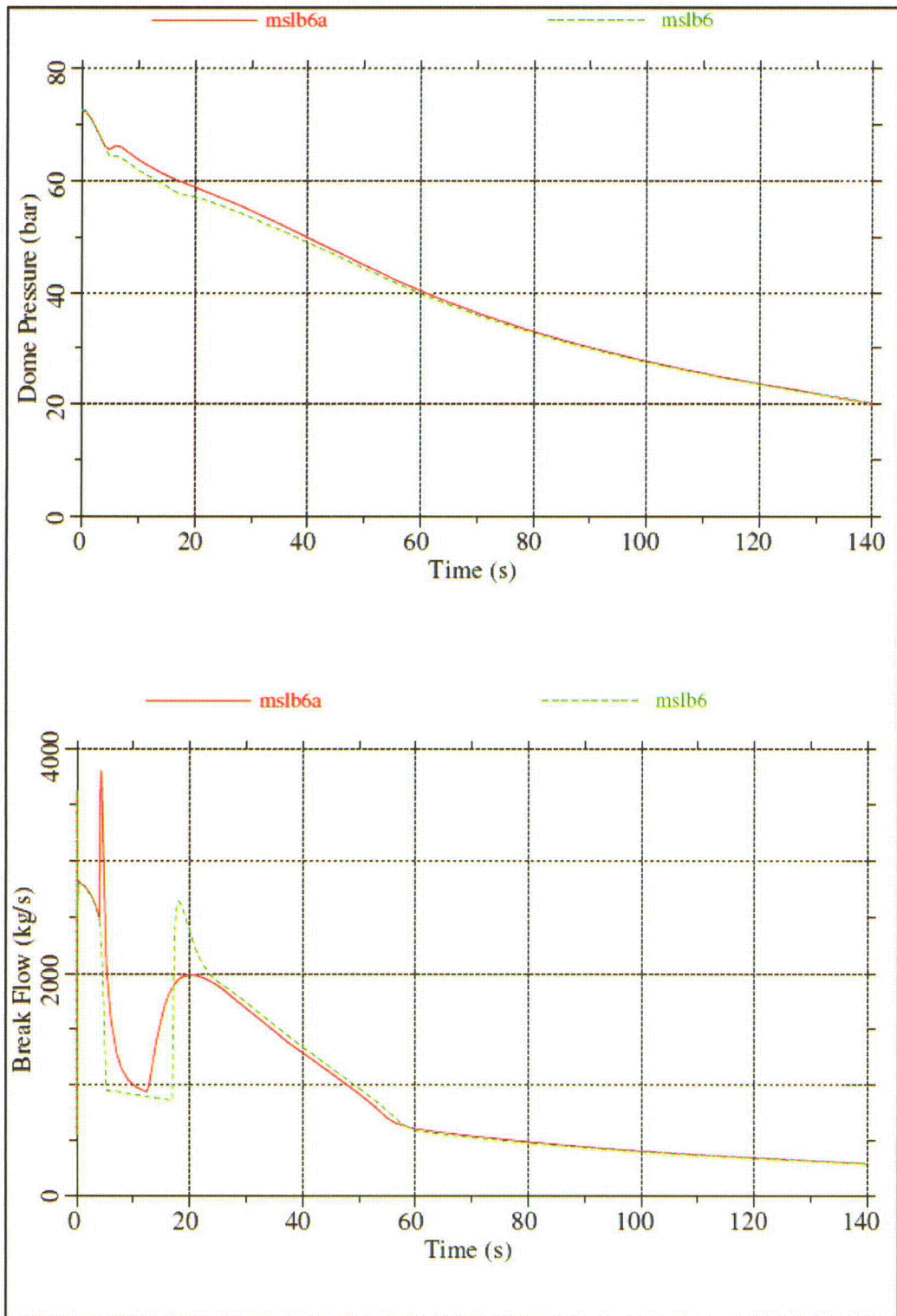


Figure 4-15 Core Flow Rate Sensitivity – Dome Pressure and Break Flow Rate

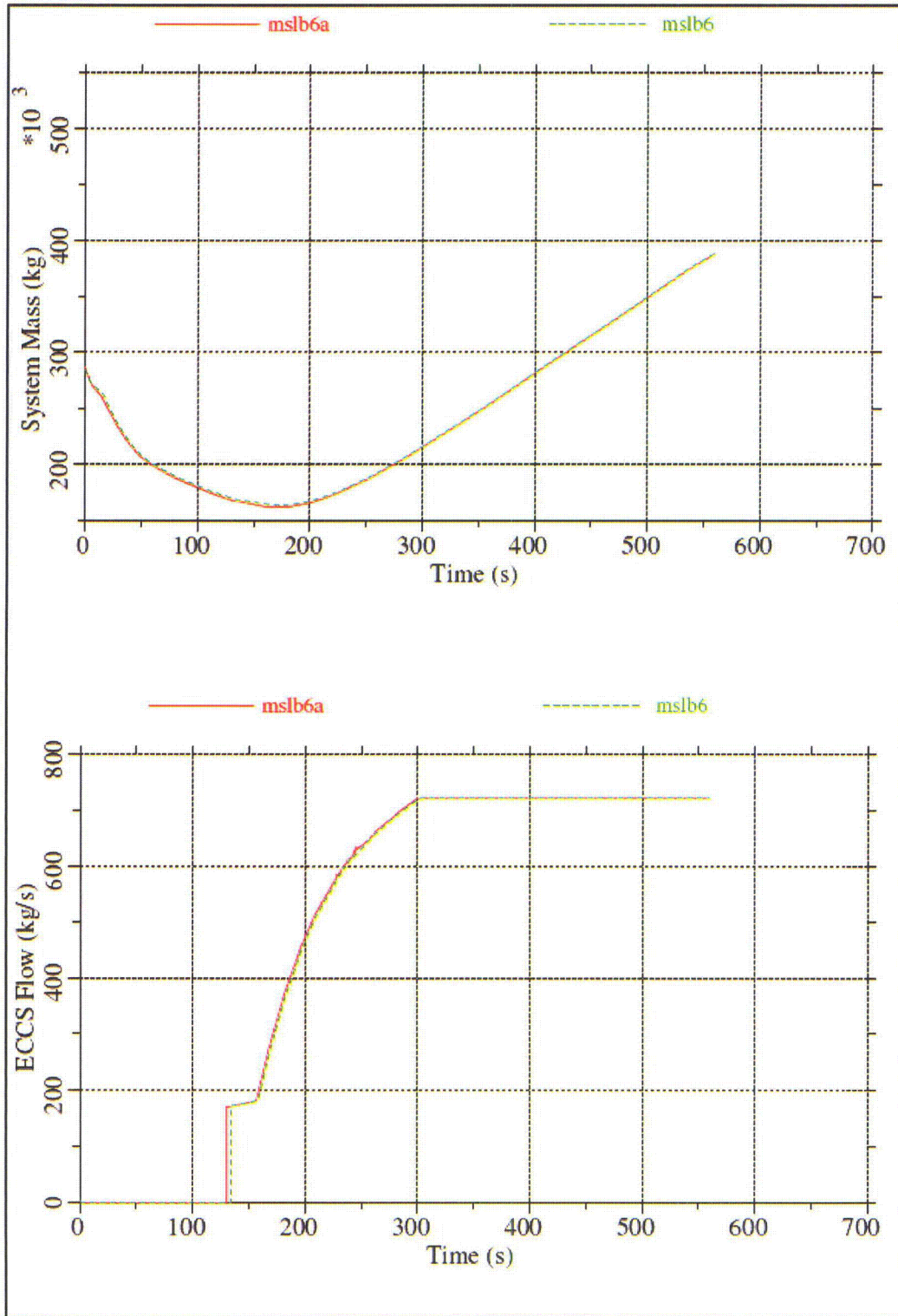


Figure 4-16 Core Flow Rate Sensitivity – System Mass and ECCS Flow Rate

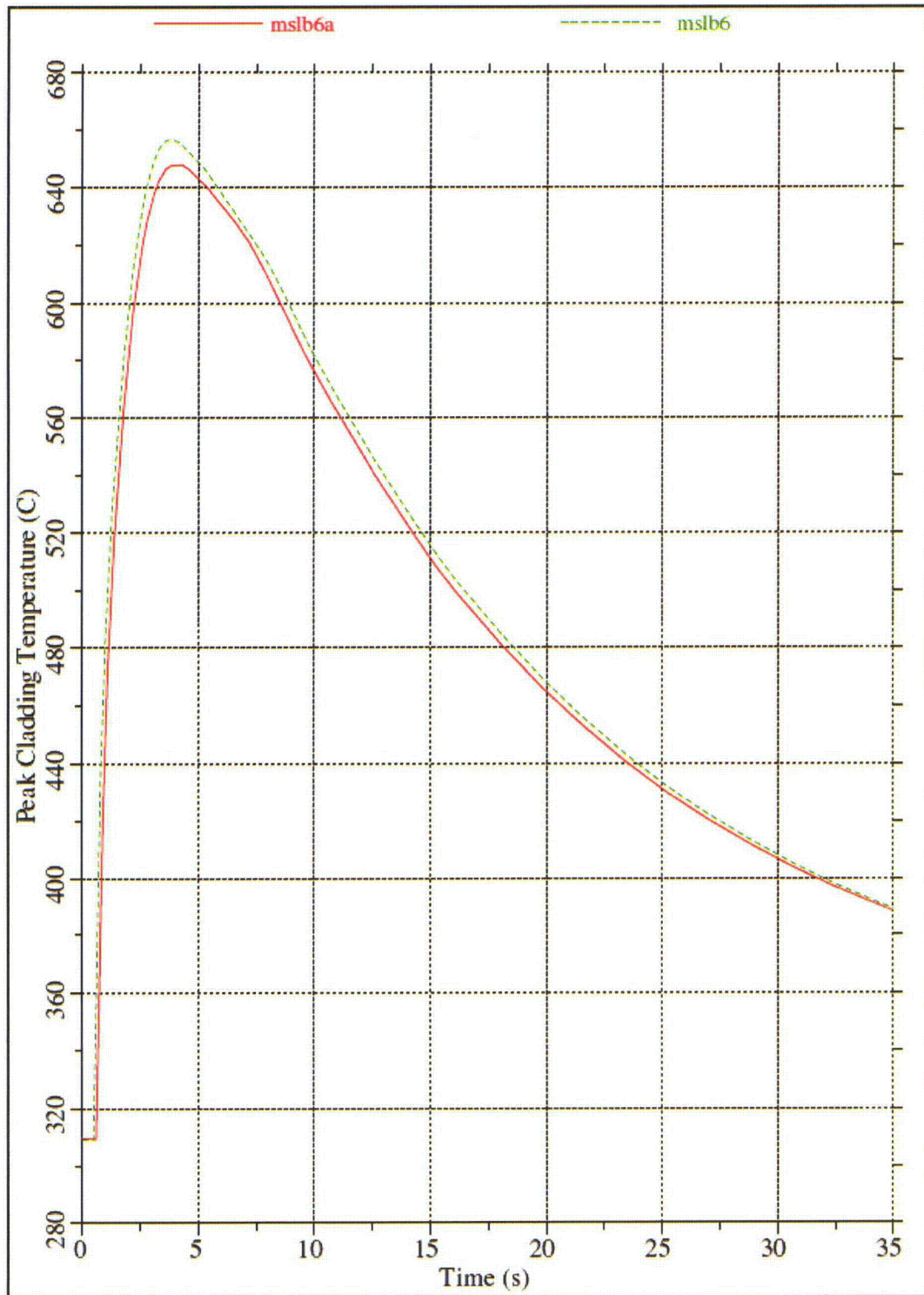


Figure 4-17 Core Flow Rate Sensitivity – GOBLIN PCTs

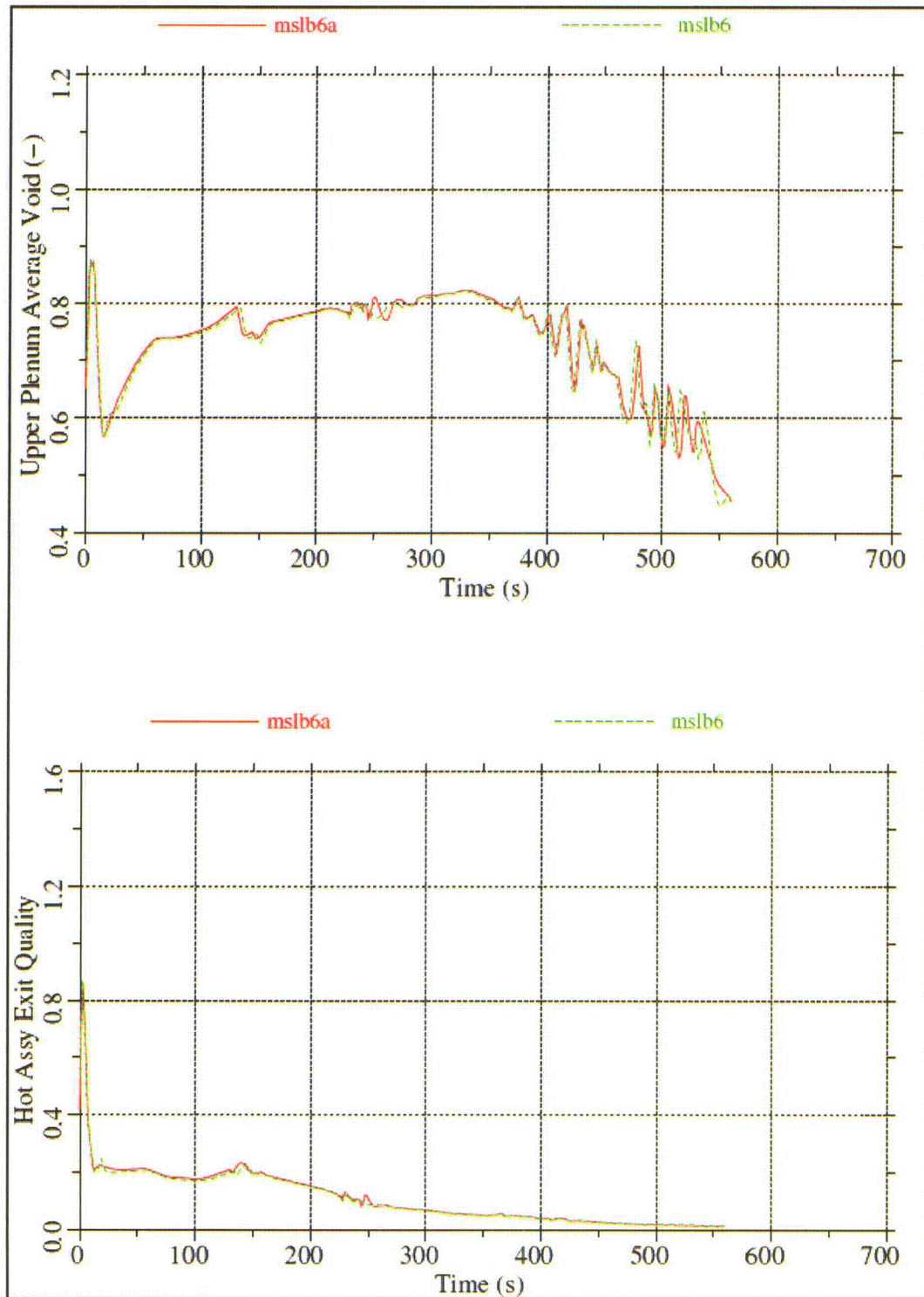


Figure 4-18 Core Flow Rate Sensitivity – Upper Plenum Void and Hot Assembly Exit Quality

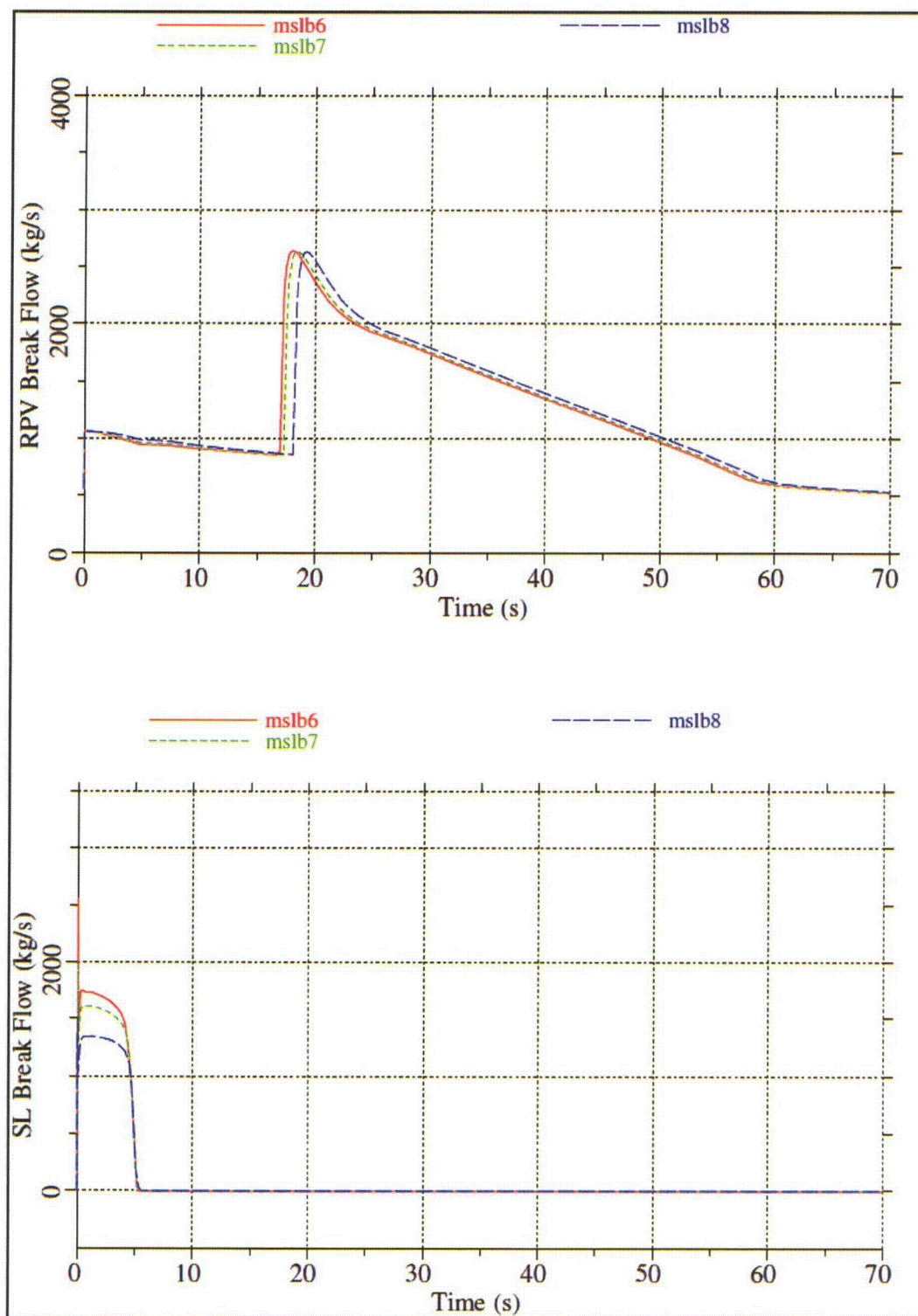


Figure 4-19 Break Size Sensitivity – Break Flow Rates

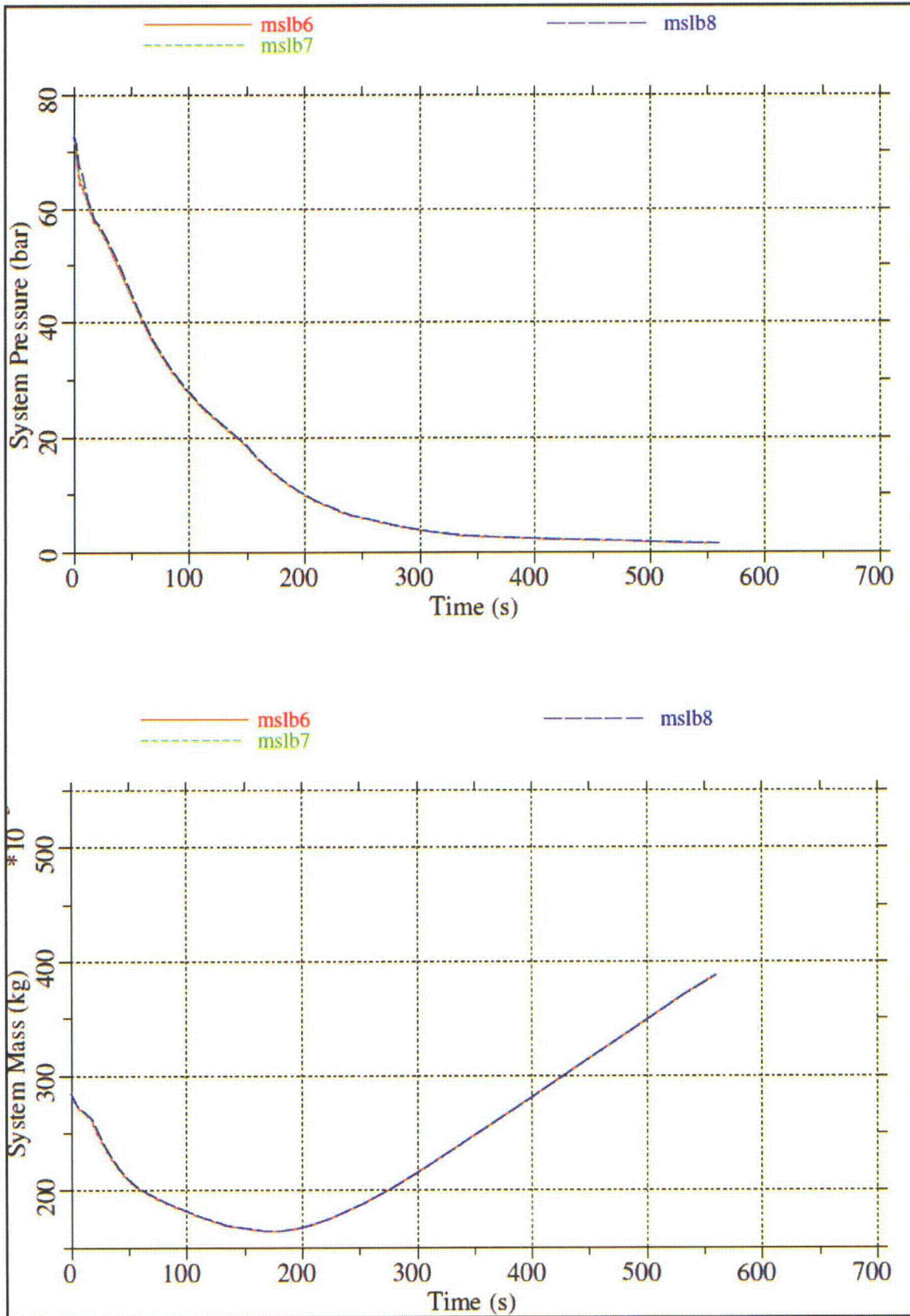


Figure 4-20 Break Size Sensitivity – Dome Pressure and System Mass

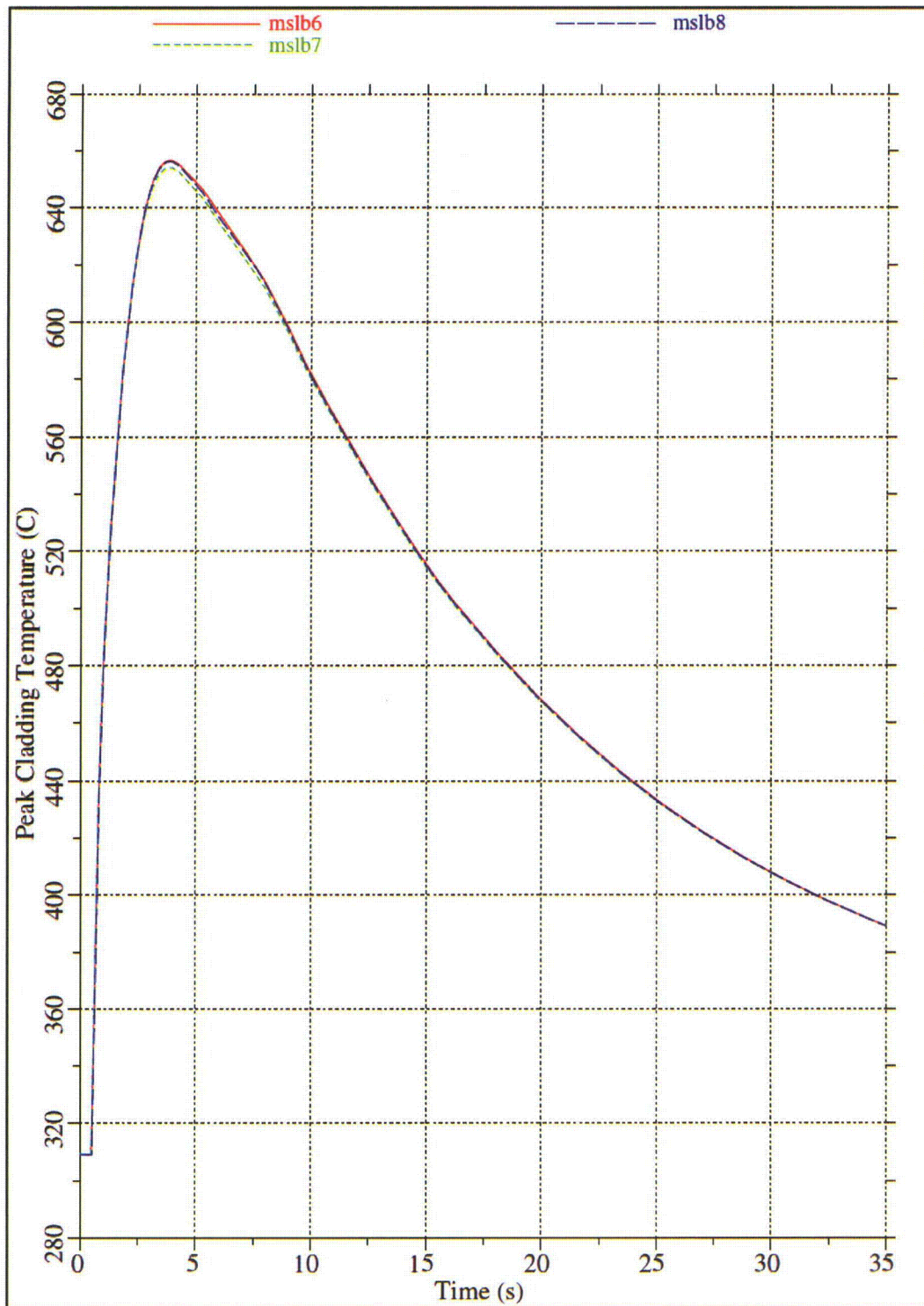


Figure 4-21 Break Size Sensitivity – GOBLIN PCTs

4.5.3 Feedwater Line Break (FWLB)

There are two feedwater lines that enter the drywell. Each feedwater line passes through two check valves, one inside the drywell and one outside the drywell. These two feedwater lines are connected to a common feedwater line outside the drywell. Inside the drywell each feedwater line branches into three lines that penetrate the RPV and connect to a sparger inside the downcomer annulus. The six feedwater spargers distribute feedwater in the annulus at an elevation corresponding to the top of the shroud dome. The three feedwater spargers associated with a single feedwater line penetrating the drywell have []^{a,c} nozzles to distribute the feedwater in the annulus.

The feedwater line break inside the containment is postulated to occur between the RPV and the first check valve, as shown in Figure 4-22. For a complete rupture of the feedwater line inside the drywell, the flow would be restricted by the available flow area through the []^{a,c} nozzles connected to the affected sparger. The check valves on the unaffected feedwater line prevents the loss of coolant through the other line.

Since one train of LPFL injects in one feedwater line and RCIC injects in the other feedwater line, the break will disable one of those systems. Failure of one of the EDGs powering a HPCF pump and a LPFL pump will result in the following equipment available:

RCIC side break: 1 HPCF + 2 LPFL + 8 ADS

LPFL side break: 1 RCIC + 1 HPCF + 1 LPFL + 8 ADS

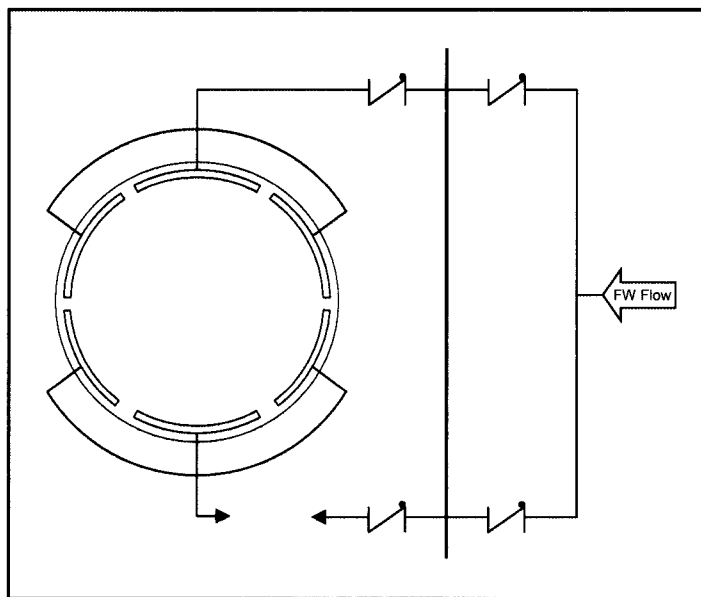


Figure 4-22 Schematic of Feedwater Line Break

4.5.3.1 Feedwater Line Break Results

Seven cases were run with the power in the hot assembly set to simulate a nodal power so that the hot rod would be at the TMOL. Table 4-4 summarizes the results of those cases. As shown, the variations in PCT are small when the steam line is isolated in the same way. Also, the variation in minimum system mass depends mainly on break size.

| Case | Core Flow | Break Location | Break Size | Steam Line Isolation | PCT (GOBLIN) | Minimum Mass |
|-------------|------------------|-----------------------|-------------------|-----------------------------|---------------------|---------------------|
| fwlb3 | 90% | RCIC side | 100% | TCV fast closure | 708°C | 126.5 E3 kg |
| fwlb4 | 111% | RCIC side | 100% | TCV fast closure | 684°C | 123.5 E3 kg |
| fwlb5 | 90% | RCIC side | 100% | Pressure Regulator | 661°C | 126.0 E3 kg |
| fwlb6 | 90% | RHR side | 100% | TCV fast closure | 708°C | 125.9 E3 kg |
| fwlb7 | 90% | RCIC side | 75% | TCV fast closure | 705°C | 136.9 E3 kg |
| fwlb8 | 90% | RCIC side | 50% | TCV fast closure | 707°C | 148.4 E3 kg |
| fwlb9 | 90% | RCIC side | 25% | TCV fast closure | 710°C | 215.6 E3 kg |

4.5.3.2 Sensitivity Studies

Core Flow Rate

Cases fwlb3 and fwlb4 compare the impact of core flow rate on the system and hot assembly responses. As shown in Table 4-4 and Figure 4-23, the GOBLIN PCT was lower for the high core flow rate case. Similar to cases described previously, this was caused by a delay in the time of boiling transition due to the higher core flow rate and increased margin to dryout. Table 4-4 also shows that the minimum system inventory was slightly lower in the case with the higher initial core flow rate.

As shown in Figure 4-24, the lower minimum system inventory was caused by a delay in HPCF injection due to the different level response resulting in later HPCF actuation.

Figure 4-25 shows that there is significant liquid in the upper plenum and that the core is cooled by a two-phase mixture throughout the transient in both cases.

Steam Line Isolation

Cases fwlb3 and fwlb5 compare the impact of steam line isolation on the system and hot assembly responses. As shown in Figure 4-26, the dome pressure increases initially when the steam line is isolated by TCV fast closure. Node 17 exhibited the highest PCT in both cases and, as shown, case fwlb3 has a larger PCT than case fwlb5. The difference is due to the initial reactor power transient prior to reactor scram (i.e., the increasing pressure in case fwlb3 results in a slower increase in average void).

As shown in Figure 4-27, the initial break flow is higher when the pressure regulator is used to isolate the steam line. This is due to the additional inventory lost from the steam line until the break is finally isolated. As a result, the minimum inventory for case fwlb5 is slightly less than for case fwlb3.

Break Location

Comparing cases fwlb3 and fwlb6 shows the effect of break location. In the first case the break is located in the feedwater line where the RCIC injects. The limiting single failure of one EDG disables one HPCF pump and one LPFL pump. In the other case, the break is located in the feedwater line where one of the LPFL pumps injects. The limiting single failure of one EDG disables one HPCF and one LPFL pump. The available ECCS systems for these cases are as follows:

fwlb3 – 1 HPCF + 2 LPFL + 8 ADS

fwlb6 – 1 RCIC + 1 HPCF + 1 LPFL + 8 ADS

As shown in Table 4-4, there is no difference in the predicted PCT, since the time of PCT occurs well before ECCS injection. There is a small effect on minimum system inventory caused by the different ECCS pumps that are available. As shown in Figure 4-28, initially there is more injection in the second case, but the injection of 2 LPFL pumps in the first case results in a faster recovery and a slightly higher minimum inventory.

Break Size

Cases fwlb3, fwlb7, fwlb8 and fwlb9 show the sensitivity to break size for feedwater line breaks. As shown in Figure 4-29, the initial system pressure responses were nearly identical because they were affected primarily by the steam line isolation. However, the long term pressure responses were quite different due to the differing break sizes. As shown in Figure 4-30, the PCTs for all cases were nearly the same.

As shown in Figure 4-31, the largest break had the greatest loss of inventory before recovery. The figure also shows that the system did not lose enough inventory for the smallest break (fwlb9) to actuate ADS and one HPCF pump provided enough injection to recover the lost inventory.

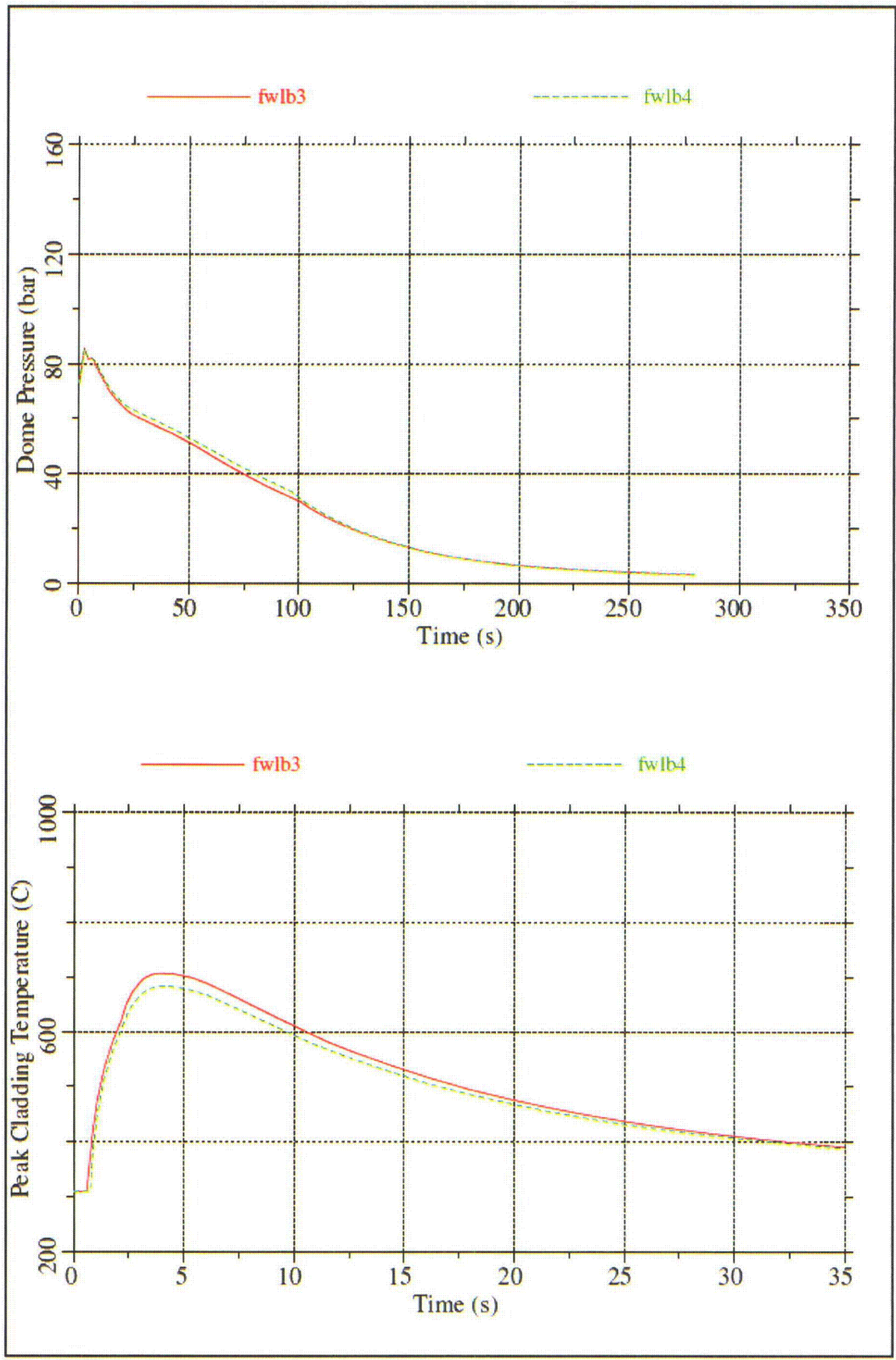


Figure 4-23 Core Flow Rate Sensitivity – Dome Pressure and GOBLIN PCTs

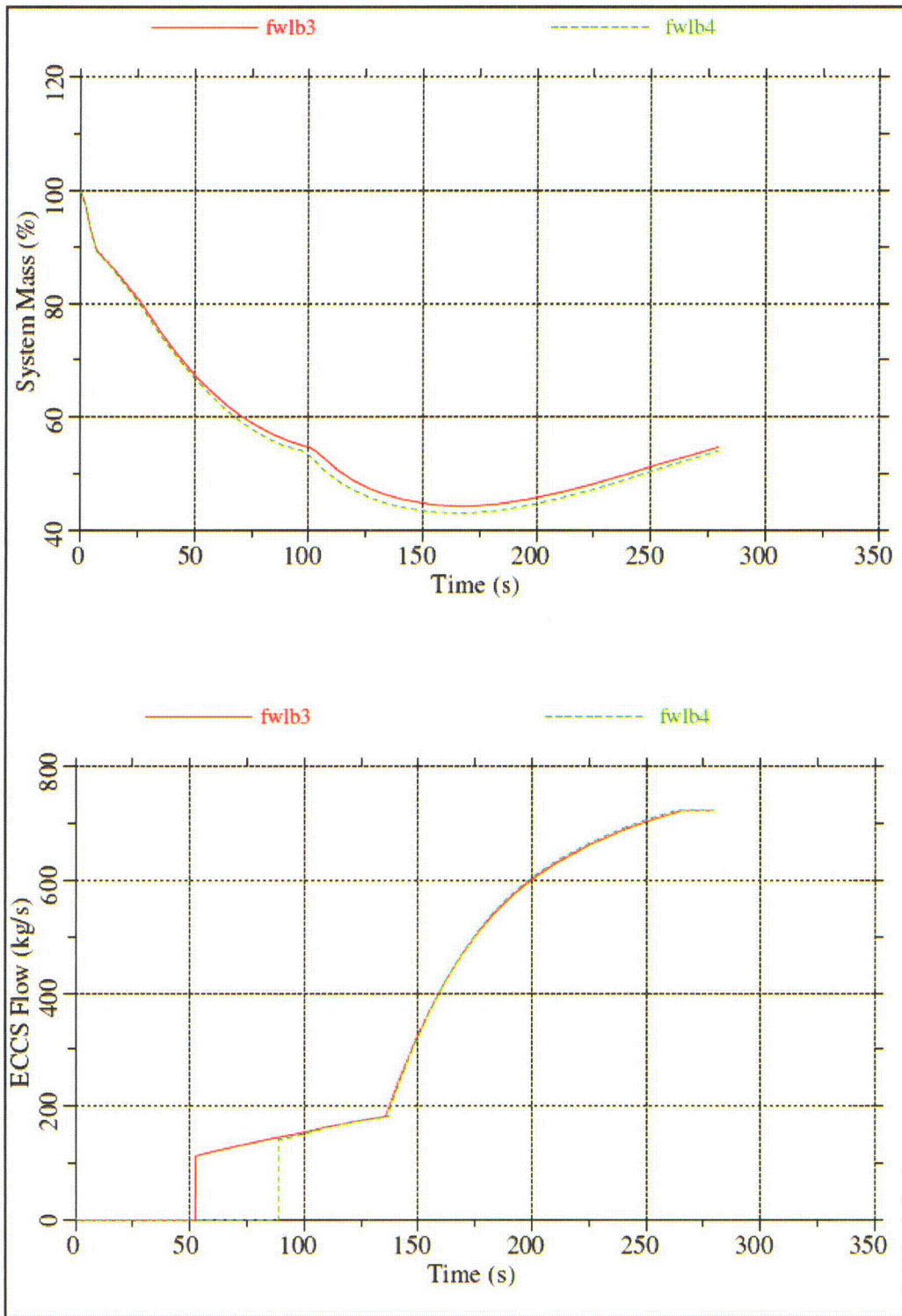


Figure 4-24 Core Flow Rate Sensitivity – System Mass and ECCS Flow Rates

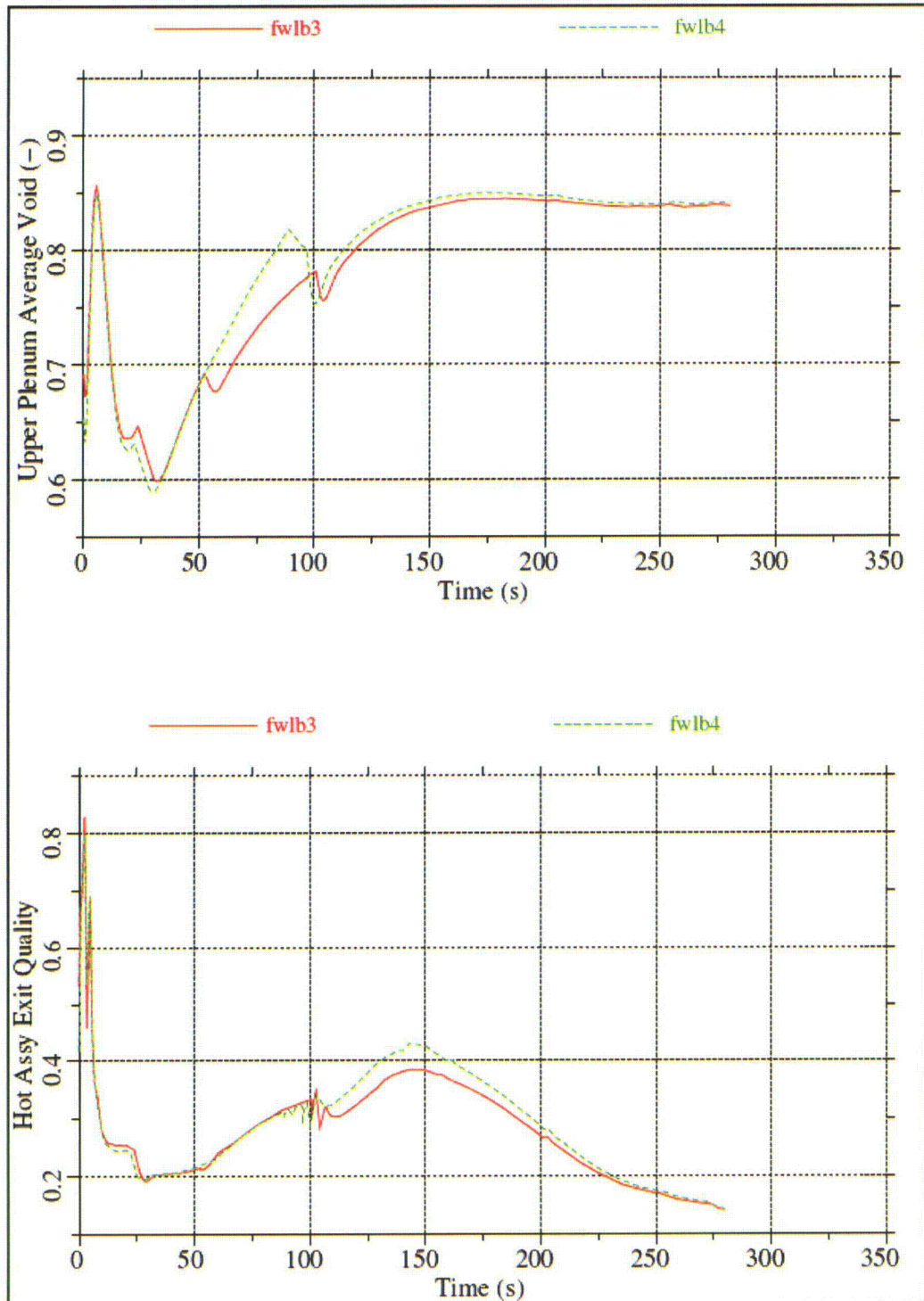


Figure 4-25 Core Flow Rate Sensitivity – Upper Plenum Void and Hot Assembly Exit Quality

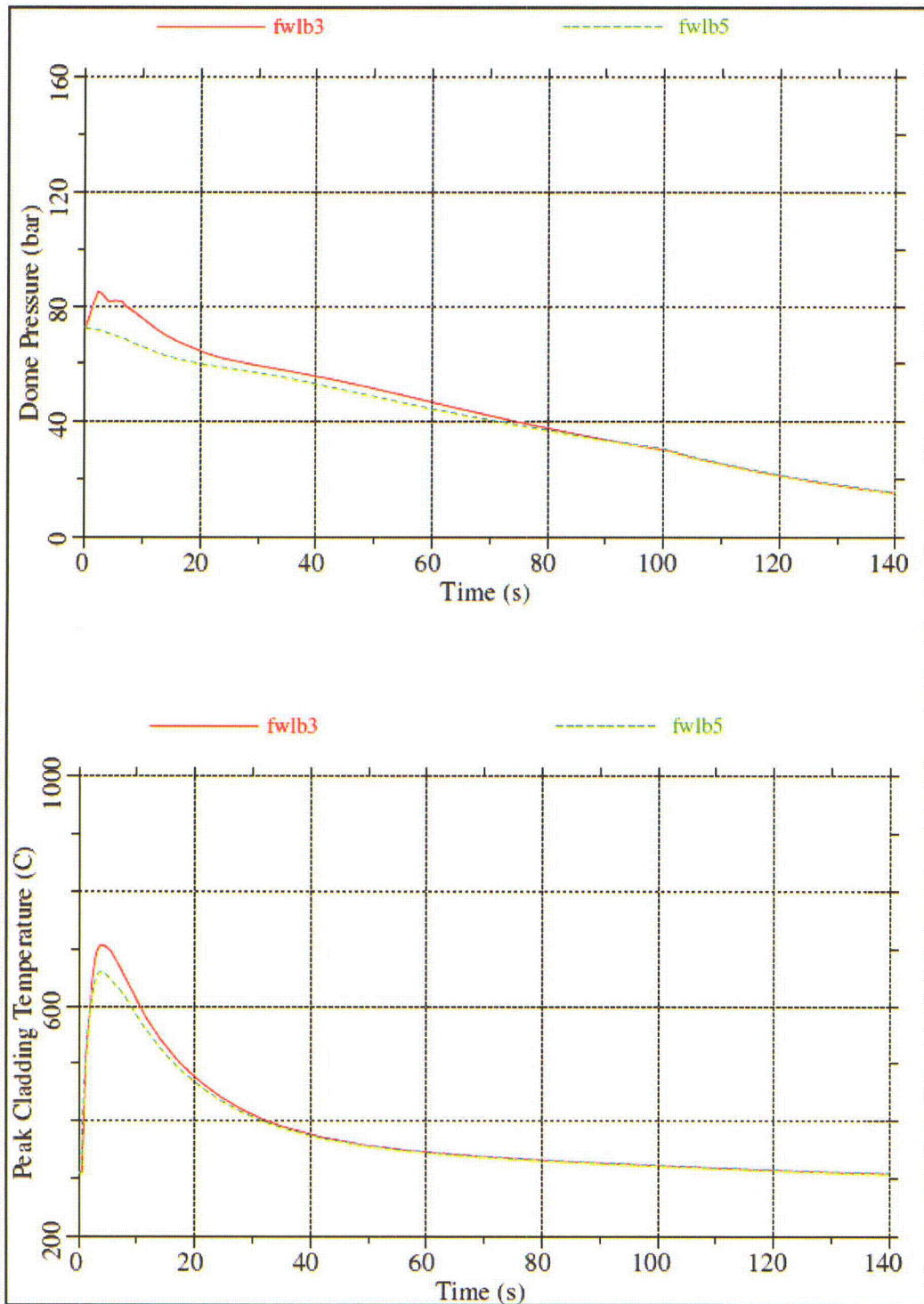


Figure 4-26 Steam Line Isolation Sensitivity – Dome Pressure and GOBLIN PCTs

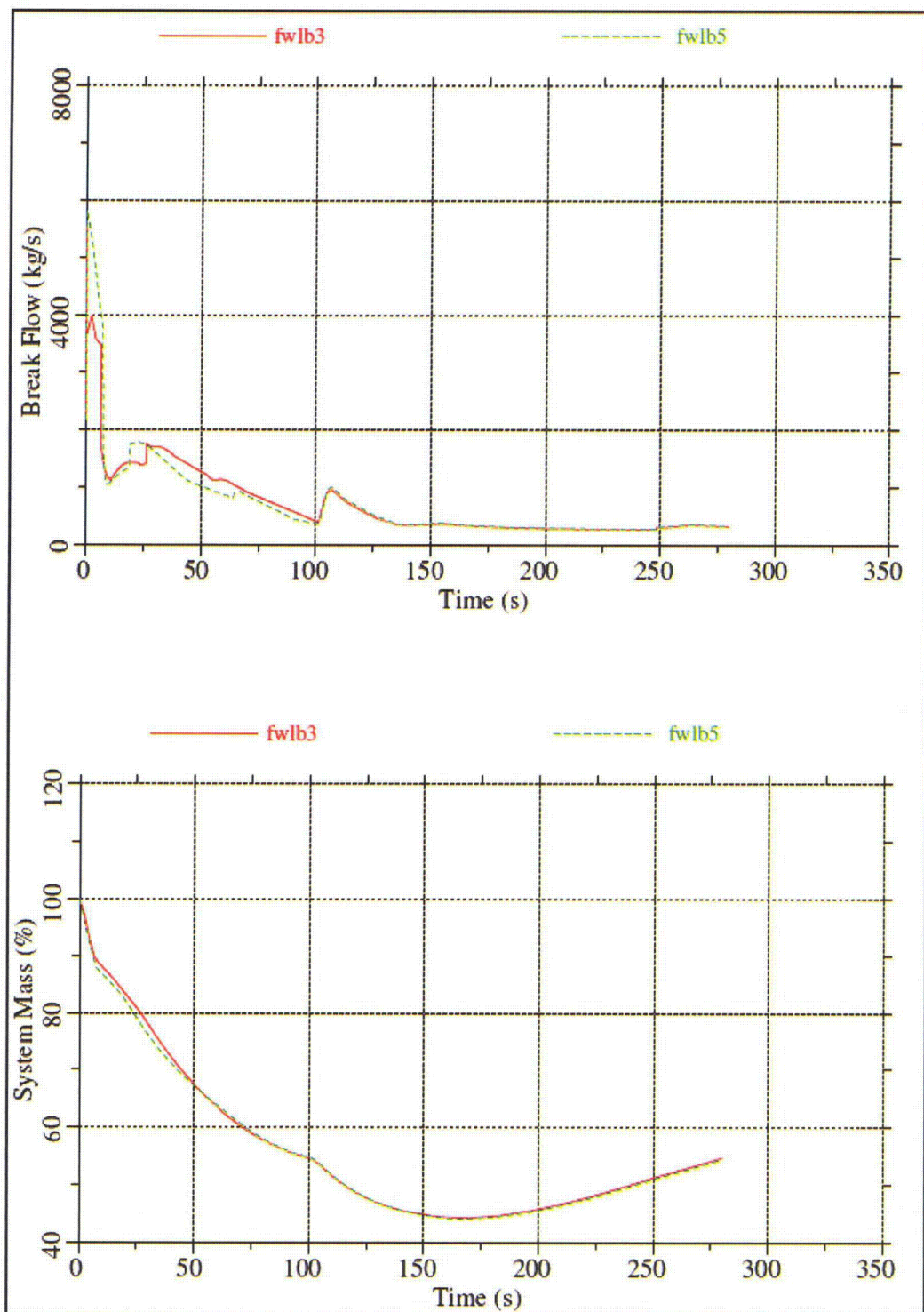


Figure 4-27 Steam Line Isolation Sensitivity – Break Flow Rate and System Mass

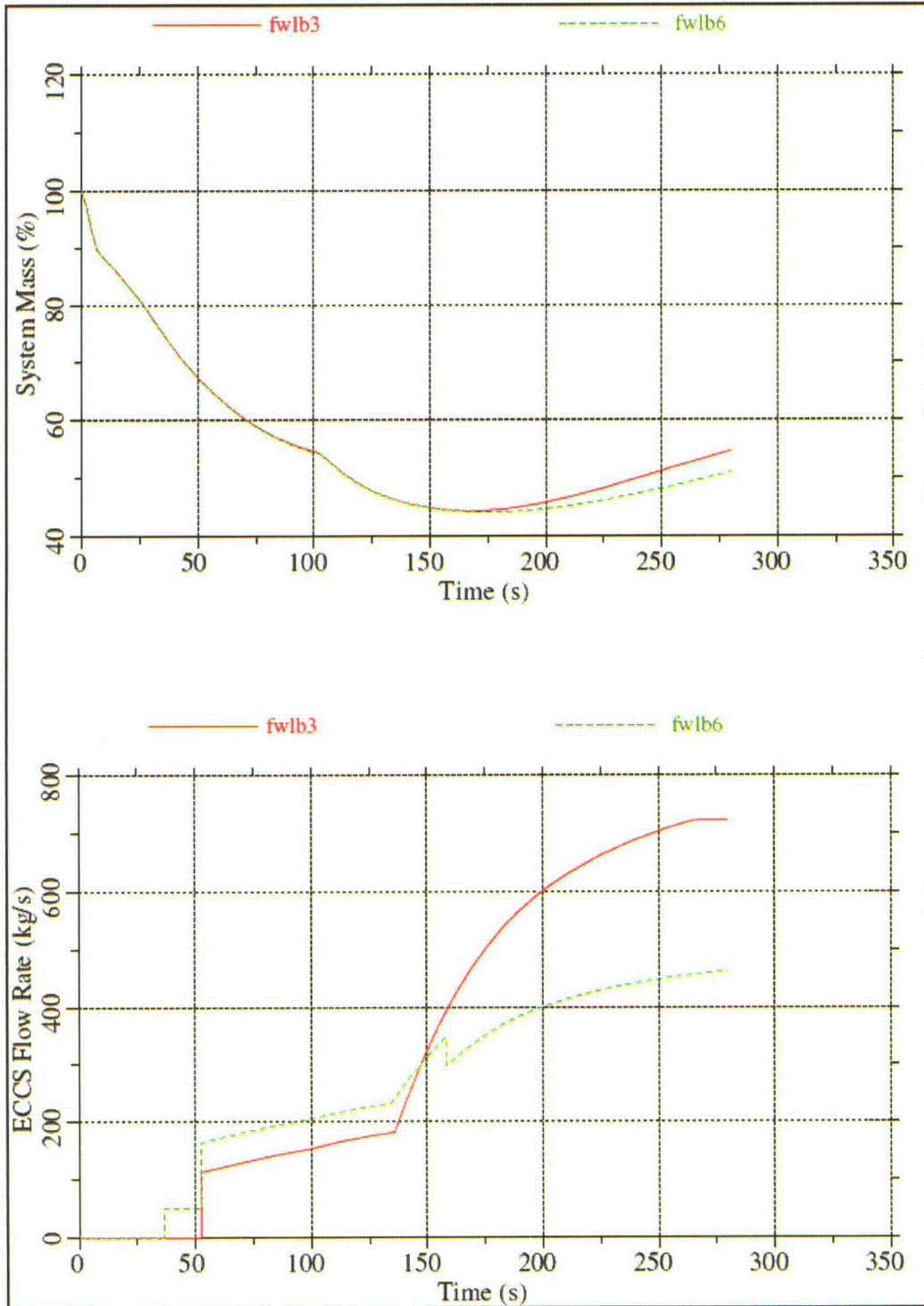


Figure 4-28 Break Location Sensitivity – System Mass and ECCS Flow Rates

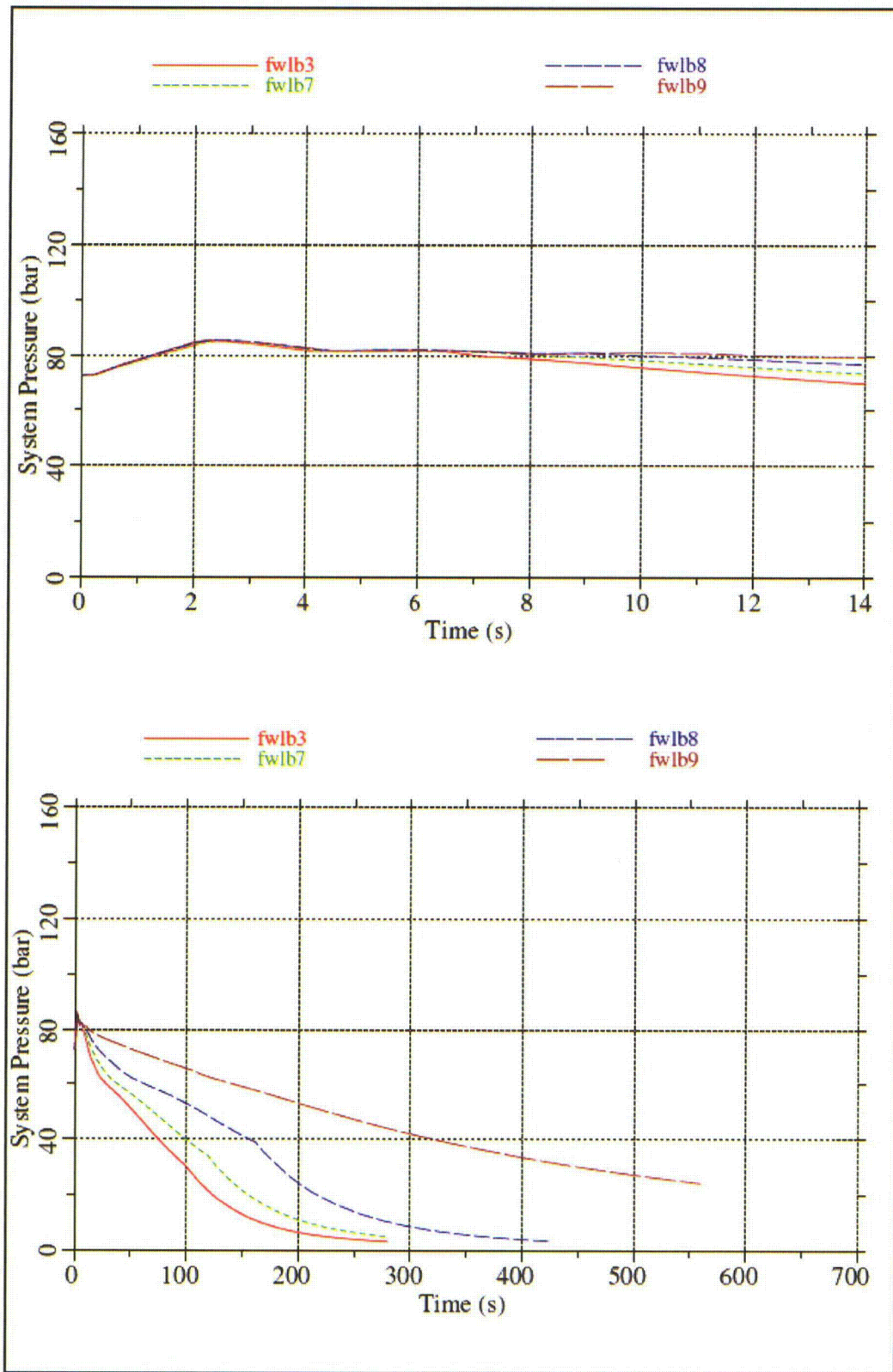


Figure 4-29 Break Size Sensitivity – Dome Pressure (Short-term and Long-term)

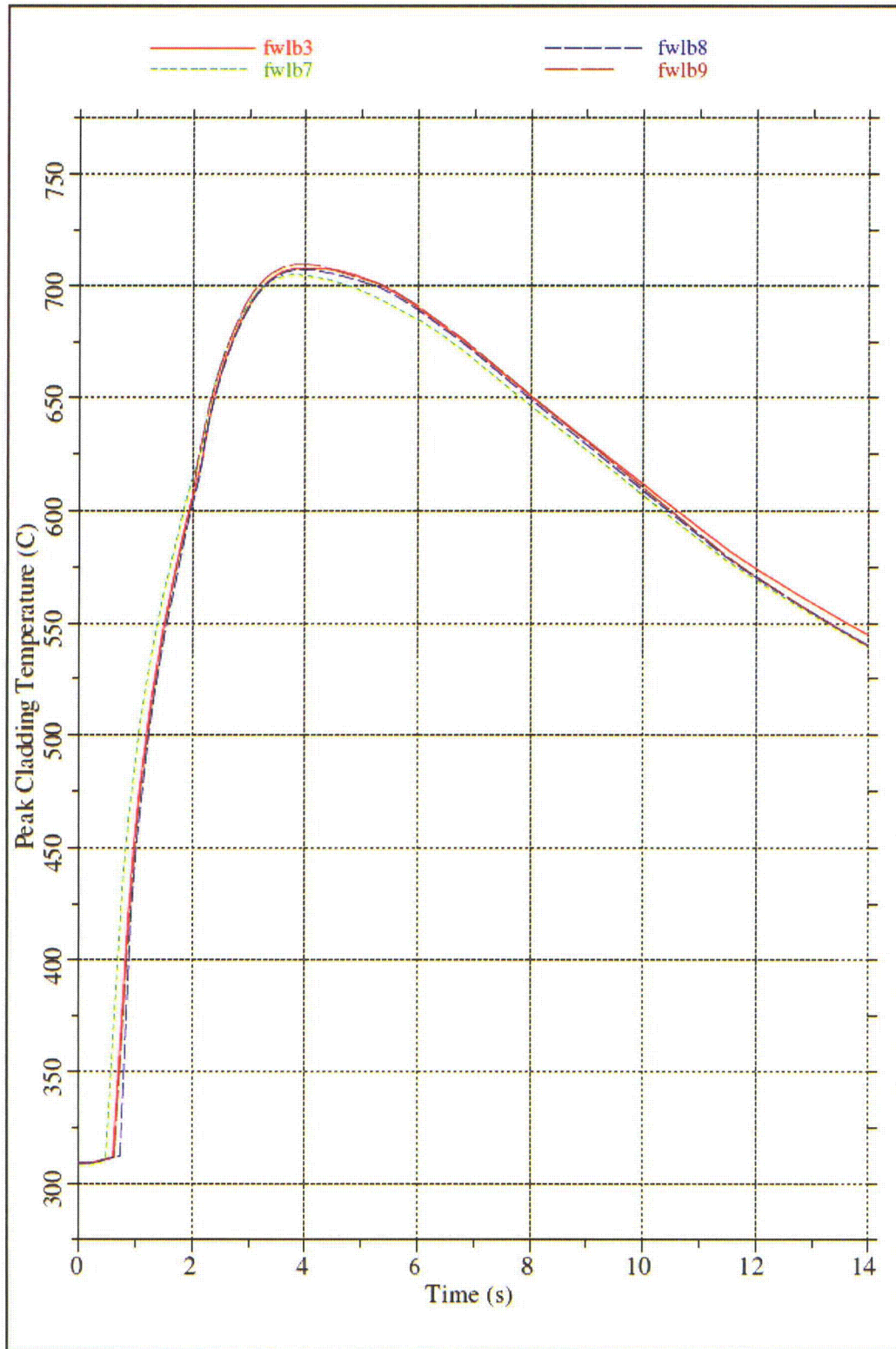


Figure 4-30 Break Size Sensitivity – GOBLIN PCTs

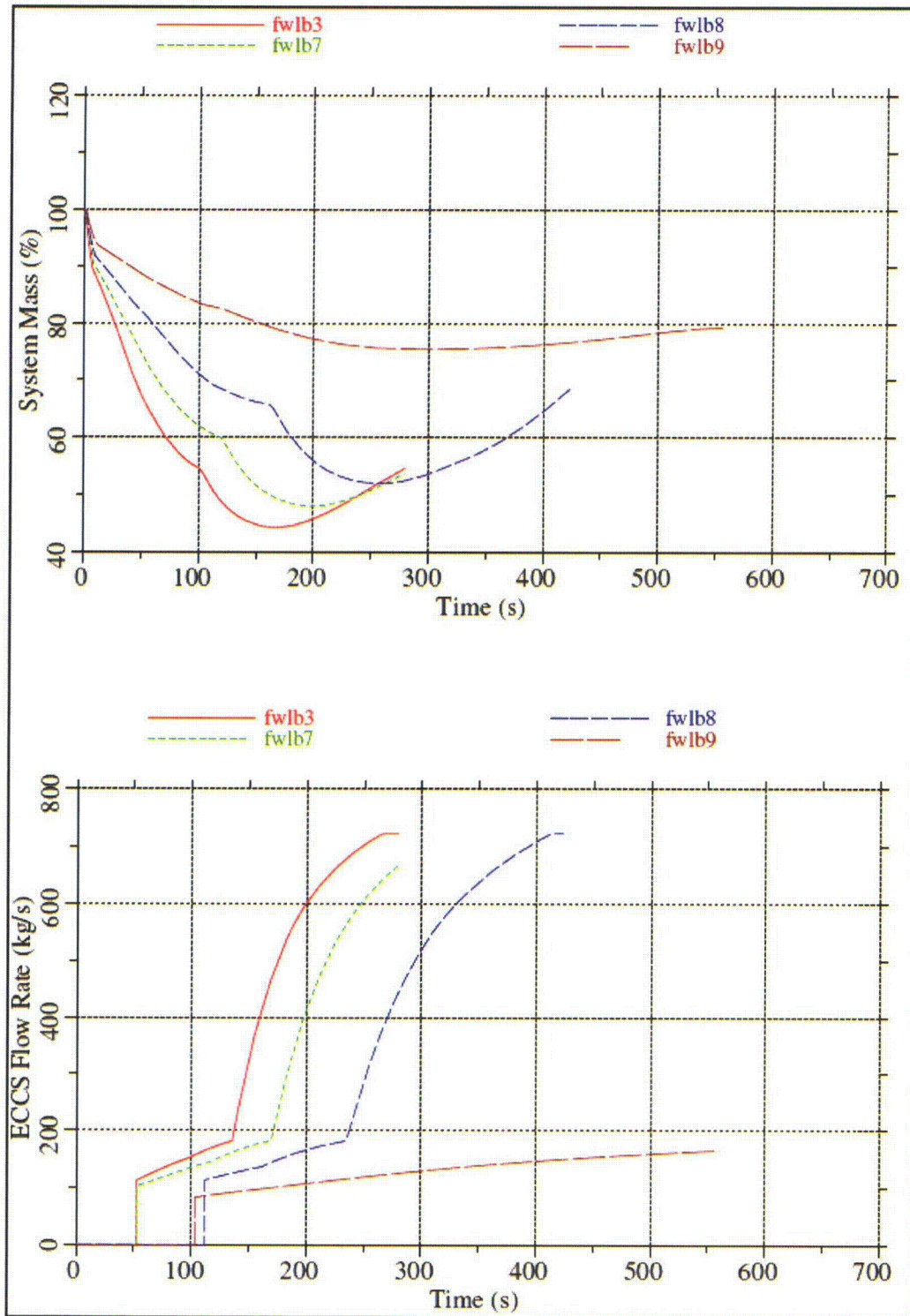


Figure 4-31 Break Size Sensitivity – System Mass and ECCS Flow Rates

4.5.4 RHR Suction Line Break

The RHR suction line nozzle is located between the elevation of the feedwater nozzle and the HPCF line nozzle. As shown in Figure 4-32, the RHR suction line also connects to the bottom head drain line. As a result, a break in the RHR suction line will result in a loss of coolant from the upper annulus and from the lower plenum of the RPV through the bottom drain line. Because of the piping configuration, the break flow from the upper annulus is limited by the flow area of the RHR suction nozzle, and the break flow from the lower head is limited by the flow area of the bottom drain nozzle. In this case the limiting single failure is that one of the EDGs that provides power to a HPCF pump does not start. This results in the following available ECCS equipment:

1 RCIC + 1 HPCF + 2 LPFL + 8 ADS

4.5.4.1 RHR Suction Line Break Results

Five cases were run with the power in the hot assembly set to simulate a nodal power so that the hot rod would be at the TMOL. Table 4-5 summarizes the results of those cases. As shown, the variation in PCT is small when the steam line is isolated in the same manner. The table also shows that the variation in minimum mass is primarily a function of break size.

| Case | Core Flow | Break Location | Break Size | Steam Line Isolation | PCT (GOBLIN) | Minimum Mass |
|-------------|------------------|-----------------------|-------------------|-----------------------------|---------------------|---------------------|
| rhrlb3dlb | 90% | RHR SL | 100% | TCV fast closure | 708°C | 133.6 E3 kg |
| rhrlb4dlb | 111% | RHR SL | 100% | TCV fast closure | 691°C | 132.1 E3 kg |
| rhrlb5dlb | 90% | RHR SL | 100% | Pressure regulator | 662°C | 133.3E3 kg |
| rhrlb7dlb | 90% | RHR SL | 75% | TCV fast closure | 709°C | 145.2 E3 kg |
| rhrlb8dlb | 90% | RHR SL | 50% | TCV fast closure | 710°C | 189.7 E3 kg |



Figure 4-32 Schematic of RHR Suction Line Break

4.5.4.2 Sensitivity Studies

Core Flow Rate

Cases rhrlb3dlb and rhrlb4dlb show the impact of initial core flow rate. As shown in Table 4-5, the minimum system masses are about the same, but the first case, rhrlb3dlb, had the highest PCT. Similar to previous sensitivity studies, the case with the higher initial core flow rate has more margin to dryout, and therefore goes through boiling transition later and have a lower peak cladding temperature. The cladding temperatures in the hot nodes are compared in Figure 4-33.

As shown in Table 4-5, the minimum inventories are nearly identical. Figure 4-34 shows that significant water is maintained in the upper plenum and that a two-phase mixture provides cooling in the hot assembly throughout the transient.

Cases rhrlb3dlb and rhrlb5dlb show the impact of steam line isolation on the LOCA transient. As shown in Table 4-5, the PCT is significantly reduced when the steam line is isolated more slowly by the pressure regulator. The minimum inventories for the two cases are nearly identical.

Figure 4-35 compares the short term dome pressure responses and the cladding temperatures of the hot nodes. As shown, fast closure of the TCVs causes the system pressure to increase initially whereas the case crediting the pressure regulator results in a slowly decreasing system pressure. Similar to previous sensitivity studies, the PCT responses are a result of different void reactivity feedback caused by the different system pressure responses.

Break Size

Cases rhrlb3dlb, rhrlb7dlb and rhrlb8dlb show the impact of break size. These cases represent a 100%, 75%, and 50% break of the RHR suction line. The drain line break size is unchanged. As shown in Table 4-5 and Figure 4-36, the minimum inventory increases as the break size is decreased, while the PCT changes minimally.

4.5.5 RHR Injection Line Break

There are two RHR injection line nozzles located below the feedwater nozzles. The RHR injection lines are used by two of the three LPFL trains. The third LPFL train injects into one of the feedwater lines. Spargers located within the annulus connect to each of the RHR injection nozzles. The break flow associated with a break in one of the RHR injection lines is limited by the []^{a,c}

nozzles on each of the RHR injection spargers. A break in one of these lines would disable one of the LPFL divisions. The limiting single failure is to the EDG which powers the other division. The remaining ECCS equipment is:

1 RCIC + 1 HPCF + 1 LPFL + 8 ADS

4.5.5.1 RHR Injection Line Break Results

Two cases were run with the power in the hot assembly set to simulate a nodal power so that the hot rod would be at the TMOL. Table 4-6 summarizes the results of these cases. As shown, the variation in minimum inventory is small, and the sensitivity to initial core flow rate is similar to other cases in that the higher initial core flow rate provides additional margin to dryout and a slightly lower PCT.

| Case | Core Flow | Break Location | Break Size | Steam Line Isolation | PCT (GOBLIN) | Minimum Mass |
|--------|-----------|----------------|------------|----------------------|--------------|--------------|
| rhrlb3 | 90% | RHR IL | 100% | TCV fast closure | 707°C | 215.0 E3 kg |
| rhrlb4 | 111% | RHR IL | 100% | TCV fast closure | 655°C | 213.1 E3 kg |

4.5.5.2 Sensitivity Studies

Core Flow Rate

Figure 4-37 compares the PCT transient predicted by GOBLIN for the hot assembly, which occurs in node 18. As shown, the case with the lower initial core flow rate is more limiting as described above. Figure 4-38 compares the system pressures and masses. The small differences in the response are due to

different actuation times for the HPCF pump. The water level recovers before actuation of the LPFL pump.

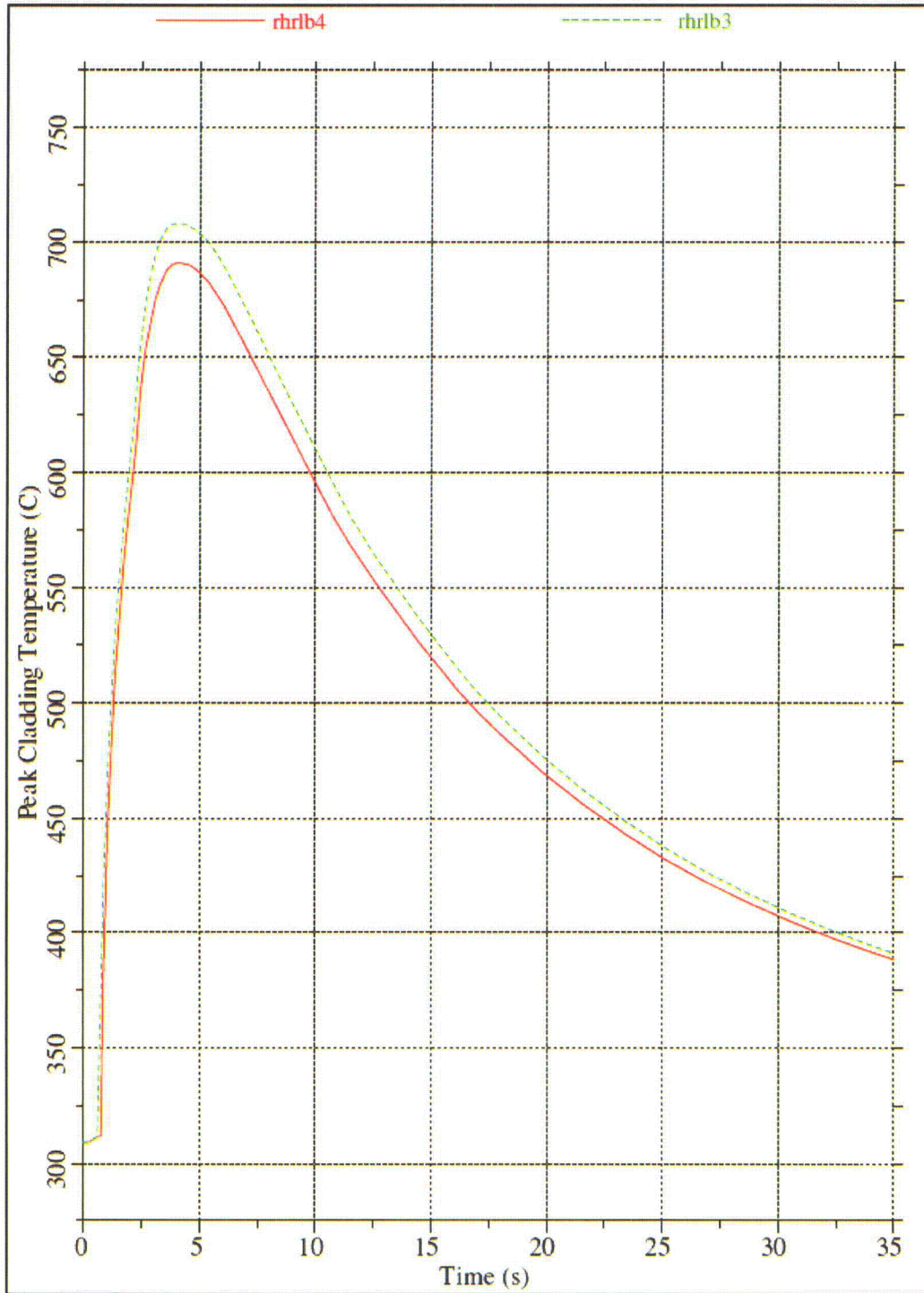


Figure 4-33 Core Flow Rate Sensitivity – GOBLIN PCTs

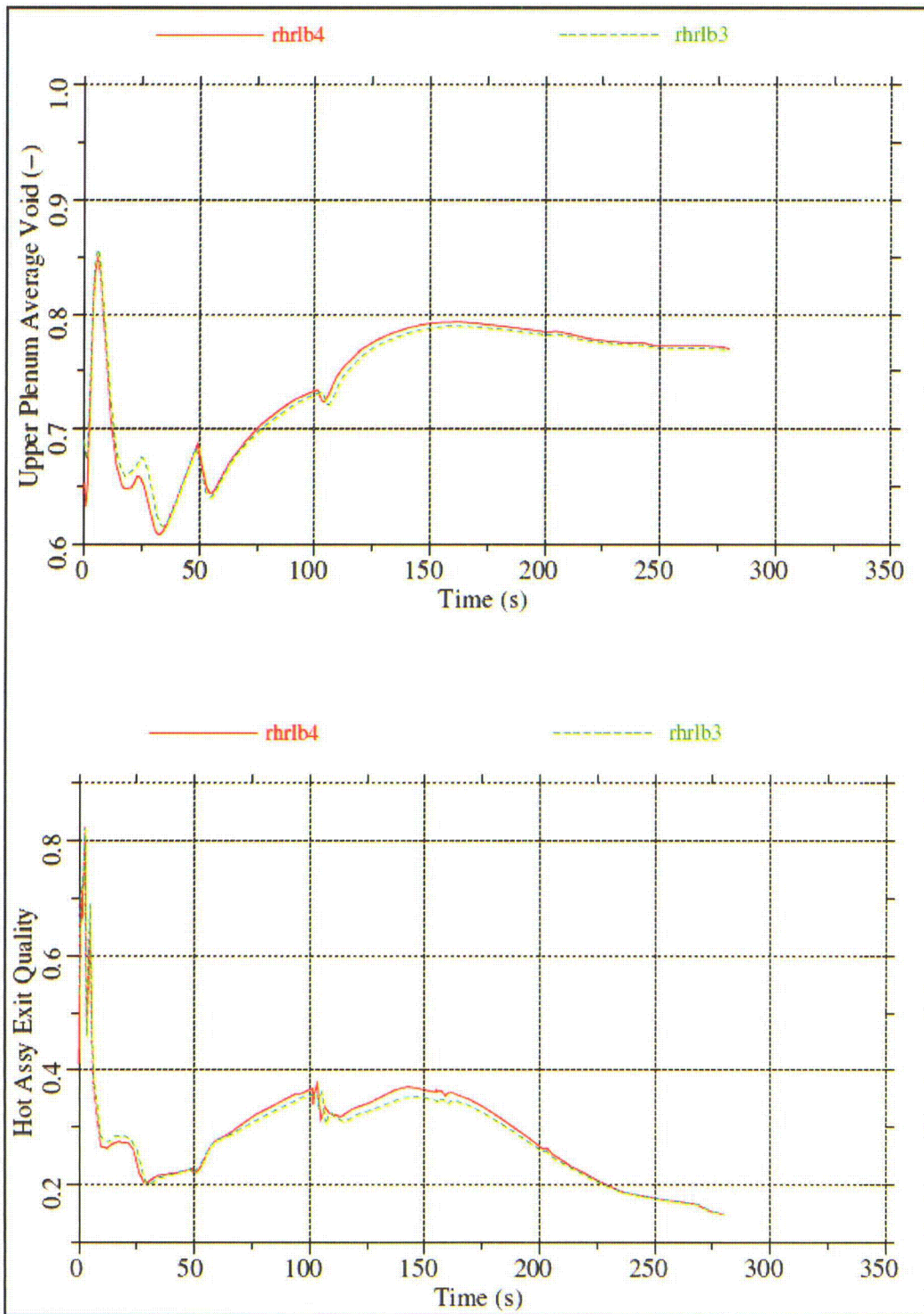


Figure 4-34 Core Flow Rate Sensitivity – Upper Plenum Void and Hot Assembly Exit Quality

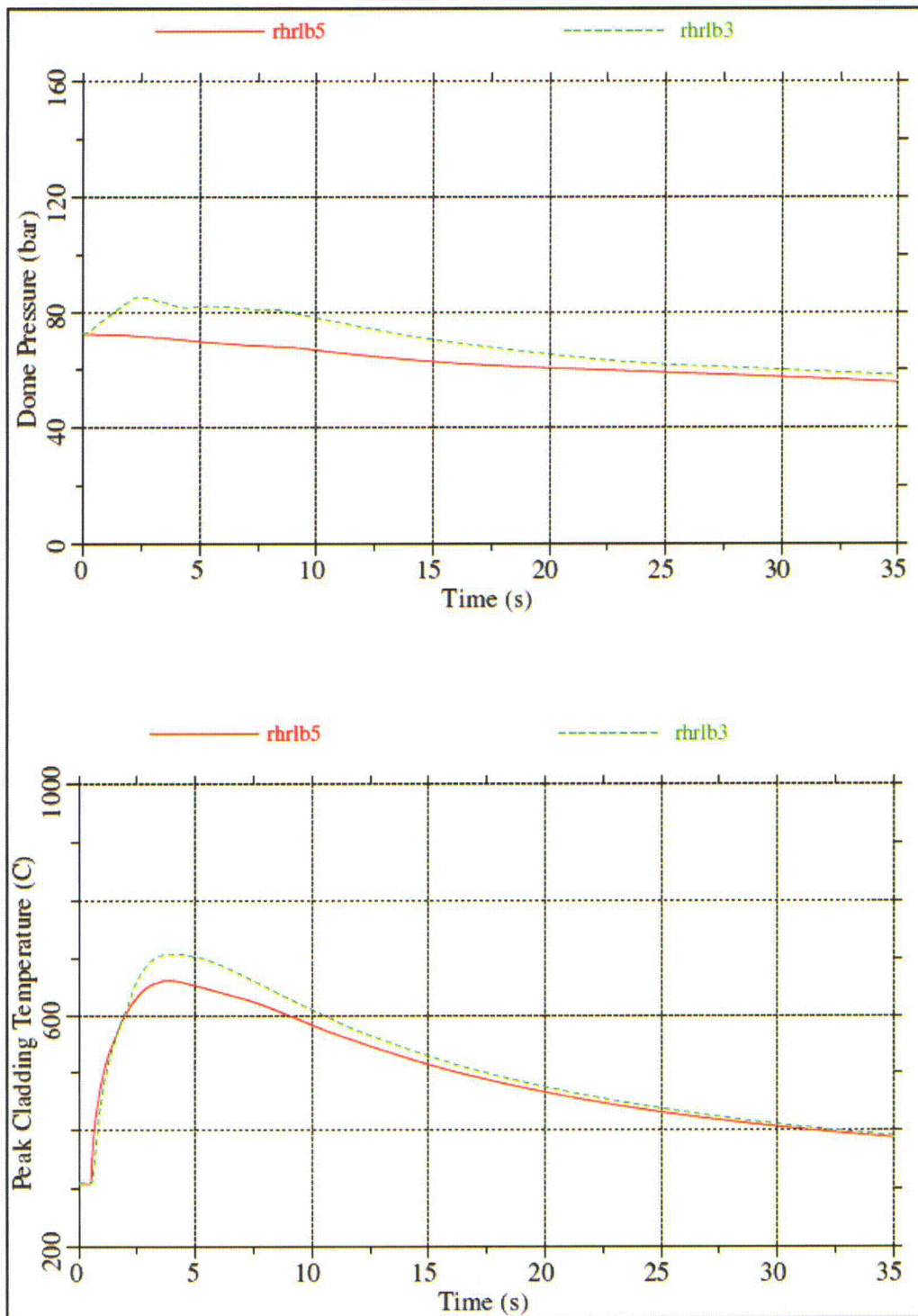


Figure 4-35 Steam Line Isolation Sensitivity – Dome Pressure and GOBLIN PCT

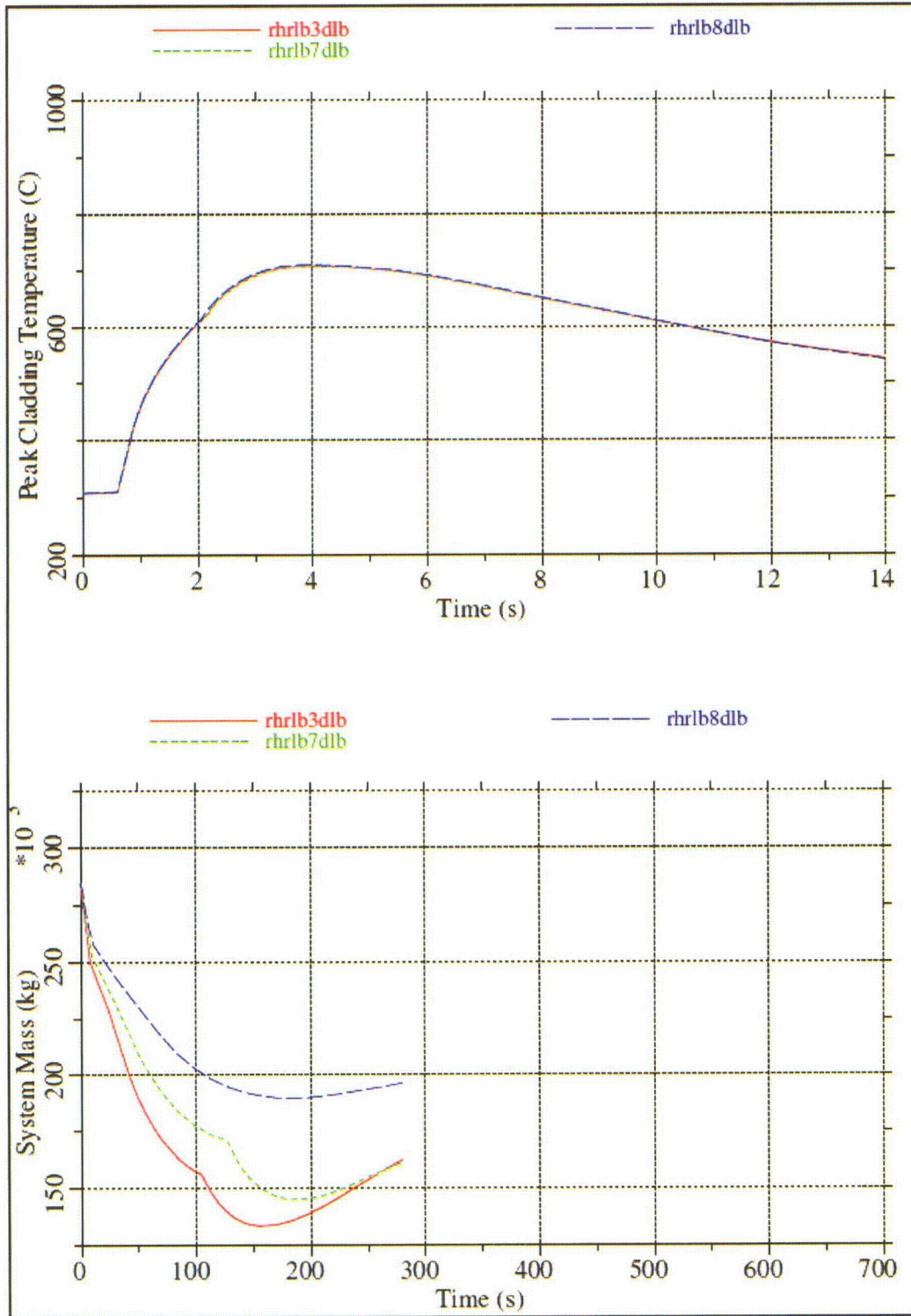


Figure 4-36 Break Size Sensitivity – GOBLIN PCT and System Mass

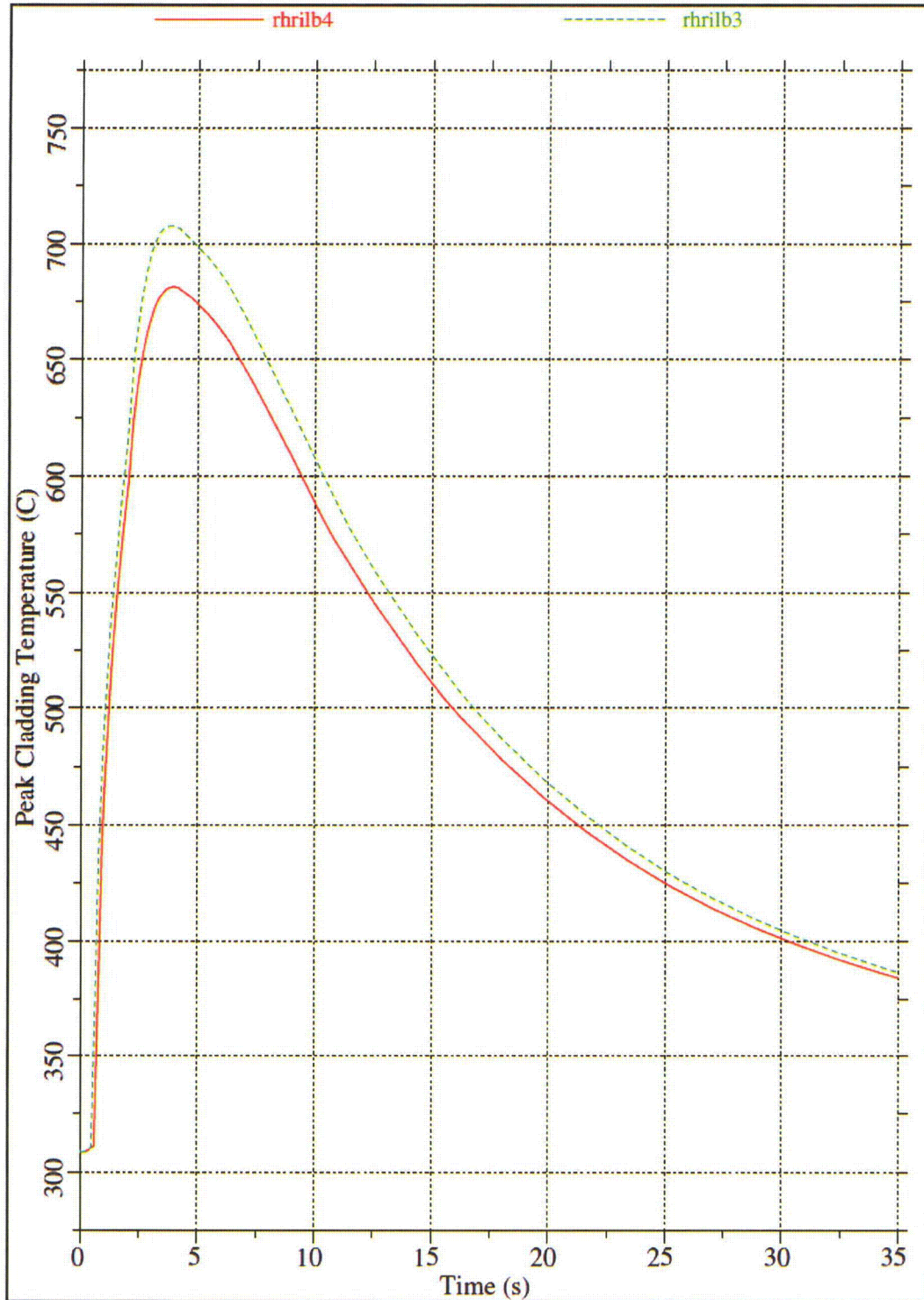


Figure 4-37 Core Flow Rate Sensitivity – GOBLIN PCT

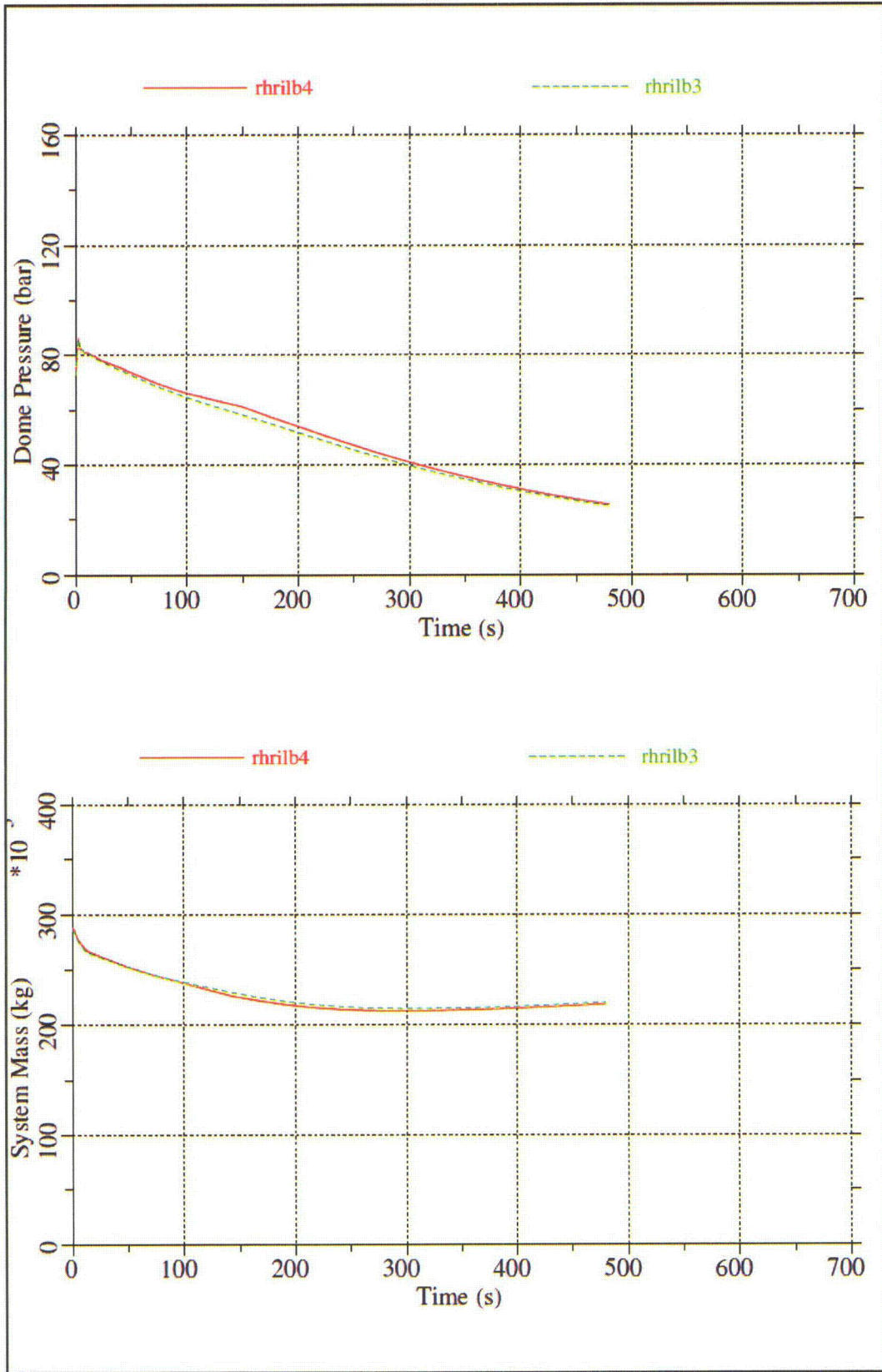


Figure 4-38 Core Flow Rate Sensitivity – Dome Pressure and System Mass

4.5.6 Drain Line Break

The drain line nozzle is connected to the bottom head. As shown in Figure 4-39, the drain line is also connected to the RHR suction line. Therefore, a break in the drain line will also result a loss of coolant from the upper annulus. In the case of a double-ended break in the drain line in the vicinity of the drain line nozzle, the break flow from the RHR suction line side of the break is limited by the smaller diameter of the piping near the bottom head drain. The limiting single failure is that one of the EDGs that provides power to a HPCF pump does not start. The remaining ECCS equipment is:

1 RCIC + 1 HPCF + 2 LPFL + 8 ADS

4.5.6.1 Drain Line Break Results

One case was run to simulate the drain line break. The results are summarized in Table 4-7. Comparing these results to those for the RHR suction line break, case rhrlb3dlb Table 4-5, shows that the PCTs predicted by GOBLIN are the same, but that the minimum inventory in this case is significantly greater as a result of the much smaller combined break flow area.

The drain line break is compared to the RHR suction line break in Figure 4-40 and Figure 4-41. As shown, the peak cladding temperature responses are nearly identical, but the drain line break loses significantly less inventory due to the smaller break size.

| Case | Core Flow | Break Location | Break Size | Steam Line Isolation | PCT (GOBLIN) | Minimum Mass |
|-------------|------------------|-----------------------|-------------------|-----------------------------|---------------------|---------------------|
| dlb | 90% | Drain Line | 100% | TCV fast closure | 708°C | 247.0 E3 kg |



Figure 4-39 Schematic of Drain Line Break

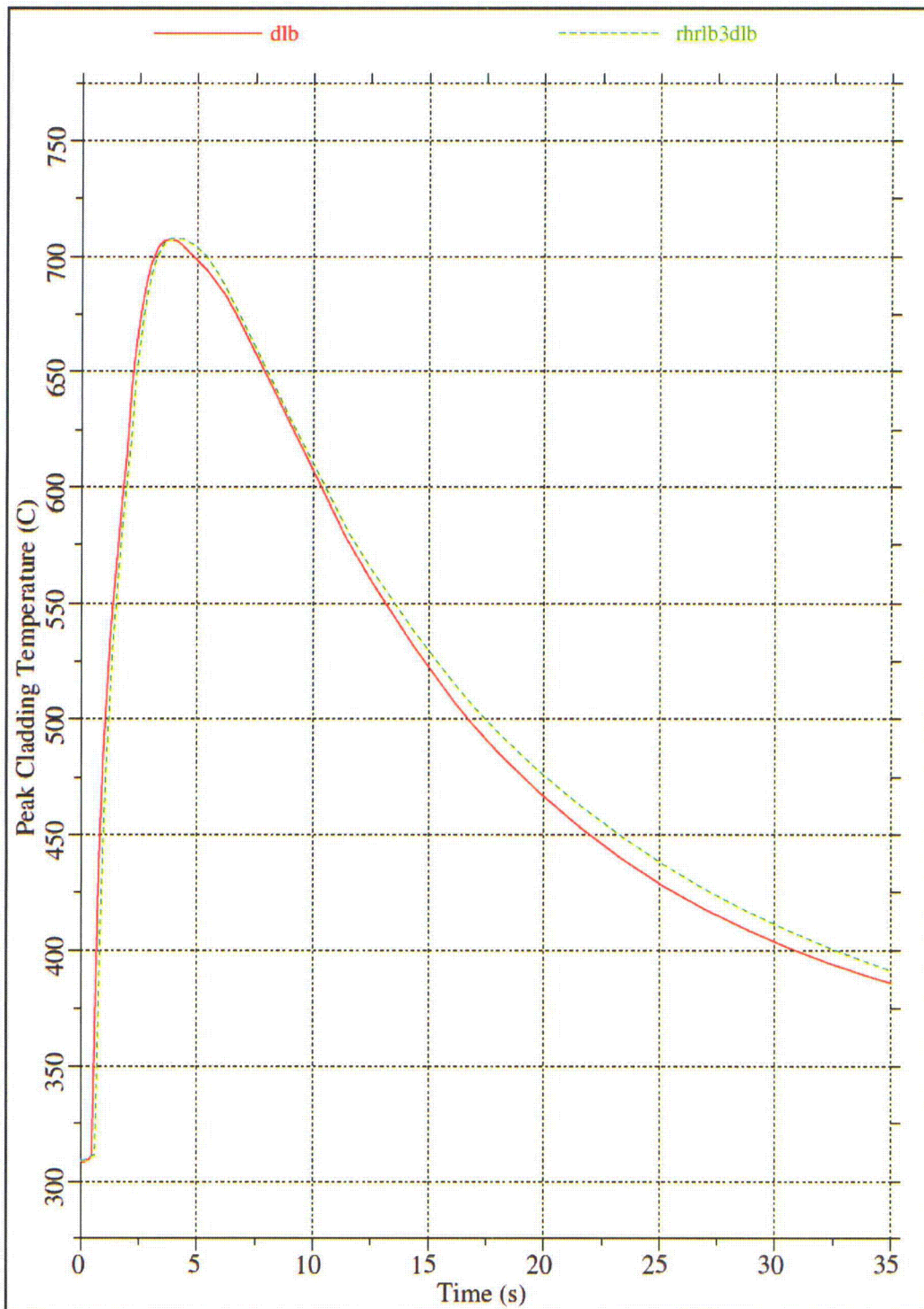


Figure 4-40 Comparison of DLB to RHRSLB – GOBLIN PCTs

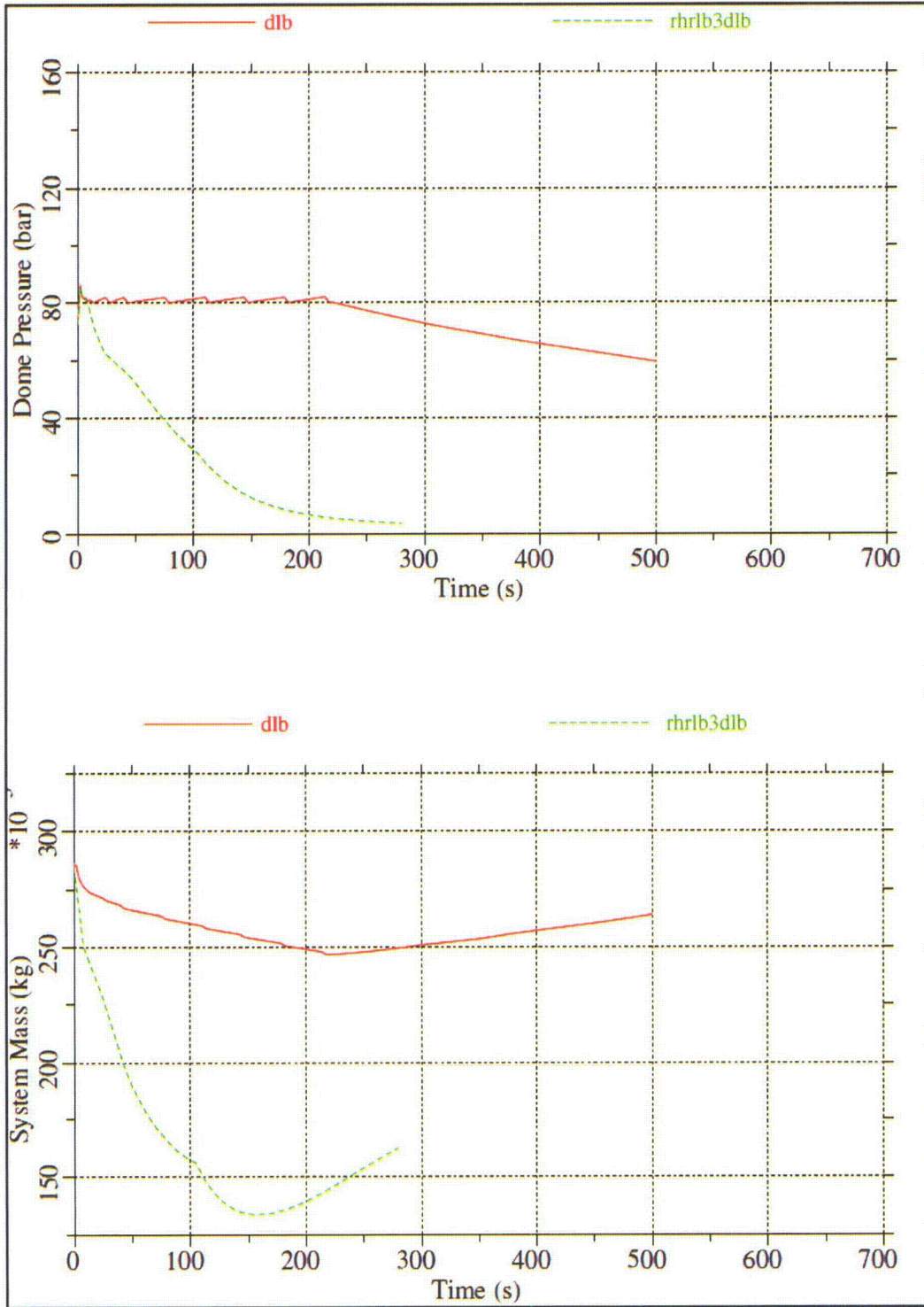


Figure 4-41 Comparison DLB to RHRSLB – Dome Pressure and System Mass

4.6 BREAKS OUTSIDE CONTAINMENT

Breaks outside of containment are characterized by isolation of the break by the MSIVs. Since the main steam line break outside the containment produces more vessel inventory loss before isolation than other breaks in this category, the results of this case are bounding for breaks in this group.

A postulated guillotine break of one of the four main steam lines outside the containment is shown schematically in Figure 4-42. A pipe rupture in this location results in mass loss from each end of the break until the MSIVs close. The MSIVs receive a close signal due to high steam flow rate through the integral flow restrictors or due to LWL 1.5. Closure of the MSIVs limits the amount of flow that will be discharged outside the containment. Once the MSIVs close, the RPV will pressurize until the SRVs open. The SRVs will control system pressure and discharge steam to the suppression pool. The RCIC system or one of the HPCF systems can provide adequate flow to the vessel to maintain core cooling.

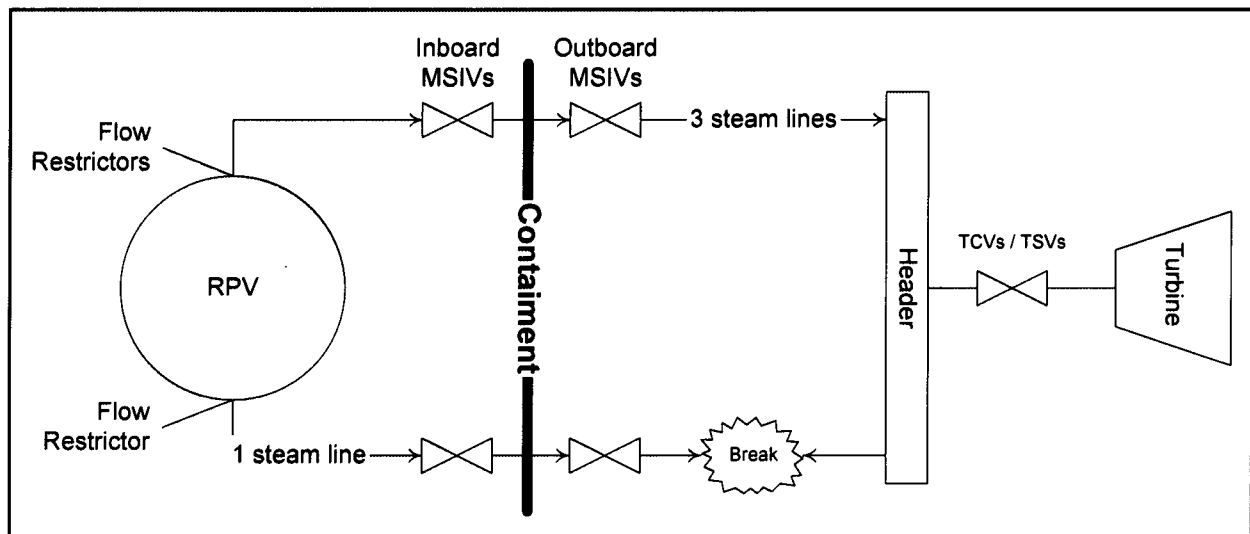


Figure 4-42 Schematic of Steam Line Break Outside Containment

4.6.1 Steam Line Break Outside Containment Results

The limiting single failure is that one of the EDGs that provides power to a HPCF pump does not start. This results in one RCIC pump, one HPCF pump, and two LPFL pumps available to mitigate the event. Although the RCIC turbine takes suction from one of the steam lines, closure of the MSIVs ensures that there is a long-term supply of steam for the RCIC turbine. However, a more limiting case is evaluated where the RCIC is assumed unavailable. In this case the assumed available equipment is:

$$1 \text{ HPCF} + 2 \text{ LPFL} + 8 \text{ ADS}$$

In this case, the LPFL systems would not actuate as the system inventory is stabilized before ADS actuation.

Table 4-8 summarizes the results for this case. As shown, the PCT and minimum system mass are not as limiting as other cases. Figure 4-43 shows that the PCT occurs early in the transient before ECCS

actuation. Figure 4-44 shows that the system pressure decreases at the beginning of the transient. However, the pressure increases after MSIV closure until actuation of the SRVs controls the pressure for the remainder of the event. Figure 4-44 also shows that the mass of the system decreases rapidly until MSIV closure, and that the system mass is maintained after HPCF injection.

| Case | Core Flow | Break Location | Break Size | Steam Line Isolation | PCT (GOBLIN) | Minimum Mass |
|-------------|------------------|------------------------|-------------------|-----------------------------|---------------------|---------------------|
| mslboc6a | 90% | SL outside containment | 100% | MSIV closure | 668°C | 241.4 E3 kg |

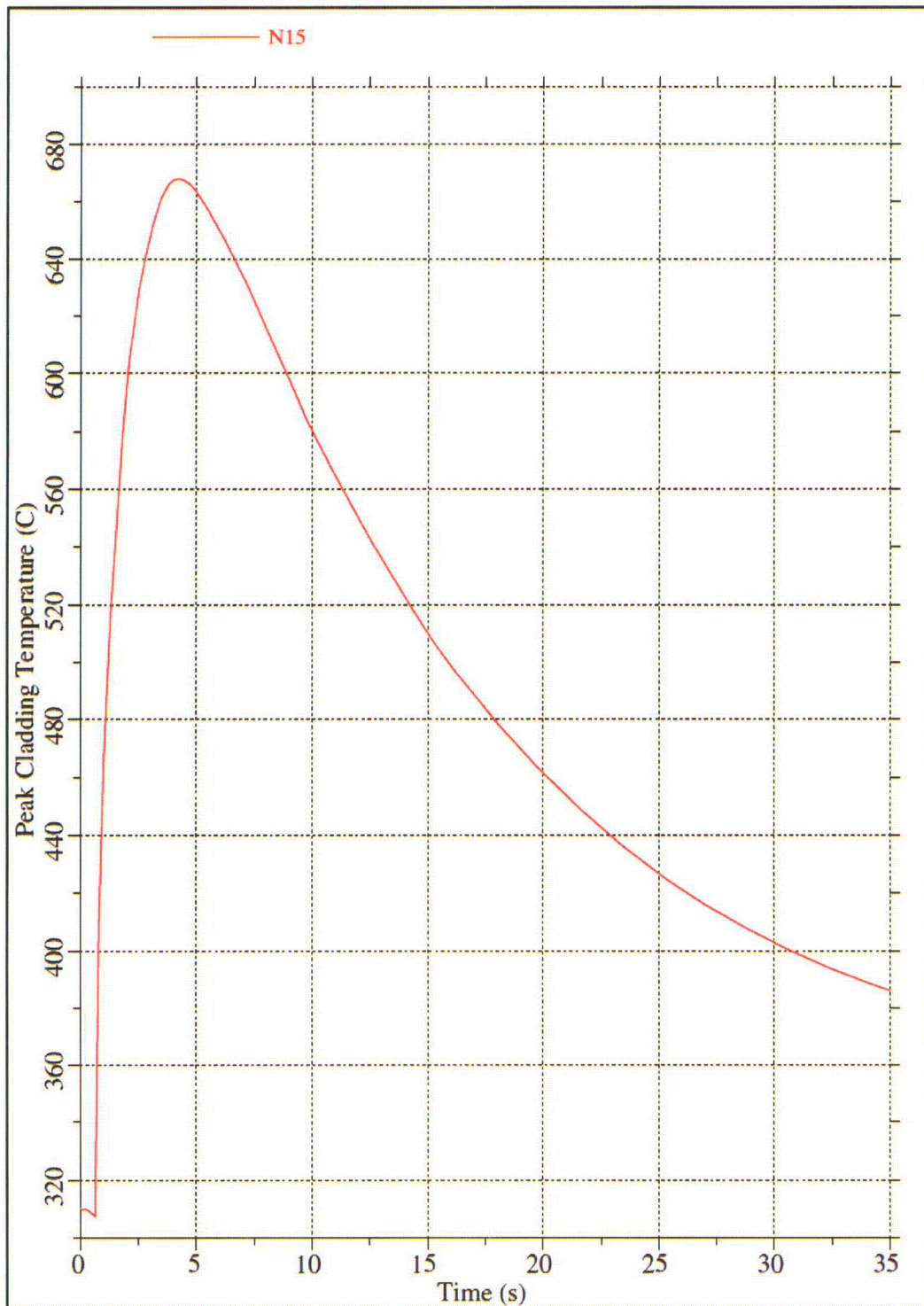


Figure 4-43 Steam Line Break Outside Containment – GOBLIN PCT

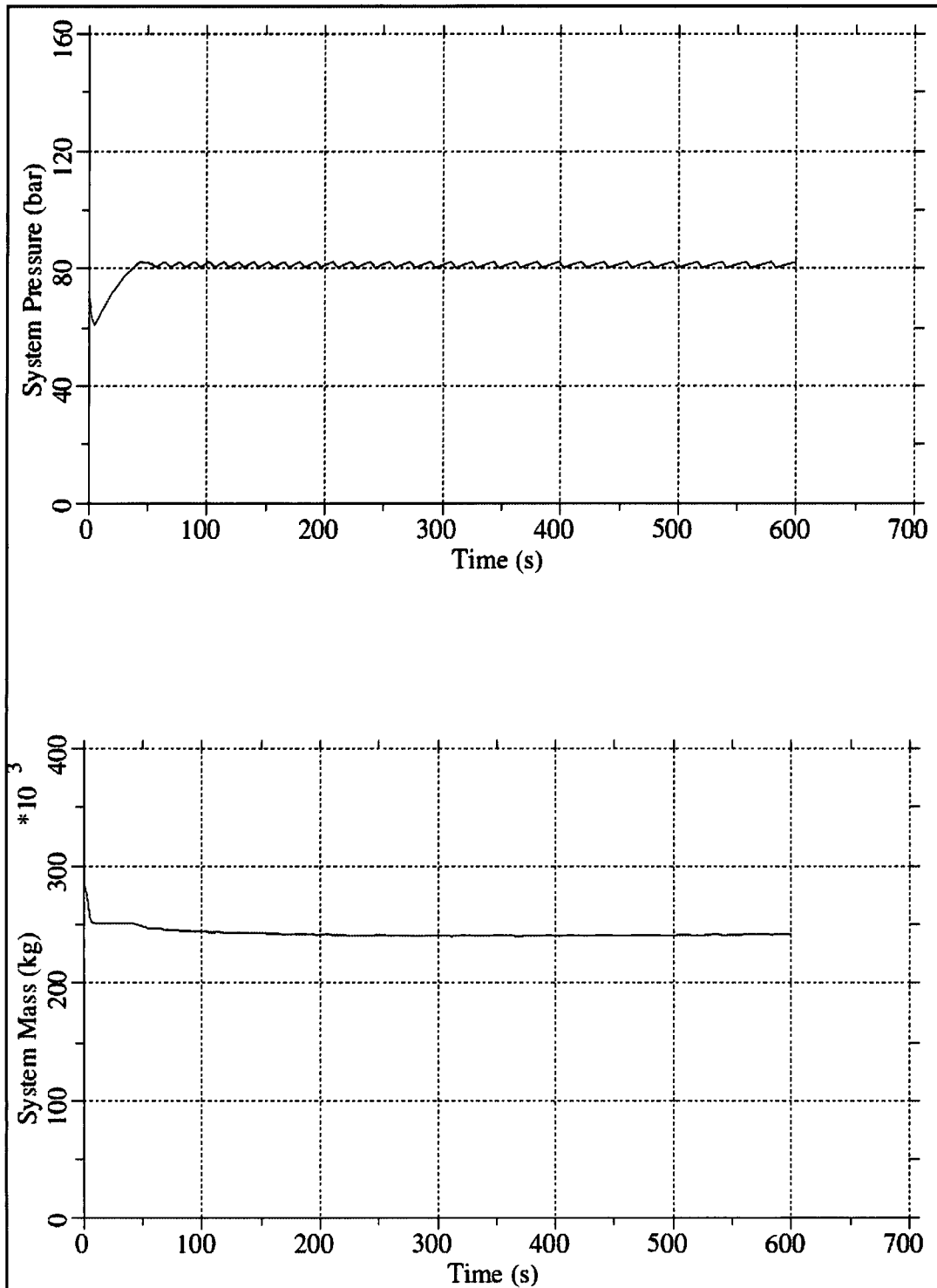


Figure 4-44 Steam Line Break Outside Containment – Dome Pressure and System Mass

4.7 SUMMARY OF LIMITING CASES

The resulting peak cladding temperature and minimum system inventory for each case is presented in Table 4-9. These results are shown as a function of break size in Figure 4-45 and Figure 4-46.²

As shown in Figure 4-44, the peak cladding temperature does not vary appreciably with break size. The variations in PCT are caused by different initial conditions such as high core flow rate vs. low core flow rate and the method assumed for isolating the steam line. As shown, the higher PCTs result from cases that are initiated from the lower core flow rate and cases where the steam line was isolated quickly (fast closure of the TCVs).

As shown in Figure 4-46, the minimum inventory varies with break size. For a similar set of available ECCS equipment, minimum inventory decreased as break size increased.

| Case | Core Flow | Break Location | Break Size | Steam Line Isolation | PCT (GOBLIN) | Minimum Mass |
|-------------|------------------|-----------------------|-------------------|-----------------------------|---------------------|---------------------|
| hpcf3 | 90% | HPCF Line | 100% | TCV fast closure | 708°C | 133.3 E3 kg |
| hpcf4 | 111% | HPCF Line | 100% | TCV fast closure | 692°C | 132.2 E3 kg |
| hpcf5 | 90% | HPCF Line | 100% | Pressure regulator | 661°C | 133.7 E3 kg |
| hpcf7 | 90% | HPCF Line | 75% | TCV fast closure | 708°C | 138.1 E3 kg |
| hpcf8 | 90% | HPCF Line | 50% | TCV fast closure | 708°C | 143.6 E3 kg |
| hpcf9 | 90% | HPCF Line | 25% | TCV fast closure | 708°C | 151.3 E3 kg |
| mslb6 | 90% | SL – RCIC side | 200% | TCV fast closure | 657°C | 164.1 E3 kg |
| mslb6a | 111% | SL – RCIC side | 200% | TCV fast closure | 648°C | 162.6 E3 kg |
| mslb7 | 90% | SL – RCIC side | 150% | TCV fast closure | 654°C | 164.1 E3 kg |
| mslb8 | 90% | SL – RCIC side | 100% | TCV fast closure | 656°C | 164.1 E3 kg |
| fwlb3 | 90% | FWL – RCIC side | 100% | TCV fast closure | 708°C | 126.5 E3 kg |
| fwlb4 | 111% | FWL – RCIC side | 100% | TCV fast closure | 684°C | 123.5 E3 kg |
| fwlb5 | 90% | FWL – RCIC side | 100% | Pressure Regulator | 661°C | 126.0 E3 kg |
| fwlb6 | 90% | FWL – RCIC side | 100% | TCV fast closure | 708°C | 125.9 E3 kg |
| fwlb7 | 90% | FWL – RCIC side | 75% | TCV fast closure | 705°C | 136.9 E3 kg |
| fwlb8 | 90% | FWL – RCIC side | 50% | TCV fast closure | 707°C | 148.4 E3 kg |
| fwlb9 | 90% | FWL – RCIC side | 25% | TCV fast closure | 710°C | 215.6 E3 kg |
| rhrlb3dlb | 90% | RHR Suction Line | 100% | TCV fast closure | 708°C | 133.6 E3 kg |

2. The results of the steam line break outside containment are not shown in the figures since the break isolates rapidly, preventing a meaningful comparison.

Table 4-9 Summary of Break Spectrum Study Results (cont.)

| Case | Core Flow | Break Location | Break Size | Steam Line Isolation | PCT (GOBLIN) | Minimum Mass |
|-----------|-----------|------------------------|------------|----------------------|--------------|--------------|
| rhrlb4dlb | 111% | RHR Suction Line | 100% | TCV fast closure | 691°C | 132.1 E3 kg |
| rhrlb5dlb | 90% | RHR Suction Line | 100% | Pressure regulator | 662°C | 133.3E3 kg |
| rhrlb7dlb | 90% | RHR Suction Line | 75% | TCV fast closure | 709°C | 145.2 E3 kg |
| rhrlb8dlb | 90% | RHR Suction Line | 50% | TCV fast closure | 710°C | 189.7 E3 kg |
| rhrlb3 | 90% | RHR Injection Line | 100% | TCV fast closure | 707°C | 215.0 E3 kg |
| rhrlb4 | 111% | RHR Injection Line | 100% | TCV fast closure | 655°C | 213.1 E3 kg |
| dlb | 90% | Drain Line | 100% | TCV fast closure | 708°C | 247.0 E3 kg |
| mslboc6a | 90% | SL Outside Containment | 200% | MSIV closure | 668°C | 241.4 E3 kg |

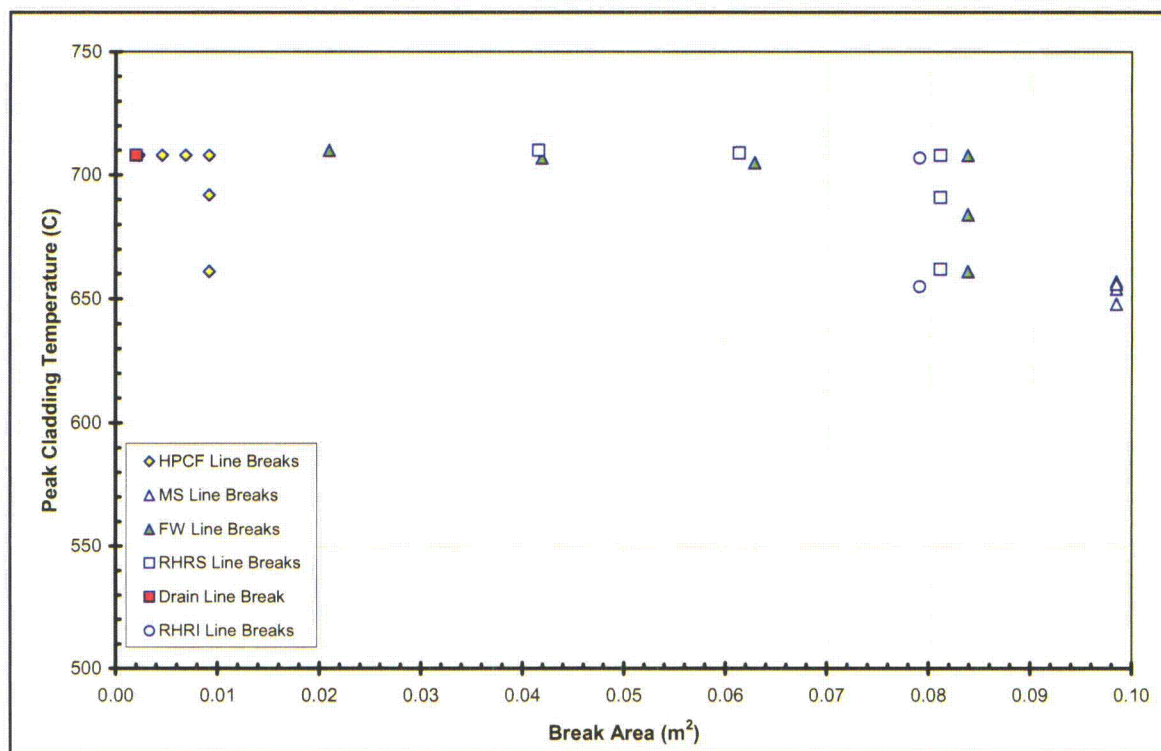


Figure 4-45 Summary of Peak Cladding Temperature Results vs. Break Size

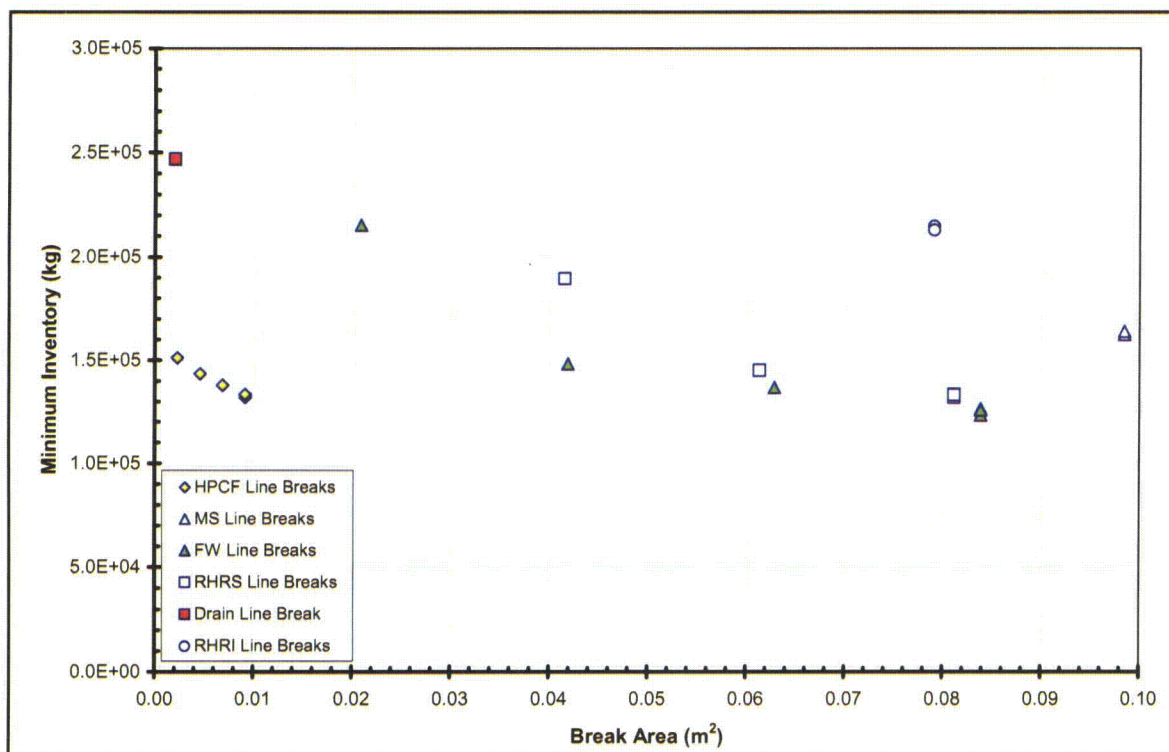


Figure 4-46 Summary of Minimum Inventory Results vs. Break Size

4.7.1 Case with Minimum Inventory

The case having the minimum system inventory was the case where the feedwater line break initiated with maximum core flow rate. Although the steam line break has a greater flow area than the feedwater line break, the feedwater line break has the smallest minimum inventory due to the lower quality fluid flowing out the break. In spite of having the least minimum inventory, the core remains cooled by a two-phase mixture throughout the transient.

4.7.2 Case with Maximum Peak Cladding Temperature

There is no clear case having the highest peak cladding temperature from the GOBLIN hot assembly analysis. As shown in Table 4-9, two cases have a PCT of 710°C as predicted by GOBLIN. The small feedwater line break initiated from 90% core flow rate, fwlb9, is selected for the heatup analysis using CHACHA.

Several exposure points are evaluated to show that the combination of nodal power and pin-to-pin peaking results in the hot rod being at the TMOL. The range of exposures encompasses beginning of life to []^{a,c}.

It is typical of BWR/ABWR fuel to have the largest pin-to-pin peaking factors early in life. However, the high power rods burn down with exposure, causing the rod power distribution to become flatter at larger cycle exposures. []

[]^{a,c} Figure 4-47 shows the results of a calculation for a typical lattice design over a range of

burnups []^{a,c}. As shown, the PCT increases slightly with burnup. However, the PCT remains below the licensing limit for ECCS performance analysis.

Due to the relatively low PCT, the maximum local oxidation and core wide oxidation are below the licensing limits.

A similar evaluation is performed for each reload to confirm that the 10 CFR 50.46 criteria are met when the []^{a,c} for the limiting LOCA event.

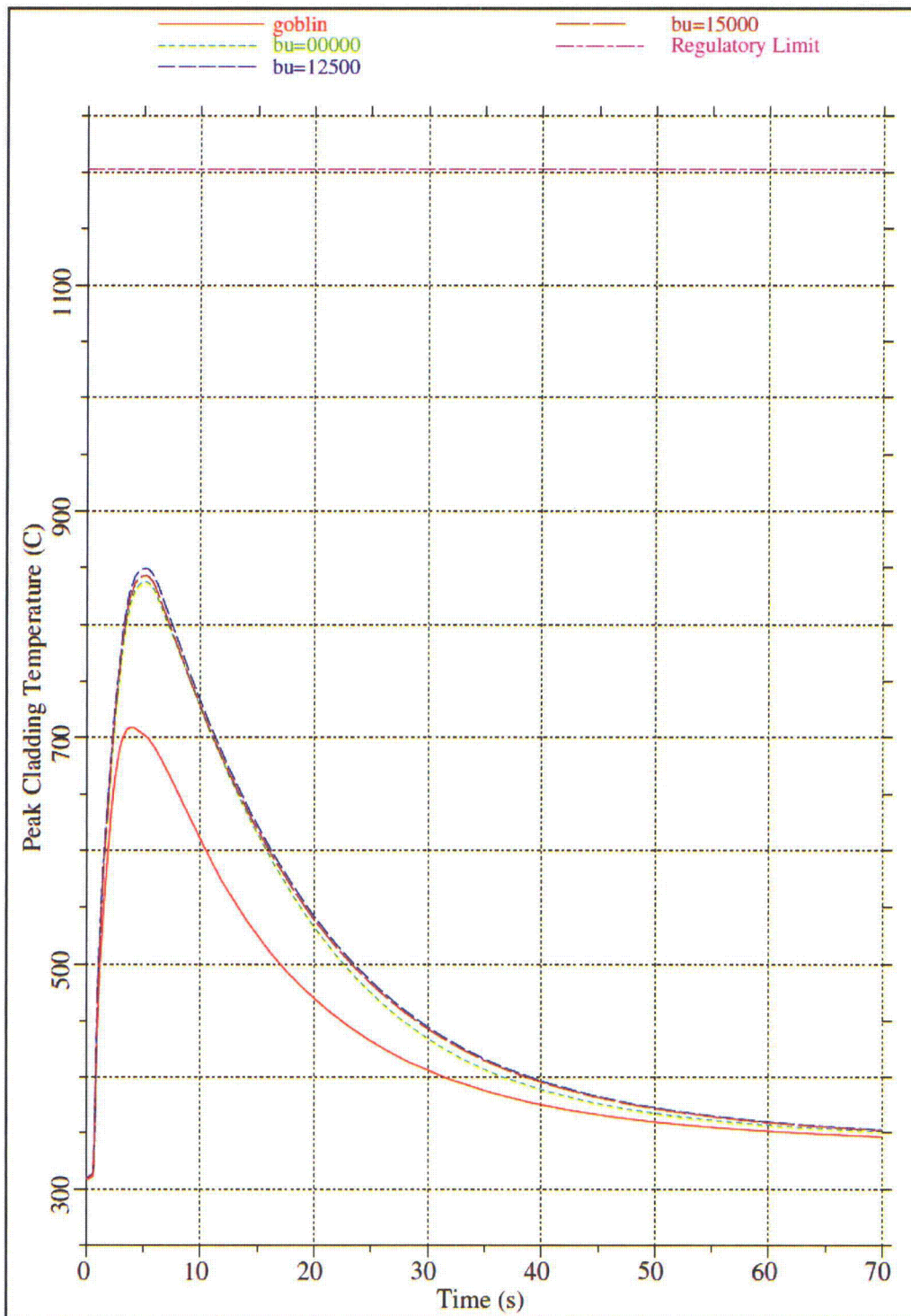


Figure 4-47 Peak Cladding Temperature For Limiting Case

5 QUALIFICATION OF ABWR EVALUATION MODEL

As described in Section 1, the main differences between a LOCA in a BWR and in an ABWR arise from the different elevations of piping connections to the RPV and the different inertias of the RIPs and external recirculation pumps. The lower inertia of the RIPs results in a faster coastdown of the pumps following a loss of power. The rapid coastdown causes an early boiling transition in the transient and a brief heat-up of the cladding. This occurs well before the ECCS actuates.

To ensure that the rapid coastdown of core flow and the effect of such a coastdown on boiling transition are accurately modeled in GOBLIN, the following two additional qualifications are performed:

- Predicted behavior of internal recirculation pumps are compared to the minimum design acceptance criterion for the ABWR RIPs and to Okiluoto 1 (OL1) plant startup test data.
- The results of GOBLIN simulations of the FRIGG loop are compared to FRIGG loop test data that simulated flow coastdown.

5.1 RECIRCULATION PUMP MODEL

The recirculation pump model is described in RPB 90-93-P-A (Reference 2). The behavior of the pumps is modeled by the conservation of angular momentum:

$$I \frac{d\omega}{dt} = T$$

where:

| | | |
|----------|---|-------------------|
| ω | = | angular velocity |
| t | = | time |
| T | = | net torque |
| I | = | moment of inertia |

The coolant conservation equations and the pump angular momentum equation are coupled in the GOBLIN code through the 4-quadrant pump homologous curves. The fluid conservation equations are solved simultaneously with the pump conservation of angular momentum equation using numerical integration techniques to obtain the transient pump coastdown. The pump angular momentum equation uses several inputs, including pump/motor assembly inertia, hydraulic torque and frictional torque.

The data that is usually provided for the pump includes the pump homologous curves for head and hydraulic torque and the following parameters:

| | | |
|------------|---|-------------------|
| ω_r | = | rated pump speed |
| W_r | = | rated pump flow |
| H_r | = | rated pump head |
| T_r | = | rated pump torque |

- ρ_r = rated density of pump fluid
 η = pump efficiency (minimum)

The GOBLIN input data include the following parameters:

- H_2 = frictional torque coefficient for high pump speed
 H_3 = lower limit of angular velocity for high speed frictional torque
 H_4 = constant frictional torque for when angular velocity < H_3
 H_6 = rated pump speed
 H_9 = rated hydraulic torque

The rated hydraulic torque is calculated using the rated torque and the minimum efficiency as follows:

$$H_9 = \eta \times T_r$$

This results in a conservatively high frictional torque at rated conditions. The frictional torque relationship in GOBLIN is assumed to vary as the square of the pump speed. The coefficient in that expression is then determined as follows:

$$H_2 = \frac{-(T_r - H_9)}{\omega_r^2}$$

The constant frictional torque at low speed (H_4) is not typically provided. However, other information is usually provided (e.g., pump coastdown time constant or pump coastdown data from a startup test), which allows the low speed frictional torque to be tuned so that the pump coastdown is simulated conservatively. The speed where these two curves cross (H_3) is then determined as follows:

$$H_3 = \sqrt{H_4 / H_2}$$

The frictional torque as a function of speed then becomes:

$$\begin{aligned}
 T_f(\omega) &= H_2 \times \omega \times |\omega| & \text{if } |\omega| > H_3 \\
 T_f(\omega) &= H_4 \times \frac{\omega}{|\omega|} & \text{otherwise}
 \end{aligned}$$

This approach is used for the initial approximation, and the results are compared to the specification for the minimum safety analysis limit for the pump coastdown time constant of []^{a,c}. If the resulting coastdown time constant is greater than this value, the model is adjusted so that this specification is met. The calculated pump coastdown transient, which is shown in Figure 5-1, demonstrates that the time constant of []^{a,c} is met []^{a,c}. In this case the pump speed does not decrease to zero. This is a result of the core flow, which transitions from forced flow to natural circulation, driving the pump rotor.



Figure 5-1 Calculated ABWR Pump Trip Transient

5.2 INTERNAL PUMP COASTDOWN

5.2.1 Okiluoto 1 Pump Trip

The OL1 reactor is an internal recirculation pump reactor operated by Teollisuuden Voima Oy (TVO) on the west coast of Finland. The plant, which is an Asea-Atom design, contains 500 fuel assemblies and 6 internal recirculation pumps. GOBLIN was used to simulate a pump trip test that was performed during plant start-up. The simulation is described in Section 6.1.8 of Reference 2. Although the purpose of the simulation was to validate the point kinetics model in GOBLIN, it also showed that the calculated flow compares well with the measured flow, Figure 5-2.

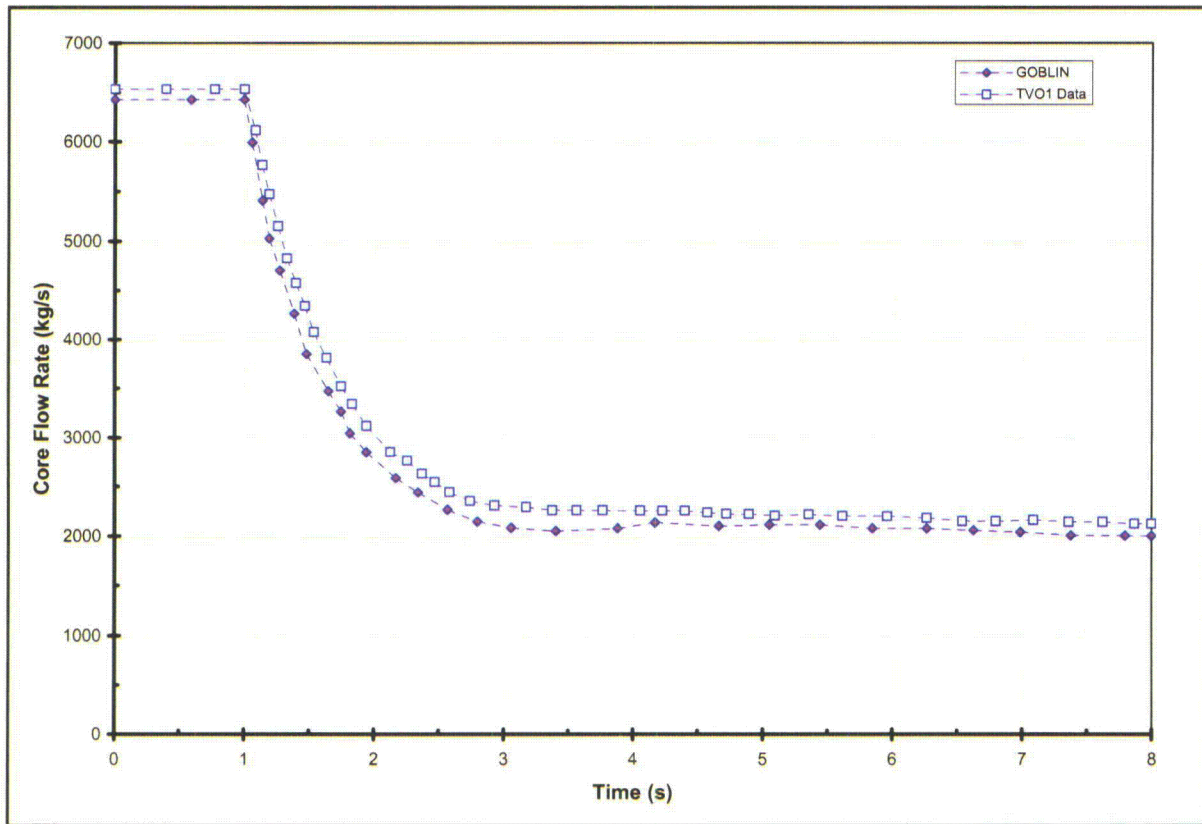


Figure 5-2 Comparison of Core Channel Inlet Flow Rate for OL1 Pump Trip Transient

5.3 PREDICTION OF BOILING TRANSITION

The ABWR LOCA event coincident with the loss of off site power is characterized by a rapid coastdown of the RIPs. The rapid decrease in coolant flow through the core causes an abrupt change of the fuel rod heat transfer regime from nucleate boiling to film boiling. The typical ABWR LOCA is characterized by departure from nucleate boiling shortly after the onset of the LOCA event. Even though the core remains covered by a two-phase mixture throughout the LOCA event, the transition to film boiling results in a cladding temperature increase until the reactor trip reduces the heat generation. Since the peak cladding temperature occurs during this time, the predicted time of boiling transition is important.

As described in Section 4.1 of Reference 5, the onset of boiling transition in GOBLIN is calculated using a boiling length CPR correlation that was developed for the fuel being analyzed. For example, the D4.1.2 CPR correlation, which has been implemented in GOBLIN, is used for the SVEA-96 Optima2 fuel design. The CPR correlation was developed from steady-state test data collected from the FRIGG loop in the Westinghouse laboratories in Västerås, Sweden. Derivation of the correlation is described in detail in Section 5 of Reference 8.

5.3.1 FRIGG Loop Comparison

In addition to the steady-state tests, another set of FRIGG transient dryout experiments was performed by increasing the bundle power and/or reducing the bundle inlet flows. These tests are described in Section 7 of Reference 8. The transient results are used for the validation of D4.1.2's implementation in GOBLIN.

The test section consists of a pressure vessel, a Zircaloy flow channel, and a replica of a SVEA-96 Optima2 sub-bundle with 24 heater rods. Each heater rod contains a heater element, electrical insulation, and Inconel-600 cladding. The heater element is made from a Monel K-500 tube. The heater rod non-uniform axial power profiles were generated by laser cutting a spiral on the Monel tube with a variable pitch. Three of the rods in each sub-bundle are part-length rods (PLRs), two being two-thirds of the length of a full-length rod and are placed adjacent to the central channel of the water cross. The other is one-third of the length of a full-length rod and is placed in the outer corner of the sub-bundle. An orifice plate is installed at the inlet of the flow channel to provide an even distribution of flow into the channel. The loss coefficient of the orifice plate closely approximates that of the lower tie plate in standard SVEA-96 Optima2 fuel. The heater rods are constrained by eight Inconel spacers of the same type used in the standard SVEA-96 Optima2 sub-bundle as seen in Figure 5-3.

[

] ^{a,c}

Eighty five of the 253 FRIGG transient tests were used to validate the GOBLIN dryout prediction capability. The test cases selected included all axial power shapes and power/flow transients that are relevant to ABWR LOCA analyses. The three axial power shapes included in the validation were a bottom-peaked shape with a 1.5 axial peak located at 22% core height; a chopped cosine shape with a 1.4 axial peak; and a top-peaked shape with a 1.5 axial peak located at 78% core height.

The power transients evaluated were typically ones where the power was rapidly increased above the initial power by 50% to 70%. Power was then held power constant for a short time and subsequently reduced to 30% of its initial value. The flow was held constant during these tests.

The flow transients typically ramped flow down from an initial value at a fixed rate until it decreased to 30% of its initial value. During the flow transients the power was ramped down at a fixed rate over 4 seconds where it reached 30% of its initial value.

A comparison of the measured vs. predicted dryout times is shown in Figure 5-4. As shown, with the exception of a few power-transient tests, the predictions are more conservative than the measurements. All of the flow transient tests are predicted conservatively.

A typical ABWR LOCA transient is characterized by a rapid decrease in flow and a slow decrease in reactor power in the first 3 seconds of the event. Therefore, the slight non-conservatism shown in the power transient tests does not impact the overall conclusion that GOBLIN predicts boiling transition time conservatively.

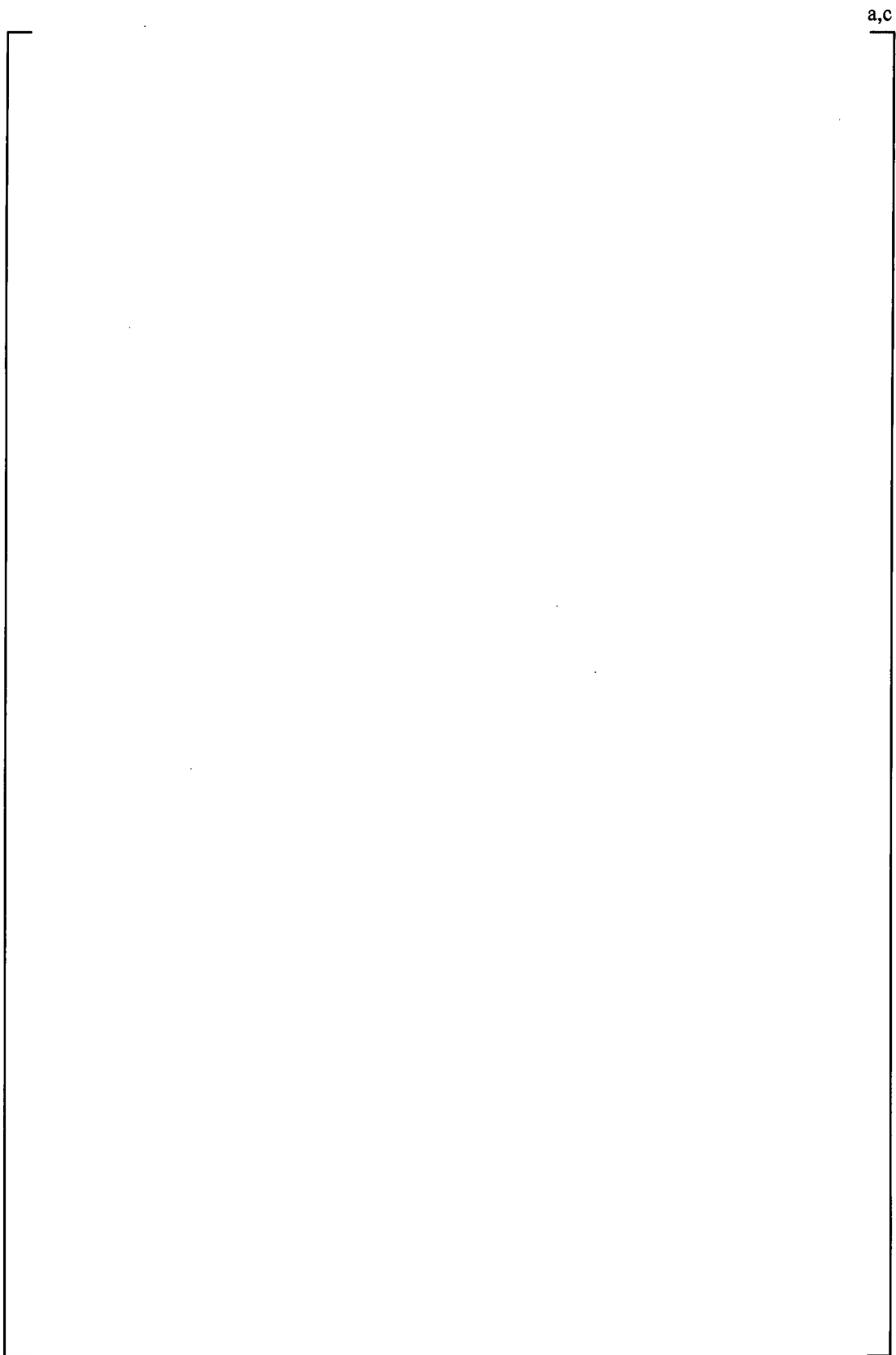


Figure 5-3 FRIGG Loop Test Section



Figure 5-4 Comparison of Measured and Predicted Dryout Times

6 COMPLIANCE WITH 10 CFR 50 APPENDIX K

This section describes the Westinghouse ABWR ECCS Evaluation Model compliance with the requirements of 10 CFR 50 Appendix K.

6.1 SOURCES OF HEAT DURING THE LOCA

Section I.A of Appendix K:

For the heat sources listed in paragraphs I.A.1 to 4 of this appendix it must be assumed that the reactor has been operating continuously at a power level at least 1.02 times the licensed power level (to allow for instrumentation error), with the maximum peaking factor allowed by the technical specifications. An assumed power level lower than the level specified in this paragraph (but not less than the licensed power level) may be used provided the proposed alternative value has been demonstrated to account for uncertainties due to power level instrumentation error. A range of power distribution shapes and peaking factors representing power distributions that may occur over the core lifetime must be studied. The selected combination of power distribution shape and peaking factor should be the one that results in the most severe calculated consequences for the spectrum of postulated breaks and single failures that are analyzed.

Evaluation Model Compliance with Section I.A:

Westinghouse may account for power level instrumentation uncertainties less than 2 percent, but no less than the power level uncertainty that has been demonstrated.

6.1.1 Initial Stored Energy in the Fuel

Section I.A.1 of Appendix K:

The steady-state temperature distribution and stored energy in the fuel before the hypothetical accident shall be calculated for the burn-up that yields the highest calculated cladding temperature (or, optionally, the highest calculated stored energy.) To accomplish this, the thermal conductivity of the UO₂ shall be evaluated as a function of burn-up and temperature, taking into consideration differences in initial density, and the thermal conductance of the gap between the UO₂ and the cladding shall be evaluated as a function of the burn-up, taking into consideration fuel densification and expansion, the composition and pressure of the gases within the fuel rod, the initial cold gap dimension with its tolerances, and cladding creep.

Evaluation Model compliance with Section I.A.1:

The [

] ^{a,c}

[
] ^{a,c}

6.1.2 Fission Heat

Section I.A.2 of Appendix K:

Fission heat shall be calculated using reactivity and reactor kinetics. Shutdown reactivities resulting from temperatures and voids shall be given their minimum plausible values, including allowance for uncertainties, for the range of power distribution shapes and peaking factors indicated to be studied above. Rod trip and insertion may be assumed if they are calculated to occur.

Evaluation Model compliance with Section I.A.2:

Fission heat is calculated by a point kinetics model as described in Section 3.7 of Reference 3. The model includes feedback effects from voiding, Doppler broadening, moderator temperature, and control rod worth. The point kinetics parameters are generated from the nuclear design code PHOENIX for a range of power distributions, peaking factors, and void fractions throughout the fuel life. Conservative values for these parameters, i.e., those which yield the highest fission heat generation, are used in the GOBLIN model. Specifically:

- The delayed neutron fraction (β) will be given its highest calculated value, typically corresponding to the beginning-of-life conditions.
- The void and Doppler reactivity coefficients will be given their highest calculated value (lowest absolute value).
- The reactivity worth of the control rods will be given a conservative (low) value.

This methodology and sensitivity studies demonstrating the conservatism of the fission heat generation are provided in Reference 4.

6.1.3 Decay of Actinides

Section I.A.3 of Appendix K:

The heat from the radioactive decay of actinides, including neptunium and plutonium generated during operation, as well as isotopes of uranium, shall be calculated in accordance with fuel cycle calculations and known radioactive properties. The actinide decay heat chosen shall be that appropriate for the time in the fuel cycle that yields the highest calculated fuel temperature during the LOCA.

Evaluation Model compliance with Section I.A.3:

The actinide decay energy release contribution is determined by calculating the equilibrium concentrations of the isotopes U^{239} and Np^{239} , and then using the energy per disintegration and half-life for these isotopes to evaluate the time dependence of the energy release after shutdown. The elements U^{239} and Np^{239} are the only significant activation products that contribute to the decay energy release in the time range of interest for LOCAs. The energy release from the activation products of U^{235} namely U^{236} and U^{237} are insignificant, approximately a factor of 20-30 less, when compared to the energy release of U^{239} and Np^{239} for this range.

The actinide decay power is determined from the decay rate equations described in the American Nuclear Society Standard 5.1 (Reference 9) and is modeled in GOBLIN as the decay power groups 12, 13, and 14 (see Section 3.7.1 of Reference 2).

The U^{239} production per fission, $Cr\sigma_{25}/\sigma f_{25}$, is chosen to yield the highest actinide decay power throughout the fuel life, typically end of life.

6.1.4 Fission Product Decay

Section I.A.4 of Appendix K:

The heat generation rates from radioactive decay of fission products shall be assumed to be equal to 1.2 times the values for infinite operating time in the ANS Standard (Proposed American Nuclear Society Standards-- "Decay Energy Release Rates Following Shutdown of Uranium-Fueled Thermal Reactors." Approved by Subcommittee ANS-5, ANS Standards Committee, October 1971). This standard has been approved for incorporation by Reference by the Director of the Federal Register. A copy of the standard is available for inspection at the NRC Library, 11545 Rockville Pike, Rockville, Maryland 20852-2738. The fraction of the locally generated gamma energy that is deposited in the fuel (including the cladding) may be different from 1.0; the value used shall be justified by a suitable calculation.

Evaluation Model compliance with Section I.A.4:

Decay of U^{235} fission products is computed by a relationship in the form of the summation of eleven decay equations. The fission product decay model is described in Section 3.7.1 of Reference 2. Comparison with the tabulated 1971 ANS proposed standard (Reference 9) is shown in Table 3-3 of Reference 2. The agreement is excellent. The local decay heat power calculated by this model is multiplied by 1.2 in accordance with the requirement in paragraph I.A.4. The fraction of gamma energy deposited in the fuel along with gamma and neutron deposition in the coolant may be specified as a function of time through the transient. The actual deposition fractions are described and justified in Reference 3.

6.1.5 Metal-Water Reaction Rate

Section I.A.5 of Appendix K:

The rate of energy release, hydrogen generation, and cladding oxidation from the metal/water reaction shall be calculated using the Baker-Just equation (Baker, L., Just, L.C., "Studies of Metal Water Reactions at High Temperatures, III. Experimental and Theoretical Studies of the Zirconium-Water Reaction," ANL-6548, page 7, May 1962). This publication has been approved for incorporation by reference by the Director of the Federal Register. A copy of the publication is available for inspection at the NRC Library, 11545 Rockville Pike, Two White Flint North, Rockville, Maryland 20852-2738. The reaction shall be assumed not to be steam limited. For rods whose cladding is calculated to rupture during the LOCA, the inside of the cladding shall be assumed to react after the rupture. The calculation of the reaction rate on the inside of the cladding shall also follow the Baker-Just equation, starting at the time when the cladding is calculated to rupture, and extending around the cladding inner circumference and axially no less than 1.5 inches each way from the location of the rupture, with the reaction assumed not to be steam limited.

Evaluation Model compliance with Section I.A.5:

The heat generation due to local metal-water reaction is considered in the cladding temperature calculation as described in Section 3.7.2 of Reference 2 for GOBLIN and Section 4.4 of Reference 2 for CHACHA. In these models, the reaction between Zircaloy cladding and steam is assumed to follow the parabolic rate law of Baker and Just.

6.1.6 Reactor Internals Heat Transfer

Section I.A.6 of Appendix K:

Heat transfer from piping, vessel walls, and non-fuel internal hardware shall be taken into account.

Evaluation Model compliance with Section I.A.6:

Heat transfer from piping, vessel walls, and non-fuel internal hardware is accounted for according to the method described in Sections 3.5 and 3.6 of Reference 2.

6.2 SWELLING AND RUPTURE OF THE CLADDING AND FUEL ROD THERMAL PARAMETERS

Section I.B of Appendix K:

Each Evaluation Model shall include a provision for predicting cladding swelling and rupture from consideration of the axial temperature distribution of the cladding and from the difference in pressure between the inside and outside of the cladding, both as functions of time. To be acceptable the swelling and rupture calculations shall be based on applicable data in such a way

that the degree of swelling and incidence of rupture are not underestimated. The degree of swelling and rupture shall be taken into account in calculations of gap conductance, cladding oxidation and embrittlement, and hydrogen generation.

The calculations of fuel and cladding temperatures as a function of time shall use values for gap conductance and other thermal parameters as functions of temperature and other applicable time-dependent variables. The gap conductance shall be varied in accordance with changes in gap dimensions and any other applicable variables.

Evaluation Model compliance with Section I.B:

Section 6.2 of Reference 5 describes the comparison of mechanistic swelling and rupture model to the applicable set of data. Section 4.1 of Reference 6 describes the revision to the Westinghouse BWR LOCA Evaluation Model, which considers burst to occur when [

] ^{a,c}

Therefore, neither the incidence of rupture nor the degree of swelling is underestimated.

6.3 BLOWDOWN PHENOMENA

6.3.1 Break Characteristics and Flow

6.3.1.1 Break Spectrum

Section I.C.1.a of Appendix K:

In analyses of hypothetical loss-of-coolant accidents, a spectrum of possible pipe breaks shall be considered. This spectrum shall include instantaneous double-ended breaks ranging in cross-sectional area up to and including that of the largest pipe in the primary coolant system. The analysis shall also include the effects of longitudinal splits in the largest pipes, with the split area equal to the cross-sectional area of the pipe.

Evaluation Model compliance with Section I.C.1.a:

The LOCA sensitivity study topical report (Reference 3) reports the results of a break spectrum analysis including the double-ended guillotine break of the largest pipe in a typical BWR design. A break spectrum analysis is used to justify the selection of the worst case in a plant-specific BWR LOCA analysis.

A similar study for the ABWR design is described in Sections 4.5 and 4.6 of this report. This study includes a series of double-ended guillotine and longitudinal split breaks of the largest pipe connected to the reactor pressure vessel, as well as breaks in other piping connected to the reactor pressure vessel. The break spectrum analysis is used to identify the limiting cases for a plant-specific ABWR LOCA analysis.

6.3.1.2 Discharge Model

Section I.C.1.b of Appendix K:

For all times after the discharging fluid has been calculated to be two-phase in composition, the discharge rate shall be calculated by use of the Moody model (F.J. Moody, "Maximum Flow Rate of a Single Component, Two-Phase Mixture," Journal of Heat Transfer, Trans American Society of Mechanical Engineers, 87, No. 1, February, 1965). This publication has been approved for incorporation by reference by the Director of the Federal Register. A copy of this publication is available for inspection at the NRC Library, 11545 Rockville Pike, Rockville, Maryland 20852-2738. The calculation shall be conducted with at least three values of a discharge coefficient applied to the postulated break area, these values spanning the range from 0.6 to 1.0. If the results indicate that the maximum clad temperature for the hypothetical accident is to be found at an even lower value of the discharge coefficient, the range of discharge coefficients shall be extended until the maximum clad temperatures calculated by this variation has been achieved.

Evaluation Model compliance with Section I.C.1.b:

The Moody model is used to calculate the two-phase discharge rate. The application and integration of the Moody model into the complete break flow model for all regimes is described in Section 3.3.6 of Reference 2.

6.3.1.3 End of Blowdown

Section I.C.1.c of Appendix K:

(Applies Only to Pressurized Water Reactors.) For postulated cold leg breaks, all emergency cooling water injected into the inlet lines or the reactor vessel during the bypass period shall in the calculations be subtracted from the reactor vessel calculated inventory. This may be executed in the calculation during the bypass period, or as an alternative the amount of emergency core cooling water calculated to be injected during the bypass period may be subtracted later in the calculation from the water remaining in the inlet lines, downcomer, and reactor vessel lower plenum after the bypass period. This bypassing shall end in the calculation at a time designated as the "end of bypass," after which the expulsion or entrainment mechanisms responsible for the bypassing are calculated not to be effective. The end-of-bypass definition used in the calculation shall be justified by a suitable combination of analysis and experimental data. Acceptable methods for defining "end of bypass" include, but are not limited to, the following:

(1) Prediction of the blowdown calculation of downward flow in the downcomer for the remainder of the blowdown period; (2) Prediction of a threshold for droplet entrainment in the upward velocity, using local fluid conditions and a conservative critical Weber number.

Evaluation Model Compliance with Section I.C.1.c:

This requirement applies only to pressurized water reactors.

6.3.1.4 Noding Near the Break and the ECCS Injection Points

Section I.C.1.d of Appendix K:

The noding in the vicinity of and including the broken or split sections of pipe and the points of ECCS injection shall be chosen to permit a reliable analysis of the thermodynamic history in these regions during blowdown.

Evaluation Model compliance with Section I.C.1.d:

Reference 3 shows the LOCA peak clad temperature sensitivity to noding near the break for a BWR. These results demonstrate that the break noding used in the evaluation model is sufficient to adequately represent the hydraulic behavior and reactor vessel geometry in the vicinity of the break.

Noding near the break in the ABWR LOCA analysis is similar to that used in the BWR LOCA analysis. Since the PCT for an ABWR occurs as a result of the rapid coastdown of the reactor internal pumps, the resulting PCT is less sensitive to break modeling than for a BWR.

6.3.2 Frictional Pressure Drops

Section I.C.2 of Appendix K:

The frictional losses in pipes and other components including the reactor core shall be calculated using models that include realistic variation of friction factor with Reynolds number, and realistic two-phase friction multipliers that have been adequately verified by comparison with experimental data, or models that prove at least equally conservative with respect to maximum clad temperature calculated during the hypothetical accident. The modified Baroczy correlation (Baroczy, C. J., "A Systematic Correlation for Two-Phase Pressure Drop," Chem. Enging. Prog. Symp. Series, No. 64, Vol. 62, 1965) or a combination of the Thom correlation (Thom, J.R.S., "Prediction of Pressure Drop During Forced Circulation Boiling of Water," Int. J. of Heat & Mass Transfer, 7, 709-724, 1964) for pressures equal to or greater than 250 psia and the Martinelli-Nelson correlation (Martinelli, R. C. Nelson, D.B., "Prediction of Pressure Drop During Forced Circulation Boiling of Water," Transactions of ASME, 695-702, 1948) for pressures lower than 250 psia is acceptable as a basis for calculating realistic two-phase friction multipliers.

Evaluation Model compliance with Section I.C.2:

The frictional losses are calculated using models that include a realistic variation of the friction factor with Reynolds number and realistic two-phase friction multipliers that are based on acceptable open literature correlations and test data as described in Section 3.3.3 of Reference 2.

6.3.3 Momentum Equation

Section I.C.3 of Appendix K:

The following effects shall be taken into account in the conservation of momentum equation: (1) temporal change of momentum, (2) momentum convection, (3) area change momentum flux, (4) momentum change due to compressibility, (5) pressure loss resulting from wall friction, (6) pressure loss resulting from area change, and (7) gravitational acceleration. Any omission of one or more of these terms under stated circumstances shall be justified by comparative analyses or by experimental data.

Evaluation Model compliance with Section I.C.3:

The momentum equation used in GOBLIN includes all of the required effects as described in Section 3.1.3 of Reference 2 and Section 4.2 of Reference 5.

6.3.4 Critical Heat Flux

Section I.C.4 of Appendix K:

- a. *Correlations developed from appropriate steady-state and transient-state experimental data are acceptable for use in predicting the critical heat flux during LOCA transients. The computer programs in which these correlations are used shall contain suitable checks to assure that the physical parameters are within the range of parameters specified for use of the correlations by their respective authors.*
- b. *Steady-state CHF correlations acceptable for use in LOCA transients include, but are not limited to, the following:*
 - (1) *W 3. L. S. Tong, "Prediction of Departure from Nucleate Boiling for an Axially Non-uniform Heat Flux Distribution," Journal of Nuclear Energy, Vol. 21, 241-248, 1967.*
 - (2) *B&W-2. J. S. Gellerstedt, R. A. Lee, W. J. Oberjohn, R. H. Wilson, L. J. Stanek, "Correlation of Critical Heat Flux in a Bundle Cooled by Pressurized Water," Two-Phase Flow and Heat Transfer in Rod Bundles, ASME, New York, 1969.*
 - (3) *Hench-Levy. J. M. Healzer, J. E. Hench, E. Janssen, S. Levy, "Design Basis for Critical Heat Flux Condition in Boiling Water Reactors," APED-5186, GE Company Private report, July 1966.*
 - (4) *Macbeth. R. V. Macbeth, "An Appraisal of Forced Convection Burnout Data," Proceedings of the Institute of Mechanical Engineers, 1965-1966.*

- (5) *Barnett. P. G. Barnett, "A Correlation of Burnout Data for Uniformly Heated Annuli and Its Uses for Predicting Burnout in Uniformly Heated Rod Bundles," AEEW-R-463, 1966.*
 - (6) *Hughes. E. D. Hughes, "A Correlation of Rod Bundle Critical Heat Flux for Water in the Pressure Range 150 to 725 psia," IN-1412, Idaho Nuclear Corporation, July 1970.*
- c. *Correlations of appropriate transient CHF data may be accepted for use in LOCA transient analyses if comparisons between the data and the correlations are provided to demonstrate that the correlations predict values of CHF which allow for uncertainty in the experimental data throughout the range of parameters for which the correlations are to be used. Where appropriate, the comparisons shall use statistical uncertainty analysis of the data to demonstrate the conservatism of the transient correlation.*
 - d. *Transient CHF correlations acceptable for use in LOCA transients include, but are not limited to, the following:*
 - (1) *GE transient CHF. B. C. Slifer, J. E. Hench, "Loss-of-Coolant Accident and Emergency Core Cooling Models for General Electric Boiling Water Reactors," NEDO-10329, General Electric Company, Equation C-32, April 1971.*
 - e. *After CHF is first predicted at an axial fuel rod location during blowdown, the calculation shall not use nucleate boiling heat transfer correlations at that location subsequently during the blowdown even if the calculated local fluid and surface conditions would apparently justify the reestablishment of nucleate boiling. Heat transfer assumptions characteristic of return to nucleate boiling (rewetting) shall be permitted when justified by the calculated local fluid and surface conditions during the reflood portion of a LOCA.*

Evaluation Model compliance with Section I.C.4:

The critical heat flux in the system and hot assembly analyses is determined using an NRC-approved CPR correlation that is applicable to the fuel design.

6.3.5 Post-CHF Heat Transfer Correlations

Section I.C.5 of Appendix K:

- a. *Correlations of heat transfer from the fuel cladding to the surrounding fluid in the post-CHF regimes of transition and film boiling shall be compared to applicable steady-state and transient-state data using statistical correlation and uncertainty analyses. Such comparison shall demonstrate that the correlations predict values of heat transfer co-efficient equal to or less than the mean value of the applicable experimental heat transfer data throughout the range of parameters for which the correlations are to be used. The comparisons shall quantify the relation of the correlations to the statistical uncertainty of the applicable data.*

- b. *The Groeneveld flow film boiling correlation (equation 5.7 of D.C. Groeneveld, "An Investigation of Heat Transfer in the Liquid Deficient Regime," AECL-3281, revised December 1969) and the Westinghouse correlation of steady-state transition boiling ("Proprietary Redirect/Rebuttal Testimony of Westinghouse Electric Corporation," USNRC Docket RM-50-1, page 25-1, October 26, 1972) are acceptable for use in the post-CHF boiling regimes. In addition, the transition boiling correlation of McDonough, Milich, and King (J.B. McDonough, W. Milich, E.C. King, "An Experimental Study of Partial Film Boiling Region with Water at Elevated Pressures in a Round Vertical Tube," Chemical Engineering Progress Symposium Series, Vol. 57, No. 32, pages 197-208, (1961) is suitable for use between nucleate and film boiling. Use of all these correlations is restricted as follows:*
- (1) *The Groeneveld correlation shall not be used in the region near its low-pressure singularity,*
 - (2) *The first term (nucleate) of the Westinghouse correlation and the entire McDonough, Milich, and King correlation shall not be used during the blowdown after the temperature difference between the clad and the saturated fluid first exceeds 300°F,*
 - (3) *Transition boiling heat transfer shall not be reapplied for the remainder of the LOCA blowdown, even if the clad superheat returns below 300°F, except for the reflood portion of the LOCA when justified by the calculated local fluid and surface conditions.*
- c. *Evaluation Models approved after October 17, 1988, which make use of the Dougall-Rohsenow flow film boiling correlation (R.S. Dougall and W.M. Rohsenow, "Film Boiling on the Inside of Vertical Tubes with Upward Flow of Fluid at Low Qualities," MIT Report Number 9079 26, Cambridge, Massachusetts, September 1963) may not use this correlation under conditions where nonconservative predictions of heat transfer result. Evaluation Models that make use of the Dougall-Rohsenow correlation and were approved prior to October 17, 1988, continue to be acceptable until a change is made to, or an error is corrected in, the Evaluation Model that results in a significant reduction in the overall conservatism in the Evaluation Model. At that time continued use of the Dougall-Rohsenow correlation under conditions where nonconservative predictions of heat transfer result will no longer be acceptable. For this purpose, a significant reduction in the overall conservatism in the Evaluation Model would be a reduction in the calculated peak fuel cladding temperature of at least 50°F from that which would have been calculated on October 17, 1988, due either to individual changes or error corrections or the net effect of an accumulation of changes or error corrections.*

Evaluation Model compliance with Section I.C.5:

The heat transfer correlations and regimes modeled in GOBLIN are described in Section 3.5 of Reference 2. The post-CHF convective heat transfer coefficient is calculated using the Groeneveld 5.7 correlation, the NRC-approved Westinghouse upper-head injection correlation, the modified Bromley correlation, and single-phase steam correlations. The Groeneveld

correlation is used for flow film boiling in the higher pressure range. For lower pressures, where the Groeneveld correlation has a singularity, a transition is made to the Westinghouse UHI correlation. This NRC-approved correlation is more conservative than the Dougall-Rohsenow correlation, which is non-conservative when compared to some heat transfer data.

The lower limit to the heat transfer coefficient is calculated using the modified Bromley correlation, which is based on zero flow. The modified Bromley correlation has been demonstrated to be a conservative lower limit when compared to a wide range of tests. A more detailed discussion of the applicability of this correlation is given Section 6.1.7 of Reference 2.

Once dryout is calculated to occur, the heat transfer mode is forced to remain in the post-dryout regime, even if rewet and transition boiling are calculated to occur.

6.3.6 Pump Modeling

Section I.C.6 of Appendix K:

The characteristics of rotating primary system pumps (axial flow, turbine, or centrifugal) shall be derived from a dynamic model that includes momentum transfer between the fluid and the rotating member, with variable pump speed as a function of time. The pump model resistance used for analysis should be justified. The pump model for the two-phase region shall be verified by applicable two-phase pump performance data. For BWR's after saturation is calculated at the pump suction, the pump head may be assumed to vary linearly with quality, going to zero for one percent quality at the pump suction, so long as the analysis shows that core flow stops before the quality at pump suction reaches one percent.

Evaluation Model compliance with Section I.C.6:

The recirculation pump model is described in Section 3.4.1 of Reference 2 and Section 3.4.1 of this report. An angular momentum balance is solved for the pump, including all contributing torques. Single-phase and degraded two-phase pump performance are modeled through user-specified performance curves.

6.3.7 Core Flow Distribution During Blowdown

Applies only to pressurized water reactors

6.4 POST-BLOWDOWN PHENOMENA; HEAT REMOVAL BY THE ECCS

6.4.1 Single Failure Criterion

Section I.D.1 of Appendix K:

An analysis of possible failure modes of ECCS equipment and of their effects on ECCS performance must be made. In carrying out the accident evaluation the combination of ECCS subsystems assumed to be operative shall be those available after the most damaging single failure of ECCS equipment has taken place.

Evaluation Model compliance with Section I.D.1:

The evaluation of the LOCA is performed assuming the single active component failure that results in the most severe consequences. The combinations of ECC subsystems assumed to be operating are those remaining after the component failure has occurred.

In an ABWR, no single active failure of ECCS equipment results in an extended uncover of the core. The limiting single failure is determined as the one that results in the least transient system inventory.

6.4.2 Containment Pressure

Section I.D.2 of Appendix K:

The containment pressure used for evaluating cooling effectiveness during reflood and spray cooling shall not exceed a pressure calculated conservatively for this purpose. The calculation shall include the effects of operation of all installed pressure-reducing systems and processes.

Evaluation Model compliance with Section I.D.2:

The ABWR Evaluation Model will assume atmospheric pressure in the containment analysis throughout the LOCA transient.

6.4.3 Calculation of Reflood Rate

Applies only to Pressurized Water Reactors.

6.4.4 Steam Interaction with Emergency Core Cooling Water

Applies only to Pressurized Water Reactors.

6.4.5 Refill and Reflood Heat Transfer

Applies only to Pressurized Water Reactors.

6.4.6 Convective Heat Transfer Coefficients for Boiling Water Reactor Fuel Rods Under Spray Cooling

Section I.D.6 of Appendix K:

Following the blowdown period, convective heat transfer shall be calculated using coefficients based on appropriate experimental data. For reactors with jet pumps and having fuel rods in a 7 x 7 fuel assembly array, the following convective coefficients are acceptable:

- *During the period following lower plenum flashing but prior to the core spray reaching rated flow, a convective heat transfer coefficient of zero shall be applied to all fuel rods.*
- *During the period after core spray reaches rated flow but prior to reflooding, convective heat transfer coefficients of 3.0, 3.5, 1.5, and 1.5 Btu-hr⁻¹-ft⁻²-°F⁻¹ shall be applied to the fuel rods in the outer corners, outer row, next to outer row, and to those remaining in the interior, respectively, of the assembly.*
- *After the two-phase reflooding fluid reaches the level under consideration, a convective heat transfer coefficient of 25 Btu-hr⁻¹-ft⁻²-°F⁻¹ shall be applied to all fuel rods.*

Evaluation Model compliance with Section I.D.6:

This requirement applies to BWRs with jet pumps. The ABWR has internal recirculation pumps with the feedwater nozzles representing the lowest of the large piping systems connected to the reactor pressure vessel. As a result, the ABWR LOCA transient does not experience the same phenomena as a BWR in that the ABWR core does not experience extended uncover during the event, even for the most limiting break location and single failure. The PCT is predicted to occur early in the transient when the reactor internal pumps coastdown due to their loss of motive power. The two-phase convective heat transfer coefficients predicted by GOBLIN will be used in the rod heatup calculation.

6.4.7 The Boiling Water Reactor Channel Box Under Spray Cooling

Section I.D.7 of Appendix K:

Following the blowdown period, heat transfer from, and wetting of, the channel box shall be based on appropriate experimental data. For reactors with jet pumps and fuel rods in a 7 x 7 fuel assembly array, the following heat transfer coefficients and wetting time correlation are acceptable.

- *During the period after lower plenum flashing, but prior to core spray reaching rated flow, a convective coefficient of zero shall be applied to the fuel assembly channel box.*
- *During the period after core spray reaches rated flow, but prior to wetting of the channel, a convective heat transfer coefficient of 5 Btu-hr⁻¹-ft⁻²-°F⁻¹ shall be applied to both sides of the channel box.*

- *Wetting of the channel box shall be assumed to occur 60 seconds after the time determined using the correlation based on the Yamanouchi analysis ("Loss-of-Coolant Accident and Emergency Core Cooling Models for General Electric Boiling Water Reactors," General Electric Company Report NEDO-10329, April 1971). This report was approved for incorporation by reference by the Director of the Federal Register. A copy of the report is available for inspection at the NRC Library, 11545 Rockville Pike, Rockville, Maryland 20852-2738.*

Evaluation Model compliance with Section I.D.7:

This requirement applies to BWRs with jet pumps. The ABWR has internal recirculation pumps with the feedwater nozzles representing the lowest of the large piping systems connected to the reactor pressure vessel. As a result, the ABWR LOCA transient does not experience the same phenomena as a BWR in that the extended uncovering of the core is not predicted during the transient and the channel box remains wet throughout the transient.

7 REFERENCES

1. RPB 90-93-P-A, "Boiling Water Reactor Emergency Core Cooling System Evaluation Model: Code Description and Qualification," October 1991
2. CENPD-300-P-A, "Reference Safety Report for Boiling Water Reactor Reload Fuel," July 1996.
3. RPB 90-94-P-A, "Boiling Water Reactor Emergency Core Cooling System Evaluation Model: Code Sensitivity," October 1991.
4. CENPD-283-P-A, "Boiling Water Reactor Emergency Core Cooling System Evaluation Model: Code Sensitivity for SVEA-96 Fuel," July 1996.
5. CENPD-293-P-A, "BWR ECCS Evaluation Model: Supplement 1 to Code Description and Qualification," July 1996.
6. WCAP-15682-P-A, "Westinghouse BWR ECCS Evaluation Model: Supplement 2 to Code Description, Qualification and Application," April 2003.
7. WCAP-16078-P-A, "Westinghouse BWR ECCS Evaluation Model: Supplement 3 to Code Description, Qualification and Application to SVEA-96 Optima2 Fuel," November 2004.
8. WCAP-16081-P-A, "10x10 SVEA Fuel Critical Power Experiments and CPR Correlation: SVEA-96 Optima2," March 2005.
9. ANS-5.1 1973 Decay Energy Release Rates Following Shutdown of Uranium-Fueled Thermal Reactors, Draft ANS-5.1 / N18.6, October 1973.
10. Code of Federal Regulations, 10 Part 50, Office of the Federal Register, National Archives and Records Administration, 1986.

APPENDIX A ROADMAP TO THE METHODOLOGY CHANGES

A.1 INTRODUCTION

The original BWR LOCA Evaluation Model, USA1, which was approved by the NRC in 1989, is described in RPB 90-93-P-A (Reference A-1) and RPB 90-94-P-A (Reference A-2). This methodology was revised in 1996 with the USA2 Evaluation Model, described in CENPD-283-P-A (Reference A-3) and CENPD-293-P-A (Reference A-4); in 2003 with the USA4 Evaluation Model described in WCAP-15682-P-A (Reference A-5); and in 2004 with USA5 Evaluation Model described in WCAP-16078-P-A (Reference A-6). The USA6 Evaluation Model is described in WCAP-16865-P (Reference A-7), which was withdrawn in February 2009. WCAP-16865-P has been revised and will be resubmitted for review and approval in late 2009. All of the documents mentioned above apply only to BWRs.

The Evaluation Model described in this report, USA7, pertains to ABWR applications. Because of the unique features of the ABWR, approval of the USA6 Evaluation Model is not required for ABWR applications.

A.2 MAJOR ASPECTS OF THE EVALUATION MODEL

A.2.1 Momentum Equation

As described in Reference A-4, Section 4.2:

The spatial acceleration term in the momentum equation has been modified to account more accurately for uneven velocities of water and steam. This change has insignificant effects on typical LOCA transients and has been introduced to improve the consistency of the fluid flow model as shown in Section 7.4 of Reference A-4. The new formulation was assessed and qualified by repeating pertinent cases in the GOBLIN qualification.

Per the NRC SER of Reference A-4:

The Technical Evaluation attached to the SER acknowledged the change to the momentum equation and cited a study showing that the GOBLIN code with the new formulation resulted in an early prediction of dryout time and in a slightly higher temperature than in old analysis. No limitations or conditions were placed upon the use of this modification.

A.2.2 Countercurrent Flow Limitation (CCFL) Model

As described in Reference A-3, Section 7.1:

The BWR LOCA Evaluation Model has a comprehensive CCFL model for determining the rate of liquid drainage into the SVEA-96 fuel assembly. The correlation is documented in Reference A-1, Section 3.3. The CCFL correlation was originally developed for 8 x 8 fuel

assemblies. Since its original development, the correlation has been generalized and validated for many geometries. Further, the correlation, with its general geometric dependence, has been confirmed valid for QUAD+ fuel through comparisons with experimental data (see response to Question 8 in Reference A-1). The SVEA-96 geometry is basically the same as the SVEA-64 and QUAD+ geometry. Differences in area of the flow restrictions are accounted for in the CCFL correlation. In the LOCA Evaluation Model, the CCFL correlation with the appropriate geometric parameters for SVEA-96 fuel will be used.

Per the NRC SER of Reference A-3:

The coefficients in the CCFL correlation that were shown to be insensitive for the SVEA-96 fuel should not be extended to other fuels without being validated by experimental data.

In addition, Westinghouse was required to demonstrate the acceptability the CCFL coefficient in any instance when the calculated PCT is greater than 2100°F. In this case, the CCFL correlation shall include a conservative bias that bounds the scatter in the database. The bias introduced to the base CCFL correlation will be such that conservative bounding predictions are obtained from the database of all fuel assembly components that were used to derive the basic CCFL correlation.

As described in Reference A-6, Section 5.4.2:

The change to the CCFL model removes the restriction placed on the USA2 Evaluation Model. This change was made to the CCFL correlation to apply a conservative bias such that it bounds all scatter in the correlation database.

The present CCFL correlation replaces the wetted perimeter term in one of the correlation coefficients with one composed of an effective diameter relation that is a function of the local cross-sectional flow area. The more restrictive effective diameter relation better represents the observed data and eliminates the restriction placed on earlier versions of the Evaluation Model.

To qualify the applicability of the modified CCFL model to SVEA-96 Optima2 fuel, Westinghouse performed a sensitivity study demonstrating the effect of the new fuel design and the modified CCFL correlation on the overall LOCA response.

Per the NRC SER of Reference A-6:

The staff concurred that the change to the CCFL acts in the same manner as the imposed restriction required by the SER of Reference A-3 and found that the CCFL model with appropriate geometric parameters is acceptable for applications involving SVEA-96, SVEA-96+, and SVEA-96 Optima2 fuel designs.

A.2.3 Two-Phase Level Tracking

The GOBLIN code has the capability to specify a series of control volumes in which a two-phase level is to be calculated and tracked with time. The level tracking model replaces a fixed control volume boundary with a moving boundary located at the two-phase level. The model can be used when it is important to know the location of the two-phase mixture level.

As described in Reference A-3, Section 6.1.2:

As a result of a sensitivity study on the use of level tracking in the upper plenum, it was determined that it is conservative to deactivate the level tracking option, and that the additional accuracy of tracking the upper plenum level is not warranted.

Per the NRC SER of Reference A-3:

The TER attached to the SER acknowledged the level tracking sensitivity study. The SER made no limitations or conditions regarding the use of level tracking in the upper plenum.

As described in Reference A-6, Section 5.1.1:

The level tracking model calculates the motion of the control volume interface such that it moves with the two-phase mixture level. The intent of the level tracking model is to capture the transient interaction of the mixture level with flow paths or with ECCS injection when it is impractical to do so by additional noding detail. Sensitivity studies were presented on the level tracking feature in Section 4.1.3 of RPB 90-94-P-A (Reference A-2) and Section 6.1.2 of CENPD-283-P-A (Reference A-3). The focus of these sensitivity studies was the use of level tracking in the upper plenum. Section 6.1.2 of CENPD-283-P-A (Reference A-3) provided the basis for not using the level tracking feature in the upper plenum.

The focus of the sensitivity study presented in this section is on the use of level tracking in the lower plenum. Cases were run with the level tracking feature activated and deactivated in the lower plenum. The results were virtually identical. Since level tracking in the lower plenum does not affect the timing of these key events, the heat transfer coefficients that are used to determine the cladding temperature response of the hot plane will be identical. As a result, the cladding temperature response will also be identical. This sensitivity shows that the use of the level tracking feature in the lower plenum is not warranted. Therefore, standard practice will be to not use level tracking in the lower plenum of the USA5 Evaluation Model unless warranted by the specific application.

However, level tracking remains an option to capture important thermal-hydraulic phenomena when it is not practical to do so with fixed control volumes. Level tracking continues to be used in the reactor vessel annulus to ensure that conditions upstream of the break are determined correctly.

Per the NRC SER of Reference A-6:

The SER indicated that the use of the optional level tracking model in the lower plenum of the GOBLIN vessel model is acceptable.

A.2.4 Convective Spray Heat Transfer Coefficients

As described in Reference A-3, Section 4.3:

Convective spray heat transfer coefficients as specified in 10 CFR 50 Appendix K are applicable for 7 x 7 fuel designs. Convective heat transfer coefficients have been derived for open lattice 8 x 8, SVEA-64/QUAD+ fuel from the coefficients prescribed in 10 CFR 50 Appendix K. These coefficients also were confirmed by experimental tests for 8 x 8 and SVEA-64/QUAD+. An extension of this application provides spray heat transfer coefficients for SVEA-96 fuel.

The approved values of convective heat transfer coefficients per Reference A-3 are presented in Table A-2.

Per the NRC SER of Reference A-3:

The SER concurred with the procedure to show conservatism in the method used to determine the spray cooling heat transfer coefficients. However, since the procedure was not supported by experimental data, it should not be extended to other fuels without experimental verification.

As described in Reference A-6, Section 6.1.1:

The convective spray heat transfer coefficients described in Section 7.2 of CENPD-283-P-A (Reference A-3) are applied without modification to analyses determining the hot plane heatup response for a reactor containing SVEA-96 Optima2 fuel. The spray cooling heat transfer coefficients are given in Table A-3.

Per the NRC SER of Reference A-6:

Because of the similarity of the lattice layout to the SVEA-96/96+ fuel design, the staff found applying SVEA-64 spray coefficients to the Optima2 fuel to be conservative and acceptable.

A.2.5 Critical Power Ratio (CPR) Correlation

As described in Reference A-3, Section 4.2:

The SVEA-96 CPR correlation was developed through a full-scale thermal-hydraulic verification program in the ABB Atom FRIGG loop. The resultant correlation is documented in Reference A-7, which has been approved by the U.S. NRC. This correlation, denoted by XL-S96, is implemented into the GOBLIN/DRAGON code. The implementation is analogous to the previous approved QUAD+ CPR correlation application.

Per the NRC SER of Reference A-3:

The SER (Reference A-8) on UR-89-210-P-A (Reference A-7) approved the use of the XL-S96 CPR correlation with the BISON computer code. However, Reference A-8 requires that when this correlation is implemented in other computer codes, the vendor must submit documentation of adequate implementation to the NRC. The SER also requires that the correlation be used to evaluate the SVEA-96 fuel assemblies for the revised range of applicability.

The adequacy of implementation of the XL-S96 CPR correlation into the GOBLIN series will be reviewed with CENPD-293-P (Reference A-4), since this version of GOBLIN/DRAGON/CHACHA-3C was viewed to be an intermediary state.

As described in Reference A-4, Section 4.1:

A CPR correlation using the critical quality-boiling length formulation has been introduced in the thermal-hydraulic code system GOBLIN/DRAGON.

The GEXL correlation, also described in Reference A-7, is chosen as the basis for all critical quality-boiling length type CPR correlations. The implementation of this base correlation is described in Section 4.1.2 of Reference A-4. As a sample case of the critical quality-boiling length CPR correlation, the implementation of the XL-S96 correlation is described in Section 4.1.3 of Reference A-4, and verification of proper implementation of the correlation is given in Section 7.1 of Reference A-4.

Per the NRC SER of Reference A-4:

The SER placed a condition on the use of the XL-S96 CPR correlation requiring that it be subject to the SER conditions in UR 89-210-P-A (Reference A-7) and Reference A-8.

As described in Reference A-6, Section 5.4.1:

CPR correlations are part of the heat transfer model in GOBLIN and DRAGON. The CPR correlation is used to determine the initial power of the hot assembly. The CPR correlation may also determine when boiling transition occurs during the LOCA transient if the fluid conditions are within the range of applicability of the correlation. The Westinghouse USA5 BWR ECCS Evaluation Model will use the SVEA-96 Optima2 CPR correlation that is approved by the NRC for applications involving the SVEA-96 Optima2 fuel design.

An NRC-approved CPR correlation that is applicable to the fuel-design being analyzed is used in the ECCS Evaluation Model RPB 90-93-P-A (Reference A-1). At the time this topical report was written, the CPR correlation for SVEA-96 Optima2 had not been approved by the NRC. Qualification of the SVEA-96 Optima2 CPR correlation was subsequently provided. The CPR correlation was installed in the GOBLIN code in accordance with the process described in Section 3.3.2.2 of Reference A-6 and has been used for licensing. The NRC will be informed of the resulting change to the GOBLIN code via the 10 CFR 50.46 reporting process.

Per the NRC SER of Reference A-6:

The SER indicated that the SVEA-96 Optima2 CPR correlation was being reviewed by the staff. After it is approved, Westinghouse may implement it into the USA5 EM model and report to the NRC through the 10 CFR 50.46 annual report process.

A new fuel design normally requires a specific CPR correlation approved by the NRC. The implementation of a new CPR correlation into GOBLIN has become a routine code update process, which includes the source code development, new CPR correlation validation, and non-Westinghouse fuel justifications. Westinghouse requested that this process be evaluated through the 10 CFR 50.46 annual report process. Therefore, the staff does not necessarily review the details of the implementation process. The staff has previously reviewed the proposed process from Reference 10 and determined that the requested process is acceptable as long as the new CPR correlation has been approved by the NRC and the change to the LOCA method is reported to the NRC through the 10 CFR 50.46 reporting process.

For version USA5, the currently approved CPR correlations (i.e., XL-S96, ABBD1.0, ABBD2.0) can still be used within the approved ranges of applicability. However, the new CPR correlation for SVEA-96 Optima2 fuel has not yet been approved by the NRC. Therefore, the current version of the SVEA-96 Optima2 fuel CPR correlation in USA5 cannot be used until it has received the approval of the staff.

On December 9, 2004, the NRC staff issued its safety evaluation (SE) approving Topical Report WCAP-16081-P-A, "10x10 SVEA Fuel Critical Power Experiments and CPR Correlation: SVEA-96 Optima2." As provided in the FSER for NRC license amendments issued on April 4, 2006 for the transition of the Quad Cities and Dresden units to Westinghouse Fuel, the NRC staff verified that all the conditions and limitations of the NRC-approved BWR LOCA methods were satisfied for this application.

A.2.6 Fuel Rod Conduction Model

As described in Reference A-4, Section 5.1:

The fuel rod conduction model described in Section 4.1 of Reference A-1 is unchanged. An optional feature is added to explicitly model the heat resistance due to crud on the cladding surface. The effective outside surface heat transfer coefficient is a function of the previous coefficient, the depth of the crud layer, and the thermal conductivity of the crud layer.

The depth of the crud layer is calculated using an NRC-approved fuel rod performance code and the thermal conductivity of crud used is consistent with the fuel performance code properties. For example, applications in the foreseen future shall use a crud depth from the STAV6.2 code and a crud thermal conductivity of 0.5 (W/m²K), which is also consistent with STAV6.2.

Per the NRC SER of Reference A-4:

The Technical Evaluation attached to the SER acknowledged the addition of the crud resistance model. The SER placed no limitations or conditions on its use.

As described in Reference A-6, Section 5.5.2.3:

A model has been introduced in the STAV7.2 code to describe the burnup-induced degradation of the fuel pellet conductivity. This model has replaced the STAV6.2 fuel pellet conductivity model in CHACHA-3D.

Per the NRC SER of Reference A-6:

The SER acknowledged the addition of the revised fuel pellet conductivity model but placed a condition upon its use until the NRC approval of the STAV7.2 code was complete. Westinghouse provided a letter to the NRC (Reference A-9), as required by the condition, after NRC approval of the STAV7.2 code was complete. The letter indicated that the applicable STAV7.2 models have been implemented in CHACHA-3D.

A.2.7 Heat Generation Model

As described in Reference A-4, Section 5.2:

The heat generation model, as described in Section 4.3 of Reference A-4, is unchanged except for the radial power distribution within the fuel pellet, and will be supplied from the appropriate NRC-approved fuel performance code. For example, results from the STAV6.2 code will be used as input to CHACHA-3. In addition, options are available in CHACHA-3 to assume a uniform radial power distribution, or a Bessel function based radial power distribution.

Per the NRC SER of Reference A-4:

The Technical Evaluation attached to the SER acknowledged the use of the uniform radial power distribution model and the Bessel function model in CHACHA. No conditions or limitations were placed upon their use in the SER.

As described in Reference A-6, Section 5.5.2.3:

The burnup-dependent TUBRNP model in STAV7.2 has been implemented in CHACHA-3D and will be used in the USA5 Evaluation Model. This model takes into account power generation by plutonium isotopes, resulting in a more precise radial power distribution in the pellet rim region.

Per the NRC SER of Reference A-6:

The SER acknowledged the change to the pellet heat generation model, but placed a condition upon its use until NRC approval of the STAV7.2 code was complete. Westinghouse provided a letter to the NRC (Reference A-9), as required by the condition, after NRC approval of the STAV7.2 code was complete. The letter indicated that the applicable STAV7.2 models have been implemented in CHACHA-3D.

A.2.8 Metal-Water Reaction

As described in Reference A-4, Section 5.3:

The metal-water reaction model remains unchanged from that described in Section 4.4 of Reference A-1. The initial oxide depth on the cladding outer surface is calculated using an NRC-approved fuel performance code. For example, the STAV6.2 code (Reference A-10) will replace the PAD fuel rod performance code, identified in Reference A-2.

Per the NRC SER of Reference A-4:

The NRC SER indicated that acceptance of this change should be determined in the review of CENPD-285-P (Reference A-10). The NRC SER of Reference A-10 placed no restrictions on the use of the initial oxide depth except for limiting the rod average burnup range of STAV6.2 to 50 GWd/MTU.

As described in Reference A-6, Section 5.5.2.3:

The initial oxide depth of the cladding outer surface is determined by the STAV7.2 fuel performance code.

Per the NRC SER of Reference A-6:

The SER acknowledged the change from STAV6.2 to STAV7.2, but placed a condition on the use of this feature in that it could not be used until the staff's review of STAV7.2 (Reference A-11) was complete. The SER of Reference A-11 did not place any condition on the use of STAV7.2 except for limiting the rod average burnup range of STAV7.2 to 62 GWd/MTU. Westinghouse provided a letter to the NRC (Reference A-9), as required by the condition, after NRC approval of the STAV7.2 code was complete.

A.2.9 Thermal Radiation Model

As described in Reference A-4, Section 5.4:

The basic model of thermal radiation, as described in Section 4.5 and 4.5.1 of Reference A-1, remains unchanged.

The gray body factors used in the radiation model are still calculated with the BILBO code as described in Section 4.5.2 of Reference A-1. However, the gray body factors are now calculated throughout the transient. To facilitate this, the BILBO code has been incorporated into CHACHA-3. The change was done to make the radiation model consistent with the new rod deformation model (described in Section 5.6 of Reference A-4), which calculates individual time-dependent dimensions for each fuel rod. The gray body factors are first calculated by BILBO at the beginning of the CHACHA-3 calculation using the initial geometry. They are updated transiently when a significant change in geometry or emissivity has occurred.

Per the NRC SER of Reference A-4:

The SER acknowledged the change to the CHACHA code and placed no limitations or conditions on the use of the change.

A.2.10 Gas Plenum Temperature and Pressure Model

As described in Reference A-6, Section 5.5.1:

The detailed fuel heatup computer code (CHACHA-3D) has been revised to provide a new plenum type that permits a conservative prediction of the plenum temperature of the PLRs. For this plenum type, the gas temperature in the rod plenum is determined conservatively by equating it to the maximum of the plenum cladding outer surface temperature, which is calculated in the hot channel analysis, and the gas temperature determined using the conventional plenum model.

Per the NRC SER of Reference A-6:

The SER acknowledged the new PLR plenum model and found it acceptable. No limitations or conditions were placed on its use.

A.2.11 Pellet-Cladding Gap Heat Transfer Model

As described in Reference A-4, Section 5.5:

Due to the replacement of the PAD code with the STAV6.2 code, the pellet-cladding gap heat transfer model in the original CHACHA code was replaced with that from the STAV6.2 code with one modification. The contact conductance term is neglected in the CHACHA model to ensure conservatism when the clad and fuel are computed to be in contact.

Per the NRC SER of Reference A-4:

Since the model was identical to that in STAV6.2, a detailed review of this model was not performed as it was to be done as part of the review of CENPD-285-P (Reference A-10). The SER for CENPD-285-P-A did not place any restriction on the use of the STAV6.2 gap heat transfer model except for the limitation to a rod average burnup of 50 GWd/MTU.

As described in Reference A-12, Appendix A:

The input to CHACHA from STAV6.2 consists of all the data describing the fuel conditions at the initiation of the LOCA. The fuel rod heatup calculations used to derive the inputs to the CHACHA gap heat transfer model make use of bounding input for model parameters, fuel geometry, and power history. A conservative representation of a reference core limiting power history was used.

Per the NRC SER for Reference A-12:

The SER adopted the TER evaluation, which acknowledged the conservative approach and concluded that the use of the STAV6.2 initialization for LOCA was acceptable. No limitations or conditions were placed on the use of STAV6.2 to provide initial conditions for CHACHA using the approach described.

As described in Reference A-6, Section 5.5.2.3:

No changes were made to the CHACHA gap heat transfer model as a result of the change to the STAV7.2 fuel performance except that initial conditions for the model would be taken from the STAV7.2 calculations.

Per the NRC SER for Reference A-6:

The SER acknowledged that CHACHA would receive inputs from the STAV7.2 code to initialize the gap heat transfer model, but placed a condition on approval of this change pending completion of the NRC review of the STAV7.2 code. Westinghouse provided a letter to the NRC (Reference A-9), as required by the condition, after NRC approval of the STAV7.2 code was complete.

As described in Reference A-13, Section 4.4.4:

The fuel rod heatup calculations used to derive the inputs to the CHACHA gap heat transfer model are based on bounding segmented power histories and conservative fuel parameters.

Per the NRC SER for Reference A-13:

The SER acknowledged the use of the segmented power history approach to bound all operation defined by the thermal mechanical operating limit (TMOL) and concluded that the LOCA initialization methods were acceptable. No limitations or conditions were placed upon the use of this methodology other than to limit its application to a peak rod average burnup of 62 GWd/MTU.

A.2.12 Cladding Strain and Rupture Model

As described in Reference A-4, Section 5.6:

The mechanistic models described in Section 5.6 replaced the empirical correlations presented in Section 4.9 of Reference A-1. The mechanical models for the fuel rod cladding are used to determine the geometry of the fuel rods (outside diameter of the rods, size of the gap between the UO₂ pellet and the cladding, and cladding thickness).

The mechanistic model for cladding burst, which gives a burst stress as a function of material properties and temperature, accounts for the influence of surface oxide and oxygen that has diffused into the Zircaloy. The burst stress is compared to the true, actual stress to detect

a rupture. The true, actual stress is calculated as a function of the pressures inside and outside the rod and the strained dimensions of the rod.

Per the NRC SER of Reference A-4:

The SER acknowledged the revision to the cladding strain and rupture model but placed a condition on its use that requires a bias of -0.5 MPa to be placed on the burst stress.

As described in Reference A-5, Section 4.1:

In addition to the cladding burst criterion described in Section 5.6 of Reference A-4, a second criterion was added to require cladding burst upon rod-to-rod contact.

Thus, the criteria for determining fuel rod rupture became that cladding rupture occurs when either the cladding contacts a neighboring rod or the burst stress criterion is exceeded – whichever comes first. The MAPLHGR is limited to a value that ensures the 10 CFR 50.46 acceptance criteria are met.

Per the NRC SER of Reference A-5:

The NRC acknowledged the change and concluded that the change complies with 10 CFR Part 50, Appendix K, in that the swelling and rupture calculations are based on applicable data in such a way that the degree of swelling and incidence of rupture are not underestimated. No limitations or conditions were placed on the application of this change.

A.2.13 Fuel Bundle Material Properties

As described in Reference A-4, Appendix A:

The fuel properties in CHACHA were changed to be consistent with fuel performance models derived from the STAV6.2 fuel performance code of Reference A-10. This includes density, thermal conductivity, and specific heat for uranium oxide (with and without Gd₂O₃), Zircaloy-2 and Zircaloy-4, and zirconium oxide.

Per the NRC SER of Reference A-4:

The SER placed a condition on the revisions to CHACHA that were based on STAV6.2 to be subject to the review findings of Reference A-10. The only condition resulting from this review was that applications must be to peak rod average burnups less than or equal to 50 GWd/MTU.

As described in Reference A-6, Section 5.5.2:

A model to account for the burnup-induced degradation of fuel pellet conductivity was introduced in CHACHA. This model was consistent with the STAV7.2 fuel performance code.

Per the NRC SER of Reference A-6:

The SER placed a condition on the revisions to CHACHA that were based on STAV7.2 to be subject to the review findings of STAV7.2, which were ongoing at the time. Westinghouse provided a letter to the NRC (Reference A-9), as required by the condition, after NRC approval of the STAV7.2 code was complete. No limitations were placed on the model other than to limit applications to peak rod average burnups less than or equal to 62 GWd/MTU.

A.3 APPLICATION OF THE EVALUATION MODEL TO A NEW FUEL DESIGN

The U.S. version of the Westinghouse BWR ECCS Evaluation Model has been qualified and approved for application to several fuel designs. The specific designs are QUAD+, SVEA-96, SVEA-96+, and SVEA-96 Optima2. The same methodology has been applied in Europe to additional fuel designs (e.g., open lattice 8 x 8, SVEA-64, SVEA-100, and SVEA-96 Optima).

The qualification process described for various fuel designs, which is discussed in Reference A-14, is shown in Figure A-1 and summarized below.

A.3.1 Methodology

If all the qualification criteria are met, the ECCS Evaluation Model is acceptable for application to the specific fuel mechanical design. If any step described below does not fulfill the qualification criteria, then the LOCA ECCS Evaluation Model may not be applied for the new fuel mechanical design prior to specific NRC review and approval.

- Nodalization – Fuel design-specific models are developed for the GOBLIN, DRAGON, and CHACHA-3D codes that capture fuel design geometrical characteristics that are important to the key phenomena of a LOCA event.
- CPR Correlation – The CPR correlation used is NRC-approved and has been shown to conservatively predict early boiling transition in a LOCA event for the specific fuel design.
- CCFL Correlation – The CCFL model used is demonstrated as conservative relative to applicable experimental data for the specific mechanical fuel design.
- Spray Cooling Convective – The spray cooling heat transfer coefficients used are demonstrated as conservative relative to applicable experimental data for the specific mechanical fuel design.
- Transition Cores – A full core configuration of the specific fuel design is used in LOCA ECCS performance evaluation applications. Acceptability for transition cores is confirmed by comparing the following reactor system responses for analyses performed assuming a full core of the applicable co-resident fuel designs:
 - time of reactor trip
 - time of boiling transition at the midplane of the hot assembly
 - time of end of lower plenum flashing

- times of ECCS actuation
- time of reflood of the midplane of the hot assembly

The following sections provide discussion of each item above in the methodology statement.

A.3.2 Nodalization

The GOBLIN average reactor core and hot channel nodalization are selected to represent the fuel design features important to ECCS performance analysis. These features include the fuel rod dimensions, fuel assembly active cross-sectional flow areas, locations and characteristics of inter- and intra-assembly flow paths, grid spacers, and tie plates. Axial node size in the GOBLIN models is selected to ensure there is sufficient detail to characterize thermal-hydraulic conditions along the channel and at the hot plane. When it is impractical to reduce axial node size sufficiently to capture important mixture level dynamics, GOBLIN's two-phase level tracking feature may be used to determine the position of the mixture level more precisely.

The CHACHA-3D geometric model is selected to represent fuel design-specific rod or rod lattice configuration, channel configuration, fuel pellet, cladding and gap dimensions, and fuel rod plenum dimensions.

A.3.3 CPR Correlation

The CPR correlation is used to (1) determine the initial power of the hot assembly that will have it operating at bounding operating conditions, and (2) determine the time of boiling transition during the blowdown phase of the LOCA. GOBLIN has several CPR correlations available to the user. The CPR correlation applicable to the fuel design being evaluated or demonstrated to be conservative relative to a NRC-approved correlation for that fuel design is selected by the analyst to ensure that the hot assembly power and the time of dryout are predicted conservatively. To ensure that the critical power is calculated conservatively, a modified pool boiling correlation is also used to determine the critical power. The code then determines the critical power by selecting the smaller of the two calculated values. The following NRC-approved CPR correlations are currently available to the user:

| CPR Correlation | Application |
|-----------------|------------------|
| XL-S96 | SVEA-96 |
| ABBD1.0 | SVEA-96 |
| ABBD2.0 | SVEA-96+ |
| D4.1.2 | SVEA-96 Optima 2 |

CPR correlations are applicable to specific fuel designs or a group of fuel designs. The SER for RPB 90-93-P-A (Reference A-1) requires that an appropriate NRC-approved CPR correlation be used when GOBLIN is used in a licensing analysis. The NRC-approved correlation may be one that has been developed specifically for the fuel design or one shown to be conservative relative to an NRC-approved correlation for that fuel design. Changes to GOBLIN are necessary when a new CPR correlation is implemented. The process described below is used by Westinghouse to install and test NRC-approved

CPR correlations. Changes to GOBLIN following this process do not require specific NRC review and approval. Such changes will be communicated to the NRC via the 10 CFR 50.46 annual reporting process.

The process used to install and qualify a CPR correlation in GOBLIN is as follows:

1. Develop coding to represent the new correlation. The coding includes checks on correlation parameters to ensure that inputs to the correlation are within valid ranges of those parameters. If a parameter is outside its range of validity, the []^{a,c}
2. Validation of the implemented CPR correlation is performed by:
 - a. Transient code simulation of transient experimental data, or
 - b. Transient code to transient code comparisons where the reference transient code implementation of the CPR correlation has been qualified against transient experimental data.
3. Ensure NRC approval of CPR correlation for the fuel design prior to its use in licensing applications.
4. Inform the NRC of the change to GOBLIN via the 10 CFR 50.46 annual reporting process.

If a LOCA analysis of non-Westinghouse fuel is required, Westinghouse may not have direct access to the accepted correlation for the resident fuel. In this case, sufficient information is obtained from the utility company to either:

1. Allow renormalization of an NRC-approved Westinghouse CPR correlation for Westinghouse fuel to describe the CPR performance of the fuel, or
2. Show that the NRC-approved Westinghouse CPR correlation for Westinghouse fuel is conservative.

CPR correlations are valid within specified ranges of parameters (e.g., system pressure, core mass flux, inlet subcooling). When a CPR correlation is implemented in GOBLIN, it is only applied when conditions in the core are within its range of applicability. If any parameter is outside its valid range, a pool boiling CHF correlation is used. Since the system pressure and core flow decrease rapidly following a large-break LOCA, the prediction of boiling transition is often the result of exceeding the []^{a,c}. Experience has shown that the fuel-specific CPR correlation selected []^{a,c}

] ^{a,c}

[

] ^{a,c}

The process for developing the renormalized CPR correlation is described in Section 5.3.2.5 of Reference A-14. Implementation of the renormalized CPR correlation in GOBLIN follows the process outlined above.

A.3.4 CCFL Model

The CCFL model has been approved for a variety of fuel designs. In accordance with CENPD 283-P-A (Reference A-3), this correlation will not be extended to fuel designs outside the range of approved applicability without being supported by experimental data. NRC review and approval of the new CCFL model is required prior to its use in licensing applications.

The change to the CCFL model in GOBLIN that is described in Section 5.4.2 of Reference A-6 removes a restriction placed on the USA2 Evaluation Model.²

A.3.5 Spray Cooling Convective Heat Transfer

A methodology to extrapolate spray cooling heat transfer coefficients for application to a variety of fuel designs has been approved. In accordance with CENPD-283-P-A (Reference A-3), this methodology will not be extended to fuel designs outside the range of applicability without being supported by experimental data. If the spray cooling heat transfer coefficients cannot be demonstrated as applicable, spray cooling heat transfer coefficients must be determined either from a detailed analysis that has been validated by experimental data or taken directly from applicable data. NRC review and approval of the new spray cooling heat transfer coefficients are required prior to their use in licensing applications.

A.3.6 Transition Cores

The BWR fuel channel and fuel mechanical designs are established to ensure hydraulic compatibility with co-resident fuel. This means that the system response to a LOCA event for one core of mixed fuel designs will be similar hydraulically to that of a full core of a single fuel design. This observation has been demonstrated for several fuel designs in References A-2 and A-3. It became a requirement to specifically analyze a transition core during the first reload analysis following the NRC acceptance of WCAP-16078-P-A (Reference A-6). If it is confirmed that a full core of Westinghouse fuel is bounding, then the Evaluation Model can be performed using the full-core Westinghouse fuel approach. Otherwise, the mixed-core model must be used. The Westinghouse Evaluation Model may not be used to calculate the MAPLHGR limits for non-Westinghouse fuel for a mixed-core analysis. If the transition core analysis indicates that the system performance of the mixed core is more limiting than the full-core analysis of the legacy fuel, Westinghouse must request the utility to contact the legacy fuel vendor for an evaluation of the impact of the mixed core on the MAPLHGR limits for their fuel.

2. In responding to a request for additional information relative to the NRC review of CENPD-283-P-A (Reference A-3), Westinghouse committed to applying a conservative bias to the CCFL correlation to bound all the scatter in the correlation database for LOCA applications in which the calculated peak cladding temperature exceeded 2100°F.

Tables for Appendix A

| Table A-1 Roadmap to Evaluation Model Changes | | | | | | |
|--|----------------------|------------|------------|------------|------------|-------------------------|
| Evaluation Model Element | Reference No. | | | | | Road Map Section |
| | A-1 | A-4 | A-3 | A-5 | A-6 | |
| Thermal-Hydraulic Model – GOBLIN | | | | | | |
| Mass Conservation Equations | 3.1.1 | | | | | |
| Energy Conservation Equations | 3.1.2 | | | | | |
| Momentum Conservation Equations | 3.1.3 | 4.2 | | | | A.2 |
| Fluid Properties | 3.2.1 | | | | | |
| Equation of State | 3.2.2 | | | | | |
| Two-Phase Energy Flow Model | 3.3.1 | | 7.1 | | 5.4.2 | A.2.2 |
| Two-Phase Level Tracking | 3.3.2 | | 6.1.2 | | 5.1.1 | A.2.3 |
| Frictional Pressure Drop Correlations | 3.3.3 | | | | | |
| Form Pressure Drop Correlations | 3.3.4 | | | | | |
| Injection Flow – Fluid Interaction | 3.3.5 | | | | | |
| Critical Flow Model | 3.3.6 | | | | | |
| Recirculation Pump Model | 3.4.1 | | | | | |
| Jet Pump Model | 3.4.2 | | | | | |
| Separator and Dryer Model | 3.4.3 | | | | | |
| Feedwater and Steam line Systems | 3.4.4 | | | | | |
| Reactor Measurement and Protection Systems | 3.4.5 | | | | | |
| Heat Transfer Regimes | 3.5.1 | | | | | |
| Convective Heat Transfer Coefficients | 3.5.2 | | 4.3 | | 6.1 | A.2.4 |
| Critical Power Ratio Correlation | 3.5.3 | 4.1 | 4.2 | | 5.4.1 | A.2.5 |
| Transition Boiling | 3.5.4 | | | | | |
| Radiation Heat Transfer | 3.5.5 | | | | | |
| Fuel Rod Conduction Model | 3.6.1 | | | | | |
| Plate Conduction Model | 3.6.2 | | | | | |
| Material Properties | 3.6.3 | | | | | |
| Point Kinetics Model | 3.7.1 | | | | | |
| Metal-Water Reaction Model | 3.7.2 | | | | | |
| Point Kinetics Solution | 3.8.1 | | | | | |

| Table A-1 Roadmap to Evaluation Model Changes (cont.) | | | | | | |
|--|----------------------|------------|------------|------------|------------|-------------------------|
| Evaluation Model Element | Reference No. | | | | | Road Map Section |
| | A-1 | A-4 | A-3 | A-5 | A-6 | |
| Hydraulic Model Solution | 3.8.2 | | | | | |
| Heat Conduction and Transfer Solution | 3.8.3 | | | | | |
| Nodalization | 3.9 | | | | | |
| Rod Heatup Model – CHACHA | | | | | | |
| Fuel Rod Conduction Model | 4.1 | 5.1 | | | 5.5.2 | A.2.6 |
| Channel Temperature Model | 4.2 | | | | | |
| Heat Generation Model | 4.3 | 5.2 | | | 5.5.2 | A.2.7 |
| Metal-Water Reaction Model | 4.4 | 5.3 | | | 5.5.2 | A.2.8 |
| Thermal Radiation Model | 4.5 | 5.4 | | | | A.2.9 |
| Gas Plenum Temperature and Pressure Model | 4.6 | | | | 5.5.1 | A.2.10 |
| Channel Rewet Model | 4.7 | | | | | |
| Pellet-Cladding Gap Heat Transfer Model | 4.8 | 5.5.1 | | | 5.5.2.3 | A.2.11 |
| Cladding Strain and Rupture Model | 4.9 | 5.6 | | 4.1 | | A.2.12 |
| Fuel Bundle Material Properties | App. 4.A | App. A | | | 5.5.2 | A.2.13 |

| Table A-2 Extrapolated Spray Cooling Heat Transfer Coefficients per Reference A-3 | | | | |
|--|--|------------------|-------------------|----------------|
| Geometry | Extrapolated from Appendix K Values (W/m²-K) | | | |
| | Corner Rods | Side Rods | Inner Rods | Channel |
| Appendix K 7 x 7, 8 x 8, Isotropic Radiation | 17.0 | 19.9 | 8.5 | 28.4 |
| Appendix K 8 x 8, Anisotropic Radiation | 16.8 | 19.4 | 11.9 | 28.4 |
| SVEA-64, Anisotropic Radiation | 15.0 | 17.3 | 10.6 | 25.3 |
| SVEA-96, Anisotropic Radiation | 15.0 | 17.3 | 10.6 | 25.3 |

| Table A-3 Extrapolated Spray Cooling Heat Transfer Coefficients per Reference A-6 | | | | |
|--|--|------------------|-------------------|----------------|
| | Extrapolated from Appendix K Values (W/m²-K) | | | |
| | Corner Rods | Side Rods | Inner Rods | Channel |
| SVEA-96, Anisotropic Radiation | 15.0 | 17.3 | 10.6 | 25.3 |
| SVEA-96 Optima2 | 15.0 | 17.3 | 10.6 | 25.3 |

Figures for Appendix A

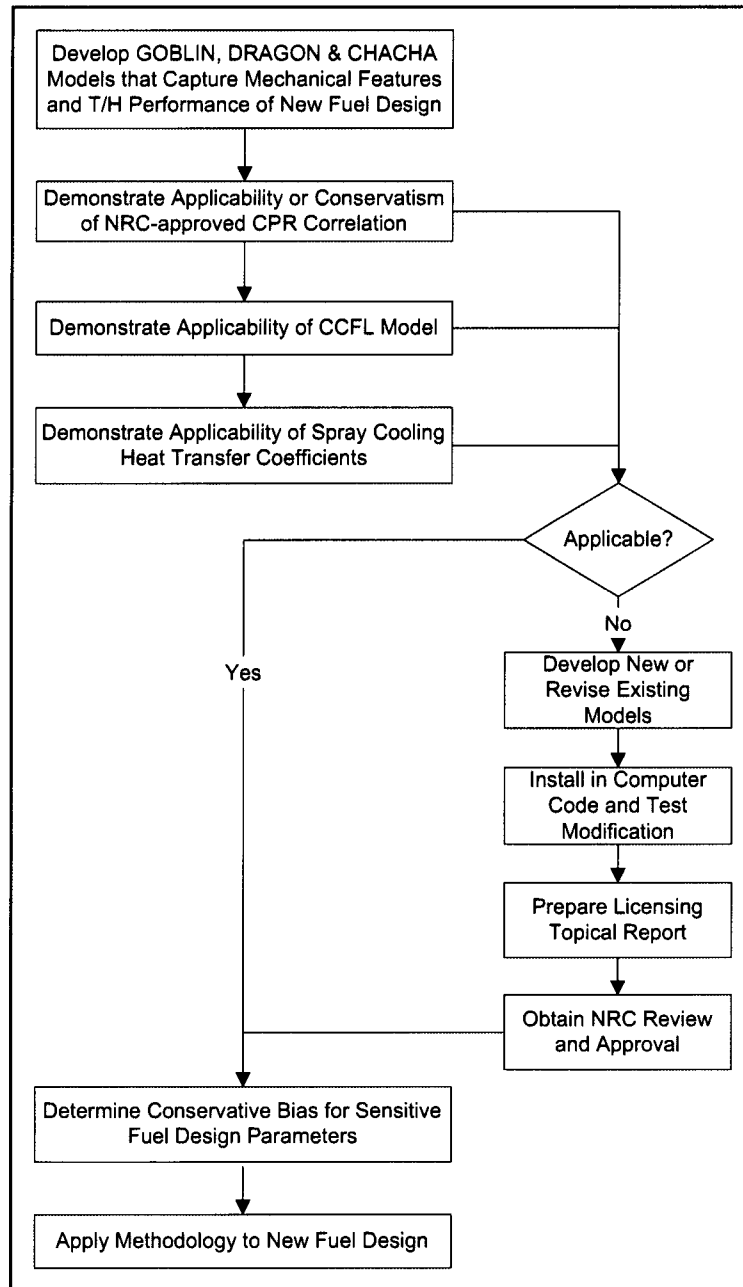


Figure A.7-1 Process for Applying Evaluation Model to New Fuel Mechanical Design

References for Appendix A

- A-1 “Boiling Water Reactor Emergency Core Cooling System Evaluation Model: Code Description and Qualification,” Westinghouse Report RPB 90-93-P-A (Proprietary), RPB 90-91-NP-A (Non-Proprietary), October 1991.
- A-2 “Boiling Water Reactor Emergency Core Cooling System Evaluation Model: Code Sensitivity,” Westinghouse Report RPB 90-94-P-A (Proprietary), RPB 90-92-NP-A (Non-Proprietary), October 1991.
- A-3 “Boiling Water Reactor Emergency Core Cooling System Evaluation Model: Code Sensitivity for SVEA-96 Fuel,” Westinghouse Report CENPD-283-P-A (Proprietary), CENPD-283-NP-A (Non-Proprietary), July 1996.
- A-4 “BWR ECCS Evaluation Model: Supplement 1 to Code Description and Qualification,” Westinghouse Report CENPD-293-P-A (Proprietary), CENPD-293-NP-A (Non-Proprietary), July 1996.
- A-5 “Westinghouse BWR ECCS Evaluation Model: Supplement 2 to Code Description, Qualification and Application,” Westinghouse Report WCAP-15682-P-A (Proprietary), WCAP-15682-NP-A (Non-Proprietary), April 2003.
- A-6 “Westinghouse BWR ECCS Evaluation Model: Supplement 3 to Code Description, Qualification and Application to SVEA-96 Optima2 Fuel,” Westinghouse Report WCAP-16078-P-A (Proprietary), WCAP-16078-NP-A (Non-Proprietary), November 2004.
- A-7 “SVEA-96 Critical Power Experiments on a Full Scale 24-rod Sub-bundle,” ABB Atom Report UR 89-210-P-A, October 1993.
- A-8 Letter from A.C. Thadani (NRC) to W. R. Russell (ABB Atom), “Waiver of CRGR Review of the Safety Evaluation of ABB Supplemental Information Regarding UR 89-210 Safety Evaluation Report,” July 12, 1993.
- A-9 Letter from B. F. Maurer (Westinghouse) to F. M. Akstulewicz (NRC), “Westinghouse response to Condition 1 in the FINAL SAFETY EVALUATION FOR TOPICAL REPORT WCAP-16078-P, “Westinghouse BWR ECCS Evaluation Model: Supplement 3 to Code Description, Qualification and Application to SVEA-96 Optima2 Fuel” (TAC NO. MB8908), October 21, 2004,” LTR-NRC-06-1, January 4, 2006.
- A-10 “Fuel Rod Design Methods for Boiling Water Reactors,” Westinghouse Report CENPD-285-P-A (Proprietary), CENPD-285-NP-A (Non-Proprietary), July 1996.
- A-11 “Fuel Rod Design Methods for Boiling Water Reactors – Supplement 1,” Westinghouse Report WCAP-15836-P-A (Proprietary), WCAP-15836-NP-A (Non-Proprietary), April 2006.

- A-12 "Fuel Rod Design Methodology for Boiling Water Reactors," Westinghouse Report CENPD-287-P-A, July 1996.
- A-13 "Fuel Assembly Mechanical Design Methodology for Boiling Water Reactors Supplement 1 to CENP-287," Westinghouse Report WCAP-15942-P-A (Proprietary), WCAP-15942-NP-A (Non-Proprietary), March 2006.
- A-14 "Reference Safety Report for Boiling Water Reactor Reload Fuel," CENPD-300-P-A (Proprietary), CENPD-300-NP-A (Non-Proprietary), July 1996.

APPENDIX B

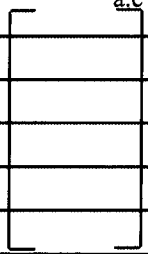
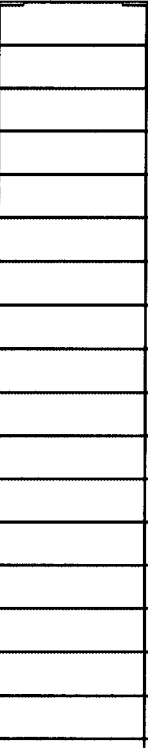
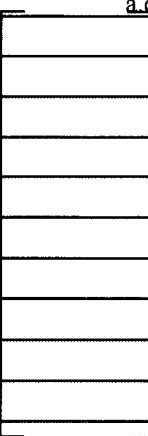
ABWR LOCA ANALYSIS MODEL INPUT PARAMETERS

Table B-1 of this appendix provides key input parameters that were used in the analyses described herein. Note that some of input parameters were revised after the analyses were completed. While the changes were small, they and any other plant specific changes will be incorporated into the final analyses prior to the first plant application of the methodology.

| Table B-1 ABWR LOCA Analysis Model Input Parameters | | |
|---|------------------|----------------|
| Parameter | Toshiba/W Values | |
| Volumes (see Figure B-1) | a,c | |
| WV-A | | m ³ |
| WV-B | | m ³ |
| WV-C | | m ³ |
| WV-D | | m ³ |
| WV-E | | m ³ |
| WV-F | | m ³ |
| WV-G (Control Rods Fully Inserted) | | m ³ |
| WV-H | | m ³ |
| WV-J | | m ³ |
| WV-K | | m ³ |
| WV-N1 | | m ³ |
| WV-N2 | | m ³ |
| WV-L | | m ³ |
| WV-M | | m ³ |
| WV-P | | m ³ |
| WV-Q | | m ³ |
| WV-R1 | | m ³ |
| WV-R2 | | m ³ |
| WV-R3 | | m ³ |
| WV-R4 | | m ³ |
| WV-R5 | | m ³ |
| WV-S1 | | m ³ |
| WV-S2 | | m ³ |
| WV-S3 | | m ³ |
| WV-S4 | | m ³ |
| WV-S5 | | m ³ |
| WV-T1 | | m ³ |
| WV-T2 | | m ³ |
| WV-T3 | | m ³ |

| Table B-1 ABWR LOCA Analysis Model Input Parameters (cont.) | | | |
|--|--|-------------------------|----------------|
| Parameter | | Toshiba/W Values | |
| VSL1-A (Main Steam Line A from RPV to first MSIV) | | a,c | m ³ |
| VSL1-B | | | m ³ |
| VSL1-C | | | m ³ |
| VSL1-D | | | m ³ |
| Elevations (from vessel zero) | | a,c | |
| Z1 | Internal pump discharge port upper end height | | m |
| Z2 | Bottom of active fuel | | m |
| Z3 | Top of active fuel | | m |
| Z4 | Upper plenum upper end (inside) | | m |
| Z5 | Feedwater sparger discharge port height | | m |
| Z6 | Normal water level | | m |
| Z7 | Steam separator upper end | | m |
| Z8 | Shroud support leg lower end height | | m |
| Z9 | Control rod guide tube lower end | | m |
| Z10 | Control rod guide tube upper end | | m |
| Z11 | Core support plate height | | m |
| Z12 | Fuel channel upper end height | | m |
| Z13 | Steam dryer skirt lower end height | | m |
| Z14 | Steam dryer lower end height | | m |
| Z15 | Steam dryer upper end height | | m |
| Z16 | Pressure vessel upper end height | | m |
| Z17 | Water level reference point height | | m |
| Z18 | HPCF sparger height | | m |
| Z19 | LPFL sparger height | | m |
| Z20 | Main steam line inlet height | | m |
| Z21 | Internal pump inlet height | | m |
| Z22 | Internal pump discharge port lower end height | | m |
| Z23-1 | Water level indicator nozzle (wide range) | | m |
| Z23-2 | Water level indicator nozzle (narrow range) | | m |
| Zcs | Top of core support mounting flange height | | m |
| Zf | Elevation of vessel flange parting line | | m |
| Zbc | Elevation of intersection of vessel bottom curvature | | m |
| Zut | Elevation of upper tap for water level measurement | | m |

| Table B-1 ABWR LOCA Analysis Model Input Parameters (cont.) | | Toshiba/W Values | |
|---|---|-------------------------|---|
| Parameter | | | |
| Dimensions of Core Structures | | | |
| Reactor Pressure Vessel | | | |
| | | a,c | |
| Di | Pressure vessel shell inner diameter | | m |
| Rhu | Top head radius | | m |
| Rhb | Bottom head radius | | m |
| TV1 | Upper head wall thickness | | m |
| TV2 | Flange thickness | | m |
| TV3 | Vessel wall thickness | | m |
| TV4 | Bottom wall thickness | | m |
| TV5 | Bottom head thickness | | m |
| TL1 | Vessel wall liner thickness | | m |
| TL2 | Bottom wall liner thickness | | m |
| Hfh | Flange head height | | m |
| Control Rod Drive (CRD) Guide Tube and Control Rod (CR) Housing (see Figure B-2) | | | |
| | | a,c | |
| Dgt | CRD guide tube outer diameter | | m |
| Tgt | CRD guide tube thickness | | m |
| Ngt | Number of CRD | | – |
| Doit | Outer diameter of index tube | | m |
| Docrd | Outer diameter of CR housing | | m |
| Dicrd | Inner diameter of CR housing | | m |
| In-core Monitor Guide Tubes (see Figure B-2) | | | |
| Dm | Outer diameter of in-core monitor guide tubes | | m |
| Tm | Wall thickness of in-core monitor guide tubes | | m |
| Nm | Number of in-core monitors | | – |
| Core Support Plate (see Figure B-2) | | | |
| Dcs | Diameter of core support plate | | m |
| Tcs | Wall thickness of core support plate | | m |
| Lbt | Total length of beams | | m |
| Dcs | Hole diameter | | m |
| Hcs | Support ring height | | m |
| Shroud (see Figure B-3) | | | |
| Dup | Inner diameter of shroud at upper plenum part | | m |
| Do | Inner diameter of shroud at core part | | m |
| Dip | Inner diameter of shroud at lower plenum part | | m |
| Tsh | Wall thickness of core shroud part | | m |
| Rsh | Shroud head curvature | | m |

| Table B-1 ABWR LOCA Analysis Model Input Parameters (cont.) | | Toshiba/W Values | |
|--|--|---|----------------|
| Parameter | | | |
| Lsh1 | Height of shroud |  | m |
| Lsh2 | Height of shroud head | | m |
| Lcy | Elevation of shroud support cylinder | | m |
| Tfl | Width of shroud head flange | | m |
| Tsl | Thickness of shroud support leg | | m |
| Tsc | Thickness of shroud support cylinder | | m |
| Separators (see Figure B-4) | |  | |
| Lsp | Length of standpipe | | m |
| Asp | Flow area of standpipe | | m |
| Dsp | Inner diameter of standpipe | | m |
| Tsp | Wall thickness of standpipe | | m |
| Dsp1~3 | Outer diameter of surface of separators | | m |
| Tsp1~3 | Wall thickness of separators | | m |
| Lsp1 | Length of separator skirts (1st) | | m |
| D1~3 | Outer diameter of inner wall surface of separators | | m |
| T1~3 | Wall thickness of inner wall surface of separators | | m |
| L1 | Length of inner wall surface of separators (1st) | | m |
| Lsp2 | Length of separator skirts (2nd) | | m |
| L2 | Length of inner wall surface of separators (2nd) | | m |
| Lsp3 | Length of separator skirts (3rd) | | m |
| L3 | Length of inner wall surface of separators (3rd) | | m |
| Zsp1 | Height at top of standpipe (from vessel zero) | | m |
| Nsp | Number of separators | | - |
| | Carry under | - | |
| | Carry over | - | |
| Steam Dryer | |  | |
| Asd | Total heating surface area | | m ² |
| Nsd | Number of packages | | - |
| Tsd | Plate thickness | | m |
| Wdr | Width of dryer unit | | m |
| Tdr1 | End thickness of dryer unit | | m |
| Tdr2 | Another end thickness of dryer unit | | m |
| Ndr | Number of dryer plate units | | - |
| Dd | Dryer skirt mean diameter | | m |
| Tds | Dryer skirt thickness | | m |
| Dsr | Dryer support ring outer diameter | m | |
| Hsr | Dryer support ring height | m | |

| Table B-1 ABWR LOCA Analysis Model Input Parameters (cont.) | | | |
|--|--|-------------------------|-------------------|
| Parameter | | Toshiba/W Values | |
| Sparger Rings | | a.c | |
| Dmfw | Mean diameter of feedwater sparger ring | [] | m |
| Dfw | Outer diameter of feedwater sparger ring tubes | [] | m |
| Tfw | Wall thickness of feedwater sparger ring tubes | [] | m |
| Afw | Cross section of feedwater sparger ring outlet nozzle | [] | m ² |
| Dmhp | Mean diameter of HPCF sparger ring | [] | m |
| Dhp | Outer diameter of HPCR sparger ring tubes | [] | m |
| Thp | Wall thickness of HPCF sparger ring tubes | [] | m |
| Ahp | Cross section of HPCF sparger ring outlet nozzle | [] | m ² |
| Dmlp | Mean diameter of LPFL sparger ring | [] | m |
| Dlp | Outer diameter of LPFL sparger ring tubes | [] | m |
| Tlp | Wall thickness of LPFL sparger ring tubes | [] | m |
| Alp | Cross section of LPFL sparger ring outlet nozzle | [] | m ² |
| Main Steam (MS) Line | | | |
| D1~4 | Inner diameter of MS line (from RPV to first MSIV) | [] ^{a,c} | m |
| Reactor Internal Pump (RIP) | | a.c | |
| Ddf | Diameter of RIP discharge | [] | m |
| Ldf | Length of RIP discharge | [] | m |
| Ath | Flow area of RIP | [] | m ² |
| Did | Inner diameter of RIP diffuser ring | [] | m |
| Ts | Thickness of shroud support leg (internal support thickness) | [] | m |
| Nrp | Number of RIP | [] | - |
| Assumed pump trip time | | [] | s |
| Rated pump speed | | [] | rpm |
| Rated pump flow rate (per pump) | | [] | m ³ /h |
| Rated pump head | | [] | m |
| Rated pump torque (includes hydraulic and frictional torque) | | [] | Nm |
| Pump moment of inertia | | [] | kg/m ³ |
| Rated density of pump fluid | | [] | kg/m ³ |
| Pump efficiency (minimum value) | | [] | % |
| Minimum inertia time constant (speed dropping to 50%) | | [] | s |
| Maximum inertia time constant (speed dropping to 50%) | | [] | s |
| Top Guide | | a.c | |
| Ttg | Thickness of top guide | [] | m |
| Wth | Weight of top guide | [] | kg |

| Table B-1 ABWR LOCA Analysis Model Input Parameters (cont.) | | | | |
|--|------------|-----------|-------------------------|-------------------|
| Parameter | | | Toshiba/W Values | |
| Material | | | | |
| Reactor pressure vessel | | | a.c. | |
| RIP diffuser ring | | | | |
| Internal support | | | | |
| Shroud support | | | | |
| Other internals | | | | |
| Initial Conditions | | | | |
| Core Thermal Power (102% of rated thermal power) | | | a.c. | |
| Core Inlet Flow Rate (90% rated) | | | MWt | |
| Core Inlet Flow Rate (111% rated) | | | kg/s | |
| Steam Flow Rate | | | kg/s | |
| Feedwater Flow Rate | | | kg/s | |
| Feedwater Enthalpy | | | kJ/kg | |
| Core Inlet Enthalpy (90% core flow) | | | kJ/kg | |
| Core Inlet Enthalpy (111% core flow) | | | kJ/kg | |
| Dome Pressure | | | MPa | |
| Water Level (slightly above scram water level) | | | m | |
| Break Areas | | | | |
| HPCI Injection Line (area of 18 sparger nozzles) | | | a.c. | |
| Main Steam Line (corresponds area of one flow limiter) | | | cm ² | |
| Feedwater Line (area of 54 sparger nozzles) | | | cm ² | |
| RHR Shutdown Cooling Suction Line | | | cm ² | |
| RHR Injection Line | | | cm ² | |
| Bottom Drain Line | | | cm ² | |
| ECCS Performance | | | | |
| High Pressure Core Flooder (HPCF) | | | | |
| | ΔP | | Flow | |
| | a.c. | | a.c. | |
| | | MPa (dif) | | m ³ /h |
| | | MPa (dif) | | m ³ /h |
| | | MPa (dif) | | m ³ /h |
| | | MPa (dif) | | m ³ /h |
| Time delay from actuation signal (includes all delays) | | | [] ^{a,c} | |
| Actuation signals | | | a.c. | |
| High drywell pressure, OR | | | MPa | |
| Low water level (LWL-1.5) | | | m | |
| Number of pumps | | | - | |

| Table B-1 ABWR LOCA Analysis Model Input Parameters (cont.) | | | | | Toshiba/W Values | |
|---|--------------------|-----------|--------------------|-------------------|--------------------|------|
| Parameter | | | | | | |
| Reactor Core Isolation Cooling (RCIC) | | | | | | |
| | ΔP | | Flow | | | |
| | [] ^{a,c} | MPa (dif) | [] ^{a,c} | m ³ /h | | |
| | [] | MPa (dif) | [] | m ³ /h | | |
| | [] | MPa (dif) | [] | m ³ /h | | |
| | [] | MPa (dif) | [] | m ³ /h | | |
| Time delay from actuation signal (includes all delays) | | | | | [] ^{a,c} | s |
| Actuation signals | | | | | | |
| High drywell pressure, OR | | | | | [] ^{a,c} | MPa |
| Low water level (LWL-2) | | | | | [] | m |
| Number of pumps | | | | | [] | - |
| Low Pressure Flooder (LPFL) | | | | | | |
| | ΔP | | Flow | | | |
| | [] ^{a,c} | MPa (dif) | [] ^{a,c} | m ³ /h | | |
| | [] | MPa (dif) | [] | m ³ /h | | |
| | [] | MPa (dif) | [] | m ³ /h | | |
| Time delay from low pressure permissive (includes all delays) | | | | | [] ^{a,c} | s |
| Pressure permissive for LPFL injection valve | | | | | [] | MPa |
| Actuation signals | | | | | | |
| High drywell pressure, OR | | | | | [] ^{a,c} | MPa |
| Low water level (LWL-1) | | | | | [] | m |
| Number of pumps | | | | | [] | - |
| Automatic Depressurization System (ADS) | | | | | | |
| Number of valves | | | | | [] ^{a,c} | - |
| Capacity per valve | | | | | [] | kg/s |
| Pressure at rated capacity | | | | | [] | MPa |
| Time delay from actuation signal | | | | | [] | s |
| Actuation signals | | | | | | |
| High drywell pressure, AND | | | | | [] ^{a,c} | MPa |
| Low water level (LWL-1), AND | | | | | [] | m |
| Indication that at least 1 LPFL or 1 HPCF pump is operating | | | | | | |

| Table B-1 ABWR LOCA Analysis Model Input Parameters (cont.) | | | | | | | |
|---|---------------------|------------|----------------------|------------|-----------------------|-------------------------|---------|
| Parameter | | | | | | Toshiba/W Values | |
| ECCS water temperature | | | | | | [] ^{a,c} | °C |
| Safety Relief Valve (safety function) | | | | | | | |
| Setpoints for spring action | | | | | | | |
| | Open _{a,c} | | Close _{a,c} | | Number _{a,c} | Capacity _{a,c} | * |
| 1 st | [] | MPa (gage) | [] | MPa (gage) | [] | [] | kg/s |
| 2 nd | [] | MPa (gage) | [] | MPa (gage) | [] | [] | kg/s |
| 3 rd | [] | MPa (gage) | [] | MPa (gage) | [] | [] | kg/s |
| 4 th | [] | MPa (gage) | [] | MPa (gage) | [] | [] | kg/s |
| 5 th | [] | MPa (gage) | [] | MPa (gage) | [] | [] | kg/s |
| * capacity is per valve | | | | | | | |
| Opening/closing time | | | | | | [] ^{a,c} | s |
| Reactor Scram | | | | | | | |
| Low water level (LWL-3) | | | | | | [] ^{a,c} | m |
| MSIV position | | | | | | [] ^{a,c} | % open |
| Time delay from actuation signal (low water level) | | | | | | [] ^{a,c} | s |
| Time delay from actuation signal (MSIV position) | | | | | | [] ^{a,c} | s |
| Scram insert time | | | | | | [] ^{a,c} | s |
| Feedwater Flow Isolation | | | | | | | |
| Time feedwater flow rate decreases to zero (from time of event) | | | | | | [] ^{a,c} | s |
| Steam Line Isolation | | | | | | | |
| Turbine control valve fast closure | | | | | | | |
| [] ^{a,c} | | | | | | | |
| A _{ti} is the steam line flow area upstream of the turbine, t is time from the loss of normal power | | | | | | | |
| Main Steam Isolation Valves (MSIVs) | | | | | | | |
| [] ^{a,c} | | | | | | | |
| A is the MSIV flow area, A _{ms} is the flow area of the main steam line, t is time from actuation signal | | | | | | | |
| Main Steam Flow Control (pressure regulator) | | | | | | | |
| [] ^{a,c} | | | | | | | |
| A _{ti} is the steam line flow area upstream of the turbine, P _d is the dome pressure in MPa. | | | | | | | |
| Actuation signals | | | | | | | |
| TCV fast closure | | | | | | | |
| Loss of normal power | | | | | | | |
| MSIV | | | | | | | |
| Low water level (LWL-1.5) | | | | | | [] ^{a,c} | m |
| High steam flow | | | | | | [] ^{a,c} | % rated |

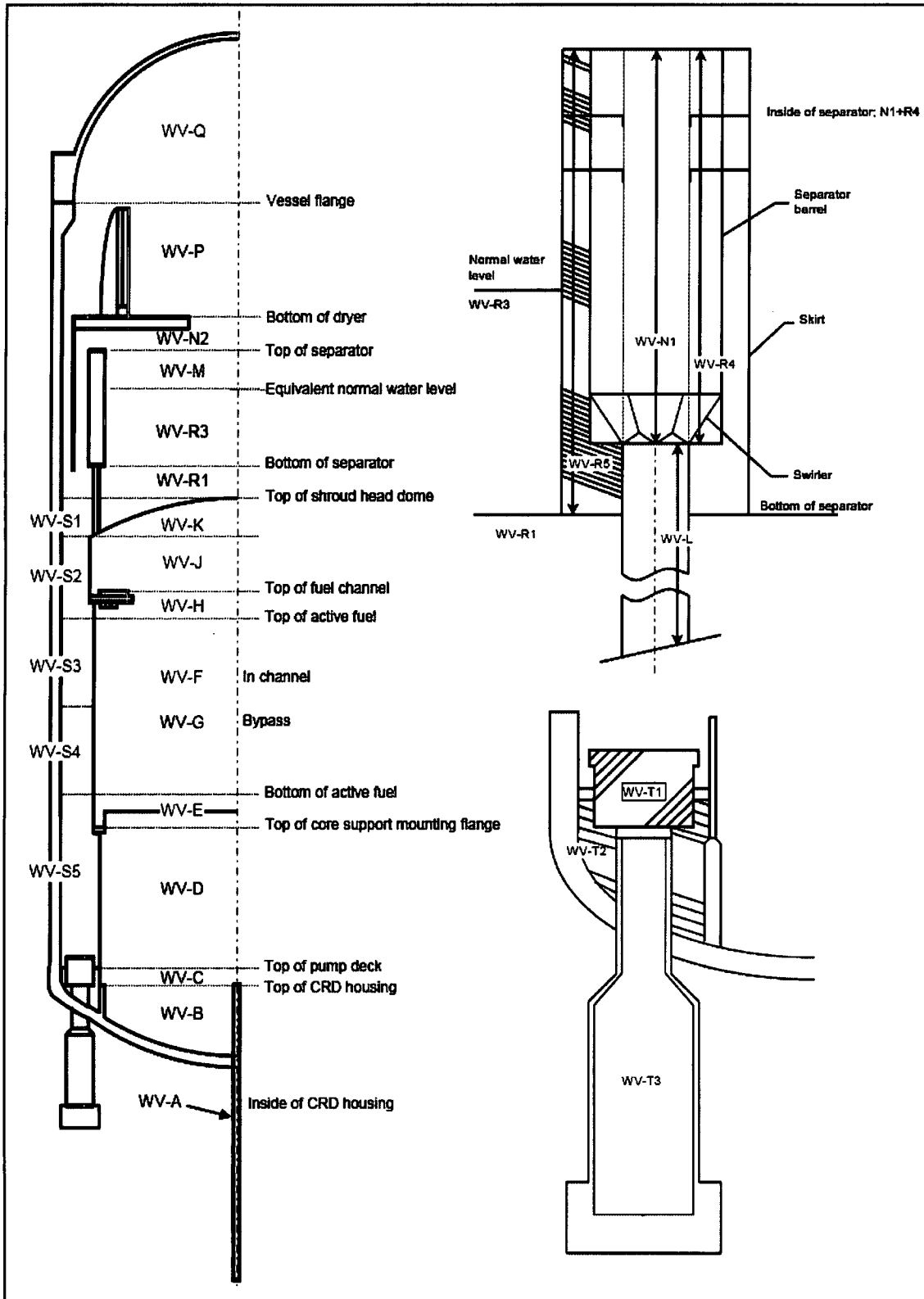


Figure B-1 Schematic of Reactor Pressure Vessel Internals

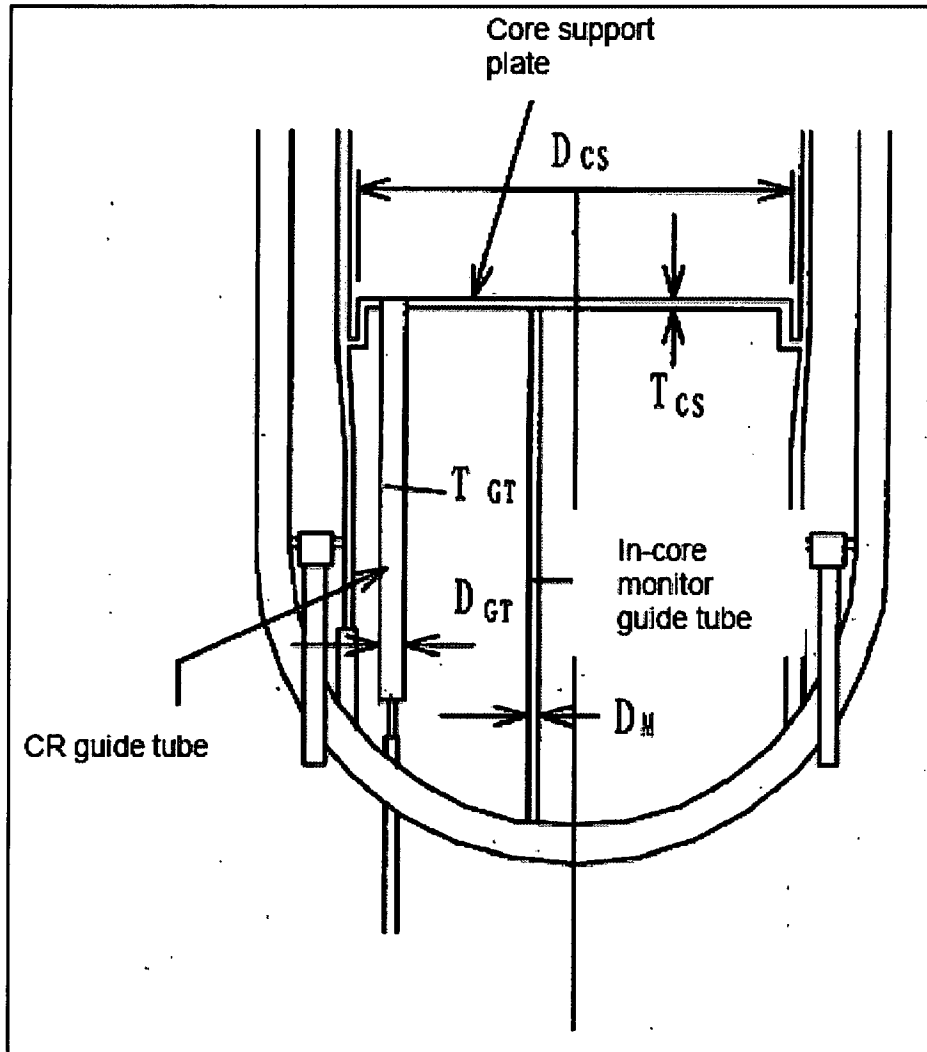


Figure B-2

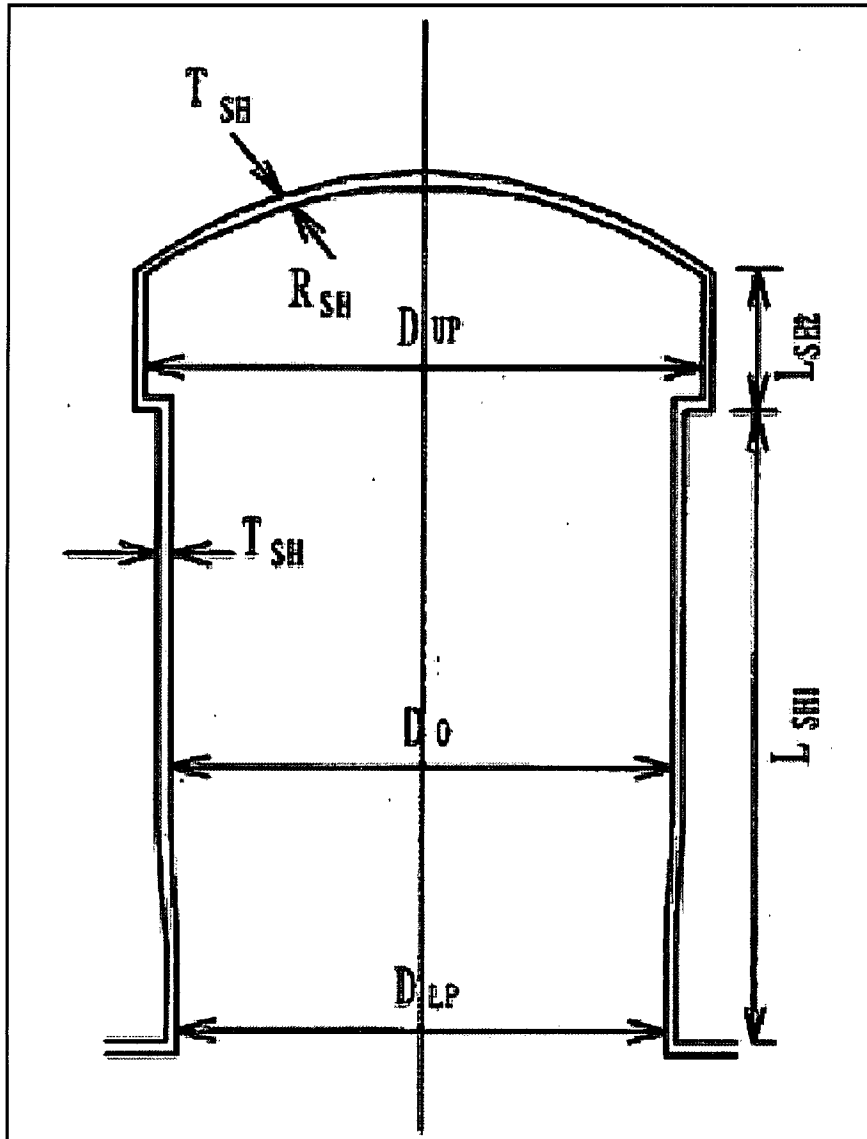


Figure B-3

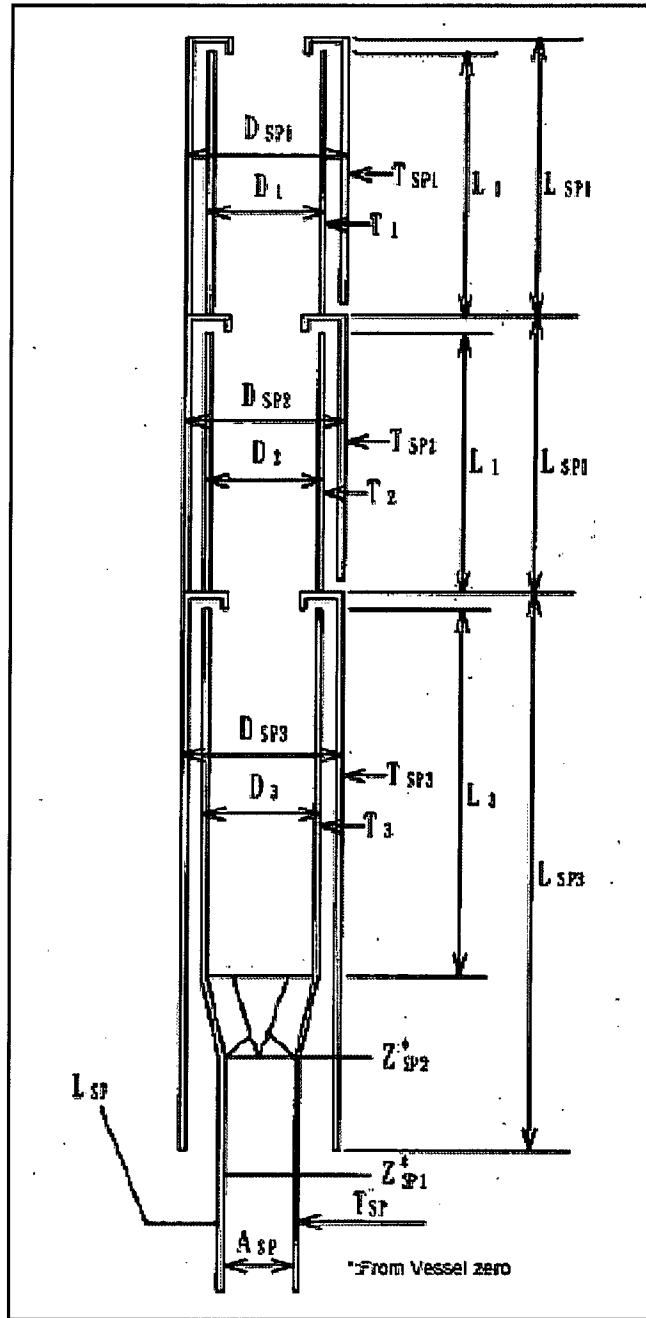


Figure B-4